



**UNIVERSIDAD DE INVESTIGACIÓN DE
TECNOLOGÍA EXPERIMENTAL YACHAY**

Escuela de Ciencias de la Tierra, Energía y Ambiente

**TÍTULO: Litho-Biostratigraphic characterization along
the Pedro Pablo Gomez – La Rinconada transect in the
coastal zone, western Ecuador.**

Trabajo de integración curricular presentado como requisito para la
obtención del título de Geólogo

Autor:

Vallejo Barzallo Alejandro Dave

Tutor:

MSc. Carlosama Morejón Felipe

Co-tutor:

PhD. Santamaría Freire Santiago

Urcuquí, Mayo 2024

Autoría

Yo, **Alejandro Dave Vallejo Barzallo**, con cédula de identidad 1725821480, declaro que las ideas, juicios, valoraciones, interpretaciones, consultas bibliográficas, definiciones y conceptualizaciones expuestas en el presente trabajo; así cómo, los procedimientos y herramientas utilizadas en la investigación, son de absoluta responsabilidad de el autor del trabajo de integración curricular. Así mismo, me acojo a los reglamentos internos de la Universidad de Investigación de Tecnología Experimental Yachay.

Urcuquí, Mayo 2024.

Vallejo Barzallo Alejandro Dave

CI: 1725821480

Autorización de publicación

Yo, **Alejandro Dave Vallejo Barzallo**, con cédula de identidad 1725821480, cedo a la Universidad de Investigación de Tecnología Experimental Yachay, los derechos de publicación de la presente obra, sin que deba haber un reconocimiento económico por este concepto. Declaro además que el texto del presente trabajo de titulación no podrá ser cedido a ninguna empresa editorial para su publicación u otros fines, sin contar previamente con la autorización escrita de la Universidad.

Asimismo, autorizo a la Universidad que realice la digitalización y publicación de este trabajo de integración curricular en el repositorio virtual, de conformidad a lo dispuesto en el Art. 144 de la Ley Orgánica de Educación

Urququí, Mayo 2024.

Vallejo Barzallo Alejandro Dave

CI: 1725821480

Dedication

To my beloved mother.

Acknowledgment

I would like to thank my advisor and co-advisor Felipe Carlosama and Santiago Santamaria for their support and guidance throughout the development of this project. They were always available and willing to help and kept pushing me forward. I would also like to thank Yaniel Vazquez and Germán Merino for being part of my thesis committee and providing important comments to improve my work. I am especially grateful to Elizabeth Mariño, who has always inspired me to challenge myself and strive for greater goals.

I am grateful to the Instituto de Investigación Geológico y Energético (IIGE) for allowing me access to their facilities and learning the techniques developed in this project. Special thanks to Ing. Rita Andrade, Ing. Jhonatan Enríquez, and Ing. Oswaldo Coronel for their guidance during the planning and field work of the thesis project. Their knowledge and experience were of great help to complete this project.

I would also like to thank the ECTEA faculty, especially all my professors who contributed in my academic formation, to whom I owe all the knowledge and experience that I have acquired during my studies at Yachay Tech.

Finally, I would like to thank my family for their unconditionally support, without them this accomplishment would not be possible.

Alejandro Vallejo

Resumen

Este estudio tiene como objetivo caracterizar las rocas sedimentarias y los microfósiles de la Formación Cayo expuestos a lo largo del transecto Pedro Pablo Gómez - La Rinconada en la zona costera de Ecuador. La Formación Cayo forma parte de la Cordillera Chongón-Colonche, una cadena montañosa formada por la acreción de fragmentos de corteza oceánica durante el Cretácico Superior. El área de estudio se dividió en seis estaciones en las que se realizaron descripciones detalladas de la litología, el estilo de estratificación y las estructuras sedimentarias. También se llevó a cabo la petrografía de secciones delgadas para determinar las texturas sedimentarias y la identificación y clasificación de 13 especies de radiolarios, foraminíferos planctónicos y bentónicos. Los resultados indican que la Formación Cayo está constituida por rocas hemipelágicas y volcanoclásticas depositadas en un ambiente marino que va desde ambientes de plataforma externa a talud medio. También se confirmó la presencia de limolitas calcáreas pertenecientes a la Formación Calentura. Los conjuntos de microfósiles sugieren una edad relativa del Santoniense al Campaniense para los estratos estudiados. Se desarrolló una correlación litoestratigráfica con estudios previos y se propuso una reconstrucción paleoambiental. Este estudio contribuye a la comprensión de la historia geológica de la región costera de Ecuador y a la evolución de la Cordillera Chongón-Colonche.

Keywords:

Micropaleontología, Formación Cayo, Bioestratigrafía, Datación Relativa, Litoestratigrafía, Zona Costanera, Chongón-Colonche

Abstract

This study aims to characterize the sedimentary rocks and microfossils of the Cayo Formation exposed along the Pedro Pablo Gomez - La Rinconada transect in the coastal zone of Ecuador. The Cayo Formation is part of the Chongón-Colonche Cordillera, a mountain range formed by the accretion of oceanic crustal fragments during the Late Cretaceous. The study area was divided into six localities where detailed descriptions of lithology, bedding style, and sedimentary structures were made. Thin section petrography to determine sedimentary textures and the identification and classification of 13 species of radiolarians, planktic and benthic foraminifera were also carried out. The results indicate that the Cayo Formation consists of hemipelagic and volcanoclastic rocks deposited in a marine environment ranging from outer shelf to middle slope environments. The presence of calcareous mudstones belonging to the Calentura Formation was also confirmed. The microfossil assemblages suggest a relative age of Santonian to Campanian for the studied strata. A lithostratigraphic correlation with previous studies was developed and a paleoenvironmental reconstruction was proposed. This study contributes to the understanding of the geological history of the coastal region of Ecuador and the evolution of the Chongón-Colonche Cordillera.

Keywords:

Micropaleontology, Cayo Formation, Biostratigraphy, Relative Dating, Lithostratigraphy, Coastal Zone, Chongón-Colonche

Contents

Dedication	v
Acknowledgment	vii
Resumen	ix
Abstract	xi
Contents	xiii
List of Tables	xvii
List of Figures	xix
1 Introduction	1
1.1 Background	1
1.2 Study area	4
1.3 Problem statement	4
1.4 Objectives	6
1.4.1 General objective	6
1.4.2 Specific objectives	6
2 Geological Framework	7
2.1 Regional geology	7
2.2 Tectonic setting	8
2.3 Stratigraphy	10
2.3.1 Piñon Formation	11
2.3.2 Las Orquídeas Formation	11
2.3.3 Calentura Formation	13

2.3.4	Cayo Formation	13
2.3.5	Guayaquil Formation	14
2.3.6	San Eduardo Formation	15
2.3.7	Las Masas Formation	15
2.4	Paleontological framework	16
2.4.1	Major groups of microfossils	16
2.4.2	Foraminifera	16
2.4.3	Ostracoda	18
2.4.4	Radiolaria	18
2.4.5	Calcareous nannoplankton	20
3	Methodology	21
3.1	Sampling methods and sedimentary description	21
3.2	Preparation of thin sections	22
3.3	Bulk sediment cleaning and fossil extraction	26
4	Results	29
4.1	Outcrop 1	29
4.2	Outcrop 2	32
4.3	Outcrop 3	34
4.4	Outcrop 4	36
4.5	Outcrop 5	38
4.6	Outcrop 6	41
4.7	Paleontological results	43
4.7.1	Radiolarians	43
4.7.2	Planktic Foraminifera	46
4.7.3	Benthic Foraminifera	47
4.7.4	Other fossils	53
5	Discussion	55
5.1	Lithofacies model	55
5.2	Relative dating	57
5.3	Lithostratigraphic correlation	60

5.4	Paleoenvironment determination	62
5.4.1	Calentura formation	62
5.4.2	Cayo Formation	63
6	Conclusions	65
A	Graphic Log Outcrop 1	67
B	Graphic Log Outcrop 2	69
C	Graphic Log Outcrop 3	71
D	Graphic Log Outcrop 4	73
E	Graphic Log Outcrop 5	75
F	Graphic Log Outcrop 6	77
G	List of Collected Samples and Location	79
	Bibliography	81

List of Tables

4.1	List of fossils identified in this study and their occurrence at each selected outcrop. See location of each outcrop in Fig. 1.2. See samples codes and coordinates in Appendix G.	43
5.1	Descriptions of the facies recognized in this study from field observations, petrography of rock samples, and microfossil content. The possible Bouma turbidite classification was also determined.	57
G.1	List of collected of rock samples (16) used for thin section analysis and bulk sediments (12) used for cleaning and physical removal of microfossils.	80

List of Figures

1.1	Typical Bouma-Sequence of internal sedimentary structures and their hydrodynamic interpretation for turbiditic deposits. Taken from Collinson et al. (2019) . . .	3
1.2	Geographical map of the Chongón-Colonche Cordillera showing the location of the studied outcrops, major towns, access roads, and major rivers. The Chongón-Colonche Fault marks the southern boundary of the Cordillera. The coordinate system is WGS 84 / UTM17S. Refer to Fig.2.1 to see the extent of the map. . .	5
2.1	Structural map of Ecuador showing the major geological terrains and fault systems. Modified after Jaillard et al. (1995) and Tamay Granda (2018)	8
2.2	Geologic map and faults of the study area showing the location and bedding measurements of each selected outcrop. The location of major rivers and towns are indicated for reference. The coordinate system is WGS 84 / UTM17S. Geologic contacts and faults are taken from Reyes and Michaud (2012) . Refer to Fig.2.1 to see the extent of the map.	10
2.3	General stratigraphic column of the Chongón-Colonche Cordillera, the Coastal Cordillera and the Neogene sedimentary cover (Manabí Basin). Maximum thickness measurements and age estimations are taken from Benitez (1995) ; Cohen et al. (2013) ; Luzieux (2007) ; Ordoñez (2006) . Modified after Benitez (1995) . . .	12
2.4	Major foraminiferal calcareous shell structures. Dashed lines represent the orientation of microcrystalline calcite. Taken from Scholle and Ulmer-Scholle (2003)	16
2.5	Most common shell morphologies of foraminifera. Taken from Scholle and Ulmer-Scholle (2003)	17
2.6	Ostracoda shell morphology and structure. Taken from Scholle and Ulmer-Scholle (2003)	18

2.7	Typical radiolarian skeletal types. Taken from Scholle and Ulmer-Scholle (2003) .	19
2.8	Schematic representation of the structure of coccoliths and their assembly into a coccosphere. Taken from Scholle and Ulmer-Scholle (2003) .	20
3.1	Materials used for thin section preparation and analysis available at Yachay Tech University. A) SystemAbele precision rock saw. B) Setting up the SystemAbele Universal Grinding Machine and the mounting instrument for polishing the samples. C) Ideal surface between the polished rock and the glass slide with minimal presence of bubbles. D) Euromex iScope series trinocular microscope used for thin section analysis.	25
3.2	Materials available at Yachay Tech University for cleaning bulk sediments, fossil extraction, and analysis. A) Bulk sediments soaking up process with H ₂ O ₂ at 30% concentration showing an exothermic reaction. B) Sieves and their standard mesh sizes used for sieving wet sediments. C) Container covered with a solution of methyl blue to avoid contamination between samples. D) Olympus SZ61 stereomicroscope used to pick up microfossils from bulk sediments.	27
4.1	A) Graphic log of Outcrop 1 describing the lithology, grain size, sedimentary structures, and sample stratigraphic position (refer to Appendix A for a detailed description). B) Outcrop 1 studied next to the Ayampe River. See location on Fig. 1.2.	30
4.2	Thin sections of rock samples from Outcrop 1 (see stratigraphic location on Fig. 4.1A). The left column is in PPL and the right column is in XPL. The scale bar is 500 μm. A) Vitric tuff with a glassy matrix and pyrolusite infill fractures. B) Greywacke texture with a clayey matrix supporting fossil fragments and mineral grains. C) Textural evolution between greywacke and lithic-arenite with strong increase in calcareous fossil fragments.	31
4.3	A) Graphic log of Outcrop 2 describing the lithology, grain size, sedimentary structures, and sample stratigraphic position (refer to Appendix B for a detailed description). B) Outcrop 2 studied next to the Ayampe River. See location on Fig. 1.2.	32

- 4.4 Thin sections of rock samples from Outcrop 2 (see stratigraphic location on Fig. 4.3A). The left column is in PPL and the right column is in XPL. The scale bar is 500 μm . A) Highly altered smectite-rich silicic tuff with a glassy matrix. B) Greywacke with moderate abundance of planktic foraminifera and fossil fragments. C) Matrix-supported microbreccia with high feldspar content. 33
- 4.5 A) Graphic log of Outcrop 3 describing the lithology, grain size, sedimentary structures, and sample stratigraphic position (refer to Appendix C for a detailed description). B) Outcrop 3 studied next to the Ayampe River. See location on Fig. 1.2. 34
- 4.6 Thin sections of rock samples from outcrops 2 and 3 (see stratigraphic location on Fig. 4.3A and Fig. 4.5A). The left column is in PPL and the right column is in XPL. The scale bar is 500 μm . A) Iddingsite and smectite alteration in an olivine crystal. B) Lithic arenite with abundant radiolarians and planktic foraminifera. C) Greywacke with a brown clayey matrix with the presence of calcite-filled fractures and radiolarians. 35
- 4.7 A) Graphic log of Outcrop 4 describing the lithology, grain size, sedimentary structures, and sample stratigraphic position (refer to Appendix D for a detailed description). B) Outcrop 4 studied next to the Ayampe River. See location on Fig. 1.2. 36
- 4.8 Thin sections of rock samples from Outcrop 4 (see stratigraphic location on Fig. 4.7A). The left column is in PPL and the right column is in XPL. The scale bar is 500 μm . A) Olivine, plagioclase and lithic fragments from a litho-feldspathic arenite. B) Altered dacite clasts and dark colored lavas surrounded by a smectitic matrix. C) Matrix-supported volcanic breccia with mineral grains of olivine, plagioclase, pyroxene, and quartz. 37
- 4.9 A) Graphic log of Outcrop 5 describing the lithology, grain size, sedimentary structures, and sample stratigraphic position (refer to Appendix E for a detailed description). B) Outcrop 5 studied next to the Grande River. See location on Fig. 1.2. C) Close-up showing wave ripples interbedded in cream and brown siltstones. D) Close-up showing convolutes and cross stratification within sandstone deposits. 39

- 4.10 Thin sections of rock samples from Outcrop 5 (see stratigraphic location on Fig. 4.9A). The left column is in PPL and the right column is in XPL. The scale bar is 500 μm . A) Arkosic arenite with a glassy matrix strongly altered to smectite. B) Centimeter-sized reworked crystal fragments from a lithic-feldspathic arenite. C) Textural evolution from greywacke to lithic arenite in sandstone 05M7. 40
- 4.11 A) Graphic log of Outcrop 6 describing the lithology, grain size, sedimentary structures, and sample stratigraphic position (refer to Appendix F for a detailed description). B) Outcrop 6 studied next to the Grande River. See location on Fig. 1.2. 41
- 4.12 Thin sections of rock samples from Outcrop 6 (see stratigraphic location on Fig. 4.11A). The left column is in PPL and the right column is in XPL. The scale bar is 500 μm . A) and B) is the representative texture of carbonate mudstone rocks at Outcrop 6 containing fossil fragments in a micritic matrix. C) Carbonate chertification with microcrystalline quartz. 42
- 4.13 Fossil specimens of *Nasellaria radiolarians*. The left column is in PPL and the right column is in XPL. The scale bar is 200 μm and the magnification is 100x. A-C) *Dictyomitra multicostata*, longitudinal section. D) *Dictyomitra multicostata*, longitudinal and transverse sections. 44
- 4.14 Fossil specimens of *Spumellaria radiolarians*. The left column is in PPL and the right column is in XPL. The scale bar is 200 μm and the magnification is 100x. A-B) *Stylospongia planoconvexa*, transverse section. C-D) Several transverse sections of *Stylospongia planoconvexa* and *Stylospongia* sp. 45
- 4.15 Fossil specimens of planktic foraminifera. The left column is in PPL and the right column is in XPL. The scale bar is 200 μm and the magnification is 100x. A-B) *Heterohelix* sp., longitudinal section. C-D) *Heterohelix* sp., transverse section. . . 46
- 4.16 Fossil specimens of planktic foraminifera. The left column is in PPL and the right column is in XPL. The scale bar is 200 μm and the magnification is 100x. A-D) *Globotruncana* sp., transverse section. 47
- 4.17 Fossil specimens of benthic foraminifera. The left column is in PPL and the right column is in XPL. The scale bar is 200 μm and the magnification is 100x. A-B) *Nodosaria* sp., longitudinal section. C-D) *Nodosaria* sp., transverse section. . . . 48

4.18	Fossil specimens of benthic foraminifera highlighting the main visible features. Images taken with an Olympus SZ61 stereomicroscope. The scale bar is 2 mm and the magnification is 45x. A) <i>Nodosaria</i> sp., 2 uniserial chambers. B-D) <i>Nodosaria</i> sp., single chambers.	49
4.19	Fossil specimens of benthic foraminifera. The left column is in PPL and the right column is in XPL. The scale bar is 200 μm and the magnification is 100x. A) <i>Cibicides</i> sp., transverse section showing sparitic composition in XPL. B-C) <i>Cibicides</i> sp., transverse section and calcareous composition. D) <i>Cibicides</i> sp., dorsal view, the test is broken or dissolved.	50
4.20	Fossil specimens of benthic foraminifera highlighting the main visible features. Images taken with an Olympus SZ61 stereomicroscope. The scale bar is 2 mm and the magnification is 45x. A) <i>Cibicides subcarinatus</i> . B) <i>Lagena</i> sp. C) <i>Gyrogoninoides</i> sp. D) <i>Hormosinella ovolum</i>	52
4.21	Fossil specimens of benthic foraminifera highlighting the main visible features. The scale bar is 2 mm and the magnification is 45x. A-C) <i>Praebulimina</i> sp. D) <i>Ellipsoglandulina</i> sp.	53
4.22	Echinoid fossils and other fragments. The left column is in PPL and the right column is in XPL. The scale bar is 200 μm and the magnification is 100x. A) Echinoid sample with sparitic composition and radial structures. B) Echinoid sample with calcareous composition and pore filled structures. C-D) Siliceous fossil fragments and spicules.	54
5.1	Stratigraphic distribion of indentified species of radiolarians (red), planktic foraminifera (green), and benthic foraminifera (blue) in the Chongón-Colonche Cordillera. The age ranges were taken from Bolli et al. (1994) ; Loeblich and Tappan (1988) ; O'Dogherty et al. (2009) ; Ordoñez (2006)	59
5.2	Lithostratigraphic correlation of the studied outcrops with previous studies, detailing approximate thickness and age. Modified after Benitez (1995) , Ordoñez (2007) and Machiels et al. (2014)	61

- 5.3 Depth assemblages of Upper Cretaceous foraminifera in marine environments. Modified after [Saraswati and Srinivasan \(2015\)](#) and [Sliter \(1972\)](#). A) Major fossil assemblages of benthic foraminifera distribution marginal marine, continental shelf, and continental slope environments highlighting the species used for this study. B) Generalized depth distribution of the planktic foraminiferal genera used in this study. 64

Chapter 1

Introduction

1.1 Background

The occurrence of marine microfossils in the sedimentary record spans a wide time range, from the Precambrian to recent times (Bellier et al., 2010; Haq and Boersma, 1998). However, the study of microfossils and the development of micropaleontology as a discipline are of relatively recent origin. In the 1940s and 1950s, the first glimpses of micropaleontology developed as exploration of the ocean floor began. Micropaleontological studies then flourished in the 1960s and 1970s with the increasing demands of the oil industry to date borehole sections and correlate them with surface strata (Haq and Boersma, 1998). This development, which reduced the cost of oil exploration, also revealed the multidimensional applications of microfossils in solving problems in the geosciences, as they are essential for seismic calibration and sequence stratigraphy (Saraswati and Srinivasan, 2015). In 1968, the Deep-Sea Drilling Project greatly expanded the available deep-sea stratigraphic record from all major ocean basins. As a result, new applications such as biochronology, biostratigraphy, and paleoenvironmental and paleoceanographic reconstructions have contributed to a better understanding of the Earth's history (Bolli et al., 1994; Saraswati and Srinivasan, 2015).

In Ecuador, important paleontological studies were carried out in the early 20th century by several authors, especially Hans E. Thalmann. Decades later, the study of microfossils in Ecuador formally began in the 1970s, when oil exploration was developing in the Ecuadorian territory and the paleontological control of perforations was needed. For this reason, the first biostratigraphy laboratory was created by the national oil company CEPE, now known as PETROECUADOR, under the direction of the Ecuadorian geologists Martha Ordoñez, Nelson

Jimenez and Italo Zambrano. Important progress has been made since then, but a proper microfossil database has not yet been developed due to the extensive microfossil species richness in the Ecuadorian territory. Further paleontological and stratigraphic studies in Ecuador will therefore contribute to the development of the Ecuadorian petroleum industry (Ordoñez, 2006).

The study of microfossils in various fields of geology is enhanced by their small size, ease of fossilization, abundance, and wide geographic distribution in sedimentary deposits of all ages and in most of the marine environments (Haq and Boersma, 1998). Microfossils are typically studied using microscopy techniques, such as light microscopy, scanning electron microscopy (SEM), and transmission electron microscopy (TEM). These techniques allow scientists to examine microfossils in detail and classify them to the species level (Ordoñez, 2006).

Some of the most important types of marine microfossils include benthic and planktonic foraminifera, radiolaria, calcareous nannofossils, diatoms, ostracodes, and palynomorphs (Bellier et al., 2010). Planktonic microfossils, such as various types of foraminifera, radiolaria, and calcareous nannofossils are useful for monitoring past changes in the oceanic environments, specially changes in temperature (Ordoñez, 2006). Benthic microfossils, such as ostracodes, diatoms, and some foraminifera, show distribution patterns that are commonly related to depth, sediment type, and physical or chemical changes in bottom waters. Palynomorphs, on the other hand, are organic remnants of continental species of plants and animals, but their presence and distribution in near-shore marine sediments allows interpretations of continental paleoclimates (Haq and Boersma, 1998).

The Ecuadorian continental margin has a high geological diversity due to multiple accretionary episodes occurred since the Triassic. The coastal region is formed by several sections of the Caribbean oceanic plateau that collided with the continental margin at the end of the Cretaceous. During these events, the deposition of several sequences of seafloor turbidites grouped within the present-day Cayo Formation took place. This study will focus on the Cayo Formation, which has been studied previously due to its economic implications in determining the oil reserves distributed along the Ecuadorian coast. The origin of this formation is a matter of discussion with several theories that try to explain the way in which the strata belonging to the Cayo Formation were deposited. Due to their age (i.e., Cretaceous) the outcrops of the Cayo Formation are slightly deformed with their fossil contents disturbed. Therefore, the accurate age of the Cayo Formation is not firmly constrained.

To fully understand the stratigraphy of the Cayo Formation, the identified turbiditic sequences must be studied in detail. The most important process of sediment transport and deposition in clastic marine and pelagic environments are turbidity currents. Turbidity currents are the result of turbulent suspension of particles surrounded by water. Due to their high velocities, turbidity currents are able to transport large particles to deeper environments, forming turbidite deposits (Prothero and Schwab, 2004). Most turbidite deposits have a regular sequence of sedimentary features known as the Bouma sequence (Fig. 1.1). The complete sequence shows structureless sand (T_A) overlain by parallel laminated sand (T_B). This is followed by ripple cross-lamination (T_C) and a diffuse textural change from sandy to cross-laminated silty sediments (T_D). Finally, structureless fine-grained mudstone and siltstone overlie the turbidite sequence (T_E , Collinson et al., 2019).

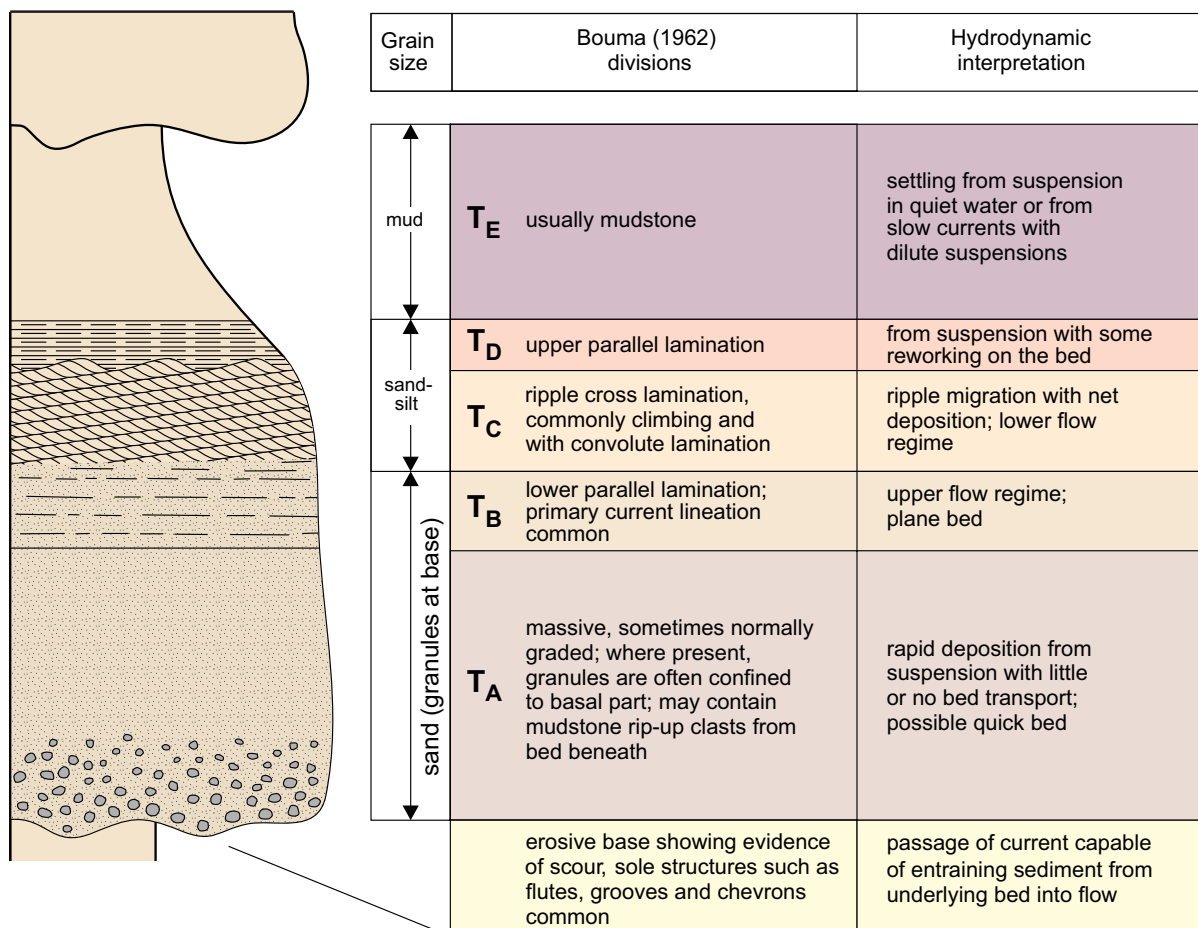


Figure 1.1. Typical Bouma-Sequence of internal sedimentary structures and their hydrodynamic interpretation for turbiditic deposits. Taken from Collinson et al. (2019).

This research project will use the applications of micropaleontology in order to characterize the past events that led to the deposition of strata in the coastal zone of Ecuador, unraveling past sedimentary environments, climate, and geological events through stratigraphy, sedimentology, and micropaleontology techniques.

1.2 Study area

The study area is located in the coastal Ecuador, on the western side of the Chongón-Colonche Cordillera, ~12 km east of the town of Ayampe, on the border between the provinces of Manabí (to the north) and Santa Elena (to the south, Fig. 1.2). Six specific outcrops of this transect located on the riverside of the Ayampe river were selected for detailed description and sampling. The outcrops can be accessed from two main secondary roads in either the Ayampe or La Rinconada districts until reaching the Guale district. Then, a gravel road along the Ayampe River is the only way to access the outcrops. This road is made up of unconsolidated material from the riverbed, so only well-equipped vehicles can use this road.

Within the study area, several tributaries flow into the Ayampe River, these are: (1) El Plátano River, (2) Blanco River, (3) Piñas River, (4) Estero Seco, (5) Chico River, and (6) Grande River (Fig. 1.2). It is recommended to visit the outcrops only during the dry season, as the flow of the rivers can increase considerably during the rainy season.

1.3 Problem statement

Micropaleontology in Ecuador is underdeveloped compared to other countries in the region. The poor quality and scarcity of outcrops in coastal Ecuador (Jaillard et al., 1995) may limit the possible information that can be obtained from the study of microfossils. Therefore, it is important to explore and describe in detail unstudied areas, in order to make the best use of the available geologic record.

The Chongón-Colonche Cordillera is a broad NNW-SSE oriented mountain range located in coastal Ecuador, between Guayaquil and Pedro Pablo Gomez. It is believed that the origin of the Chongón-Colonche Cordillera is the result of the intense accretionary events that occurred during the Late Cretaceous in the Ecuadorian margin (Jaillard et al., 1995). This mountain range contains several potential areas for geological studies. Most of the reported studies are located in the northeastern part of the cordillera, near the city of Guayaquil (e.g., Benitez,



Figure 1.2. Geographical map of the Chongón-Colonche Cordillera showing the location of the studied outcrops, major towns, access roads, and major rivers. The Chongón-Colonche Fault marks the southern boundary of the Cordillera. The coordinate system is WGS 84 / UTM17S. Refer to Fig.2.1 to see the extent of the map.

1995; Luzieux, 2007; Ordoñez, 2006). There are a few studies on the southwestern part of the Cordillera (e.g., Machiels et al., 2014), but they have not addressed properly the paleontology and stratigraphy of the area. Thus, a detailed description of the formations outcropping on this side of the Chongón-Colonche Cordillera is needed. The contribution of any geological/-paleontological study is useful to complete and reconstruct the complex geological history of Ecuador.

1.4 Objectives

1.4.1 General objective

The main purpose of this study is to characterize the sedimentary rocks and microfauna contained in the sedimentary sequence exposed along the Pedro Pablo Gomez - La Rinconada transect, located on the flanks of the Ayampe River. This will complement and correlate the current knowledge of the coastal region.

1.4.2 Specific objectives

- To characterize the sedimentary rock sequences exposed at selected outcrops along the Pedro Pablo Gomez - La Rinconada transect, recording lithology, bedding style, and sedimentary structures.
- To describe the petrography of rock samples to determine the mineral content and sedimentary textures.
- To identify microfossil specimens primarily benthic foraminifera, planktonic foraminifera, and radiolarians.
- To assign an age range to the studied strata based on microfossil assemblages.
- To develop the lithostratigraphic correlation of the identified rock sequences to complement the stratigraphic framework of the Chongón-Colonche Cordillera.
- To reconstruct the paleoenvironment and depositional depth of the stratigraphic units.

Chapter 2

Geological Framework

2.1 Regional geology

Continental Ecuador (Fig. 2.1A) can be subdivided into five physiographic regions, that exhibit distinctive lithological units of different age and tectonic evolution (Fig. 2.1B). These physiographic regions lie parallel to the regional tectonic orientation of the northern Andes with a roughly north-south orientation agreeing with the different components of the Andean orogen (Jackson *et al.*, 2019). From west to east, these regions are commonly referred to as: (1) The Coastal Region, composed of a mafic oceanic basement and covered by Paleogene to Neogene forearc deposits (Vallejo *et al.*, 2019). (2) The Western Cordillera (Cordillera Occidental), composed of mafic to intermediate volcanic and intrusive rocks tectonically juxtaposed with Late Cretaceous to Miocene sedimentary rocks (Vallejo *et al.*, 2019). (3) The Interandean Valley is a depression created between the Western and Eastern Cordilleras, which consists of a crystalline basement of metamorphic and mafic rocks hosting thick Pliocene to Pleistocene volcanic deposits (Vallejo *et al.*, 2009). The western boundary between the Western Cordillera and the Interandean Valley is considered to be part of the suture between the South American plate and the accreted crustal fragments derived from the Caribbean Large Igneous Province (CLIP) in the Late Cretaceous (Aizprua, 2021). (4) The Eastern Cordillera (Cordillera Real), composed of Paleozoic to Jurassic metamorphic rocks and Mesozoic granitoids and metasedimentary rocks (Vallejo *et al.*, 2019), corresponds to the internal hinterland segment of the fold-thrust belt (Jackson *et al.*, 2019). (5) The Subandean Zone and Oriente Basin are Late Cretaceous to Quaternary outer frontal segments of the fold-thrust belt and retro-arc foreland basin that developed in response to the growth of the Eastern Cordillera (Vallejo *et al.*, 2009).

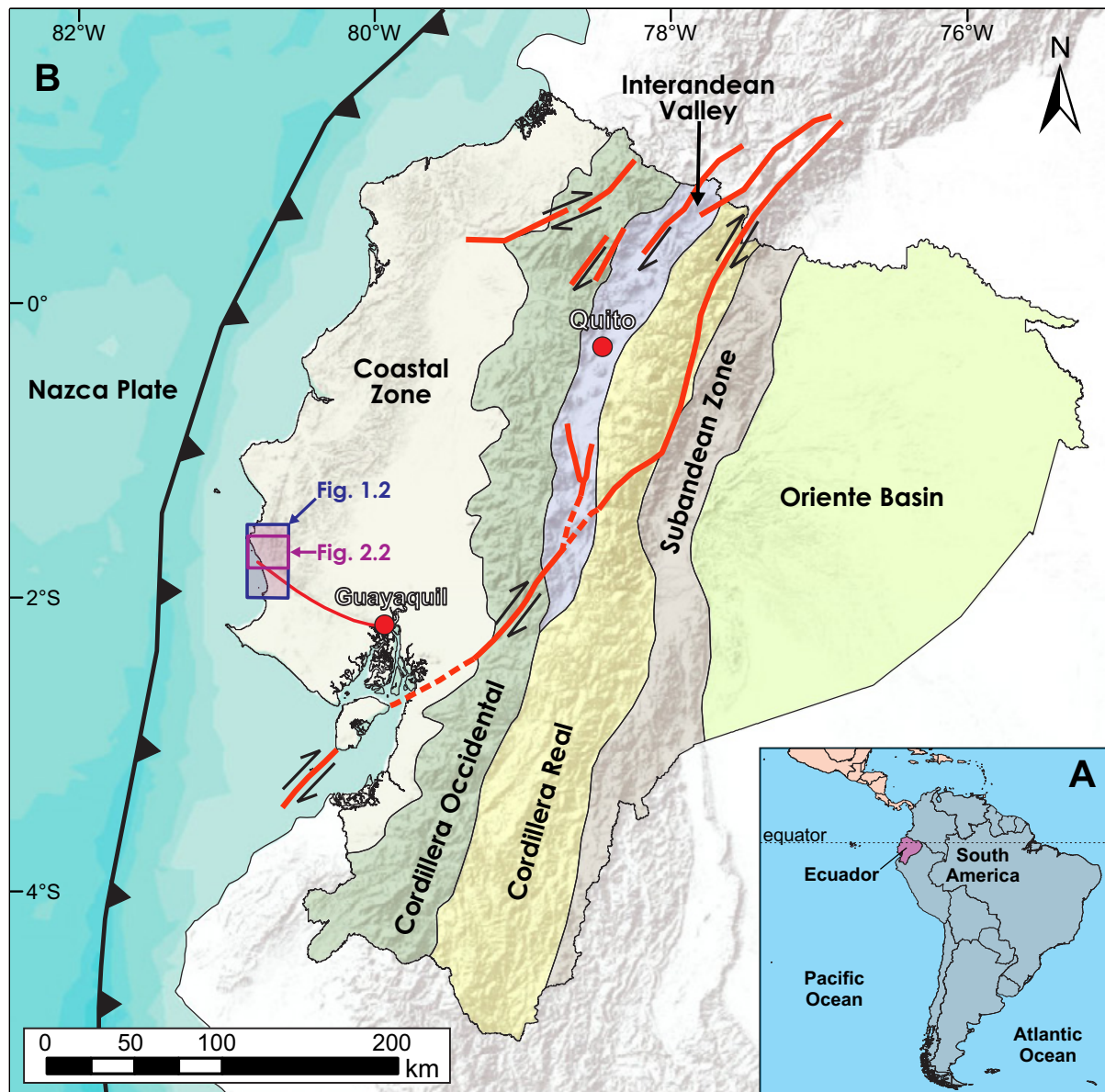


Figure 2.1. Structural map of Ecuador showing the major geological terrains and fault systems. Modified after [Jaillard et al. \(1995\)](#) and [Tamay Granda \(2018\)](#)

2.2 Tectonic setting

The Coastal Region is a 500 km long and 25 to 200 km wide geomorphologic feature of the continental Ecuador, bounded by the Cordillera Occidental to the east and the Pacific Ocean to the west (Fig. 2.1B). The morphology of the coastal Ecuador is relatively flat, with a local relief of ~100 m, except for the occurrence of three mountain ranges with elevations greater than 300 m, these being the Coastal Cordillera, the Chongón-Colonche Cordillera, and the Estancia

Mountain Range (Benitez, 1995; Feininger and Bristow, 1980).

The origin of the Coastal Region is geologically complex, including island arc related and marginal basin sedimentation, basin subsidence, and compressional tectonic pulses (Benítez et al., 1993; Jaillard et al., 1995). Several studies suggest that the basement of the northern two-thirds of the coastal Ecuador is composed of allochthonous accreted oceanic plateau remnants (Benítez et al., 1993; Goossens and Rose Jr, 1973; Reynaud et al., 1999), whereas the southern third of the coastal Ecuador, the Andean region, and the Oriente basin are underlain by continental crust (i.e., the South American Plate, Feininger and Bristow, 1980; Lebrat et al., 1985; Mégard et al., 1987).

Recent studies have determined that the basement rocks of the Coastal Region and the Western Cordillera, broadly identified as the Pallatanga, Piñon, and Macuchi terranes, are geochemically equivalent. This suggests that they may be derived from a single terrane (crustal fragments of the CLIP) that accreted towards the South American plate during the Late Cretaceous (~75 to 65 Ma, Aizprua, 2021; Spikings et al., 2015; Vallejo et al., 2009), triggering crustal fragmentation and clockwise rotations (~40° to 50°, Luzieux, 2007). There are two proposed models to explain the mode of emplacement of the basement of coastal Ecuador: (1) a single and consecutive accretionary episode during the Maastrichtian (Vallejo et al., 2009) and (2) multiple accretionary events between the Late Cretaceous and the Eocene (Jaillard et al., 2009).

Locally, the sedimentary cover south of the coastal Ecuador (i.e., Santa Elena Peninsula) is characterized by thick Late Paleocene deposits and by the development of the Progreso Basin (see Fig. 1.2, Jaillard et al., 1995). North of coastal Ecuador, the Chongón-Colonche fault (Fig. 2.1) and a sudden change in elevation marks the southern boundary of Chongón-Colonche Cordillera, which extends 90 km from Guayaquil to Pedro Pablo Gomez with a NNW-SSE direction and a homoclinal structure. A subsequent change in the orientation of the mountain range (N-S) marks the lower boundary of the Coastal Cordillera which extends from Pedro Pablo Gomez towards northwestern Ecuador (Fig. 1.2, Benítez et al., 1993; Benitez, 1995; Feininger and Bristow, 1980; Jaillard et al., 1995; Ordoñez, 2006).

2.3 Stratigraphy

The stratigraphy of the Chongón-Colonche Cordillera is characterized by Upper Cretaceous (i.e., Piñon Formation) to Middle Eocene (i.e., Las Masas Formation) sedimentary, volcanic-sedimentary, and calcareous sequences (see Fig. 2.3, Benitez, 1995; Feininger and Bristow, 1980; Jaillard et al., 1995). The study area covers only the Cayo and Calentura formations (see fig. 2.2), but it is worth describing the events that led to the deposition of the strata that occur in the Chongón-Colonche Cordillera to get a better understanding of its geological history.

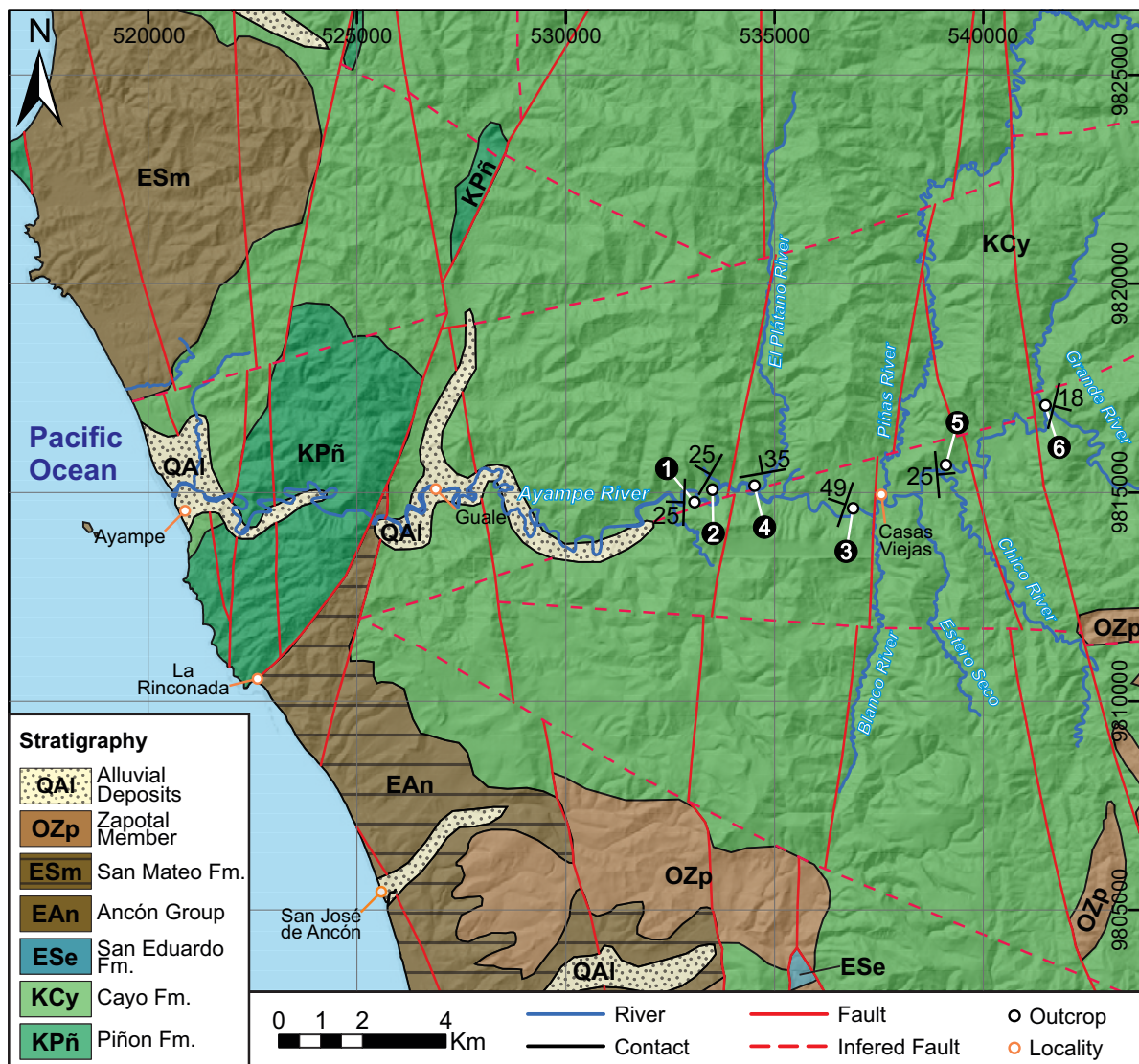


Figure 2.2. Geologic map and faults of the study area showing the location and bedding measurements of each selected outcrop. The location of major rivers and towns are indicated for reference. The coordinate system is WGS 84 / UTM17S. Geologic contacts and faults are taken from Reyes and Michaud (2012). Refer to Fig.2.1 to see the extent of the map.

The lithostratigraphic units belonging to the Chongón-Colonche Cordillera (i.e., Piñon, Las Orquídeas, Calentura, Cayo, Guayaquil, San Eduardo and Las Masas Formations; see stratigraphic position on Fig 2.3) are described in detail in the following section.

2.3.1 Piñon Formation

The Piñon Formation is widespread, with extensive outcrops in the Chongón-Colonche Cordillera and local outcrops in the Guayaquil area, the Santa Elena peninsula and the Manabí Basin (see Fig.2.2 and Fig 2.3). Therefore, it is considered to constitute the basement of the entire southwestern coastal area of Ecuador (Jaillard et al., 1995; Luzieux, 2007; Reyes and Michaud, 2012). It consists of three main lithologies: (1) mid-ocean ridge-like basalts (MORBs, aphanitic pillow basalts and intrusive dolerites), (2) island arc tholeiites (volcanic and volcanic-sedimentary cover, San Lorenzo Formation), and (3) intrusions of different ages and compositions (tonalites, diabase or gabbro sills and dacitic dikes, Benitez, 1995; Goossens and Rose Jr, 1973; Jaillard et al., 1995; Mégard et al., 1987).

The Piñon Formation corresponds to the basement of the coastal Ecuador, commonly known as a Basic Igneous Complex (BIC) due to its wide range of lithologies and ages (Goossens and Rose Jr, 1973). Radiometric dating and biostratigraphic correlations of the Piñon Formation assign ages ranging from 50 to 120 Ma (Goossens and Rose Jr, 1973). The narrowest age approximation is Coniacian (~88.8 Ma, Luzieux, 2007).

2.3.2 Las Orquídeas Formation

The Las Orquídeas Formation is poorly exposed, although a limited number of outcrops could be identified near the Guaramao River, north of the Chongón-Colonche Cordillera (Luzieux, 2007). The Las Orquídeas Formation consists of a 30-200 m thick series of andesitic to basaltic volcanic breccias containing porphyric andesitic fragments, rare basaltic flows, locally brecciated hyaloclastites, volcanoclastic debris flows, and subordinate tuffs. The lower part of the formation consists of laminated, organic-rich limestones with a fossil content rich in planktic foraminifera, radiolarians and inoceramids. The Las Orquídeas Formation overlies the Piñon basement and the age attributed to this formation is Middle Coniacian (see Fig 2.3, Jaillard et al., 2009; Van Melle et al., 2008).

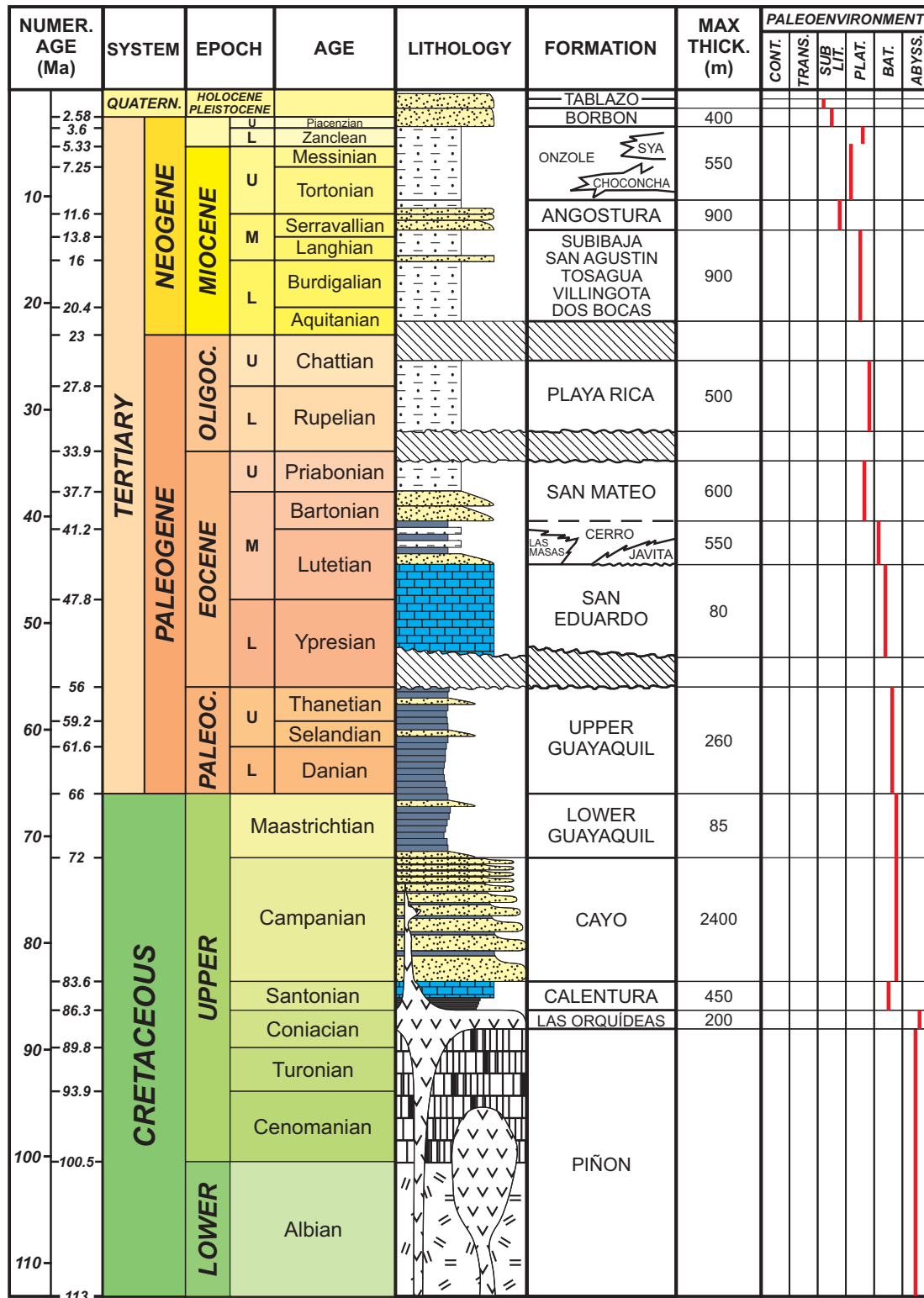


Figure 2.3. General stratigraphic column of the Chongón-Colonche Cordillera, the Coastal Cordillera and the Neogene sedimentary cover (Manabí Basin). Maximum thickness measurements and age estimations are taken from Benitez (1995); Cohen et al. (2013); Luzieux (2007); Ordoñez (2006). Modified after Benitez (1995).

2.3.3 Calentura Formation

The Calentura Formation laterally extends about 90 km along the northeastern flank of the Chongón-Colonche Cordillera from the Guayaquil area to the town of Las Delicias, in the Manabí province (Luzieux, 2007; Ordoñez, 2006). It consists of a series of deposits 250 to 450 m thick composed of multiple flow deposits of reworked andesites, tuffs, radiolarites, fine laminated limestones and cherts, and red siliceous limestones (Jaillard et al., 1997; Reyes and Michaud, 2012) formed in a pelagic anaerobic environment (Jaillard et al., 1995; Ordoñez, 2006). The Calentura Formation conformably overlies the Las Orquídeas Formation (see Fig 2.3, Jaillard et al., 1995; Reyes and Michaud, 2012).

The anaerobic environment is interpreted by the presence of widespread pyrite grains and a high organic content extending to an outer shelf environment (Luzieux, 2007; Ordoñez, 2006). The fossil content of the Calentura Formation includes microfossils such as foraminifera, radiolarians and calcareous nannofossils, which are particularly resistant to anaerobic conditions. The macrofossil content mainly consists of mollusk somatofossils and molds (Ordoñez, 2006). The high silicification of nannofossils in the Calentura Formation has made species identification difficult (Benítez, 1995). Despite this factor, the currently reported biostratigraphic assemblages are correlated with the Oceanic Anoxic Event 3 (OAE3), Coniacian to Santonian in age (90 to 84 Ma, Luzieux, 2007) or more precisely, Lower Coniacian to Middle Coniacian (Ordoñez, 2006).

2.3.4 Cayo Formation

The Cayo Formation outcrops on both sides of the coastal Ecuador, northwest of the Guayaquil area, Puerto Cayo, the Chongón-Colonche Cordillera area and along the Jama fault system (Jaillard et al., 1995; Ordoñez, 2007; Reyes and Michaud, 2012). It is particularly well exposed in the Chongón-Colonche Cordillera (see Fig 2.2) and occurs locally in the Santa Elena province. The Cayo Formation is thickest in the southern part of coastal Ecuador (i.e., Santa Elena area, Feininger and Bristow, 1980).

The Cayo Formation consists of 2-3 km thick deposits composed of normal graded sequences of volcanically derived debris flows and coarse-grained volcanoclastic turbidites resulting from the erosion of a volcanic arc (Benítez et al., 1993; Jaillard et al., 1995; Luzieux, 2007). The main lithologies found are shales, sandstones, conglomerates, siliceous shales, fine-grained tuffs and tabaceous sandstones, cherts, and few limestone beds (Benítez et al., 1993; Ordoñez, 2007).

The Cayo Formation conformably overlies the Calentura Formation (see Fig 2.3, [Jaillard et al., 1995](#)).

The microfossil content is mainly planktonic and benthonic foraminifera, in addition to the occurrence of trace fossils, which are widespread within the formation with an increasing trend towards the top. This indicates that there was a significant bioturbation activity at the time of deposition ([Luzieux, 2007](#)). Several authors have proposed a possible age for the Cayo Formation, most of them attribute that the deposition occurred in the Upper Cretaceous ([Benítez et al., 1993](#); [Feininger and Bristow, 1980](#); [Jaillard et al., 1995](#)). The closest approximation is Upper Santonian to Maastrichtian age, based on microfossil assemblages ([Luzieux, 2007](#)).

2.3.5 Guayaquil Formation

The Guayaquil Formation crops out only in the north of the coastal Ecuador, in the southern flank of the Chongón-Colonche Cordillera up to 80 km west of the Guayaquil area, specifically in the Via Perimetral, and as olistostromes in the Santa Elena peninsula ([Benitez, 1995](#); [Bristow and Hoffstetter, 1977](#); [Jaillard et al., 1995](#); [Luzieux, 2007](#); [Ordoñez, 2006](#)). The Guayaquil Formation consists of ~400 m thick, slightly deformed sequences of pelagic dark shales, black chert nodules, siliceous tuffs and thin-bedded volcanoclastic turbidites ([Deniaud, 1998](#); [Jaillard et al., 1997](#); [Reynaud et al., 1999](#)). It conformably overlies the Cayo Formation and is further divided into two units: Lower Guayaquil and Upper Guayaquil (see Fig 2.3, [Benitez, 1995](#); [Ordoñez, 2006](#)).

The origin of the Lower Guayaquil Formation is attributed to pelagic sedimentation resulting from mild to distal volcanic activity, far from any continental source ([Jaillard et al., 1995](#)), deposited in a deep marine environment with low salinity at depths between 500 and 1000 m ([Ordoñez, 2006](#); [Benitez, 1995](#)). The Upper Guayaquil Unit shows shallowing trends with an increase in calcareous microfossil content ([Luzieux, 2007](#); [Ordoñez, 2006](#)). Available microfossil assemblages based on planktonic foraminifera and radiolarian species suggest a Maastrichtian to Upper Paleocene age ([Bristow and Hoffstetter, 1977](#); [Deniaud, 1998](#); [Jaillard et al., 1995](#); [Ordoñez, 2006](#)). Stratigraphic and paleontological studies have established the existence of the KT limit (66 Ma), which marks the boundary between the Lower and Upper Guayaquil Units ([Ordoñez, 2006](#)).

2.3.6 San Eduardo Formation

The San Eduardo Formation crops out north of the coastal Ecuador along the southwestern flank of the Chongón-Colonche Cordillera. It is composed of a 30-120 m thick sequence of calciturbidites, siliceous shales, and limestones that paraconformably overlie the Upper Guayaquil Formation (see Fig 2.3, [Benítez et al., 1993](#); [Jaillard et al., 1995, 1997](#)). The San Eduardo Formation corresponds to non-continuous beds thinned or compacted by erosion caused by a diachronous Ypresian transgression and erosion, called the Lower Eocene Hiatus ([Feininger and Bristow, 1980](#); [Jaillard et al., 1995](#); [Ordoñez, 2006](#)).

The San Eduardo Formation is interpreted to have been deposited from cyclic calcareous flysch derived from material collapsed from algal reefs in deep-water turbidity currents ([Feininger and Bristow, 1980](#)). The sediments of the San Eduardo Formation contain algae, benthic foraminifera, planktonic foraminifera, nannofossils and oncolites dated to the Middle-Late Ypresian to Early Lutetian ([Benítez et al., 1993](#); [Jaillard et al., 1995, 1997](#)).

2.3.7 Las Masas Formation

The Las Masas Formation consists of a 200 m thick sequence of laminated shales, marlstones and siltstones, systematically found above the San Eduardo Formation in an apparently conformable contact (see Fig 2.3, [Benitez, 1995](#); [Luzieux, 2007](#)). The Las Masas Formation is interpreted to have been deposited in a calm hemipelagic environment that records a relative sea-level rise. It has been suggested that the Las Masas Formation and the San Eduardo Formation were deposited simultaneously ([Benitez, 1995](#); [Luzieux, 2007](#)). It contains a high abundance of radiolarians, fine sponge spicules and planktonic foraminifera, but simple methods to extract microfauna from this formation have not been successful ([Benitez, 1995](#)).

2.4 Paleontological framework

2.4.1 Major groups of microfossils

All six kingdoms of living organisms have microscopic forms of life, but only a few of these are geologically useful for sedimentary studies. Microfossils are considered to be any remains of a living organism, which may be microscopic fossils or detached skeletal fragments of larger organisms (Ordoñez, 2006). Fragments of sponge spicules, coral plates, and echinoderm spines are included in micropaleontological studies due to their small size and therefore can be identified only through a microscope (Saraswati and Srinivasan, 2015). Some of the most abundant and consequently most important marine microfossil species studied in Ecuador are: foraminifera, ostracoda, radiolaria, and calcareous nannoplankton. The following sections describe each type of microfossil in detail.

2.4.2 Foraminifera

Foraminifera are unicellular organisms (Protozoa) found in all marine environments. They are composed of chemically variable shells or tests, which can be calcareous, siliceous, or agglutinated (cementing together exogenous grains). The shells can also exhibit different degrees of crystallization and crystal orientations (Fig. 2.4).

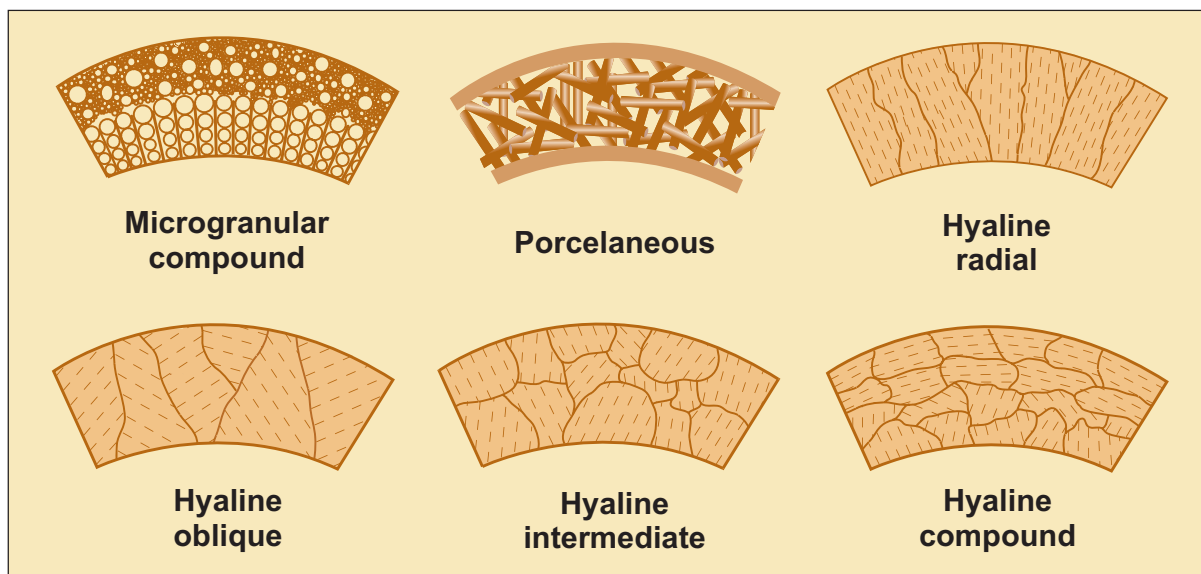


Figure 2.4. Major foraminiferal calcareous shell structures. Dashed lines represent the orientation of microcrystalline calcite. Taken from Scholle and Ulmer-Scholle (2003)

The arrangement of the shells is morphologically diverse, generally consisting of successive chambers arranged serially (uniserial, biserial, or triserial) or spirally (planispiral or conically spired, Fig. 2.5). Overall, foraminifera are divided into benthic and planktonic species. The benthic species live on the seafloor, either on the surface of the sediment or buried in it, and are useful for paleoenvironmental interpretation. The planktonic species float passively on water moved by currents and have been successfully used in biostratigraphy. The common foraminifera size typically ranges from about 0.3 mm to 0.1 mm, although some species can reach diameters of about 10 cm (Bellier et al., 2010; Bolli et al., 1989; Ordoñez, 2006).

Stratigraphically, foraminifera have appeared since the Early Cambrian. Nowadays, about 55,000 species of foraminifera have been recognized (Camacho, 1966; Saraswati and Srinivasan, 2015). Foraminifera are the most important microfossil species due to their wide environmental and stratigraphic distribution. They are increasingly used for environmental (paleoecological) interpretations and chronological correlations (Horowitz et al., 2012; Ordoñez, 2006).

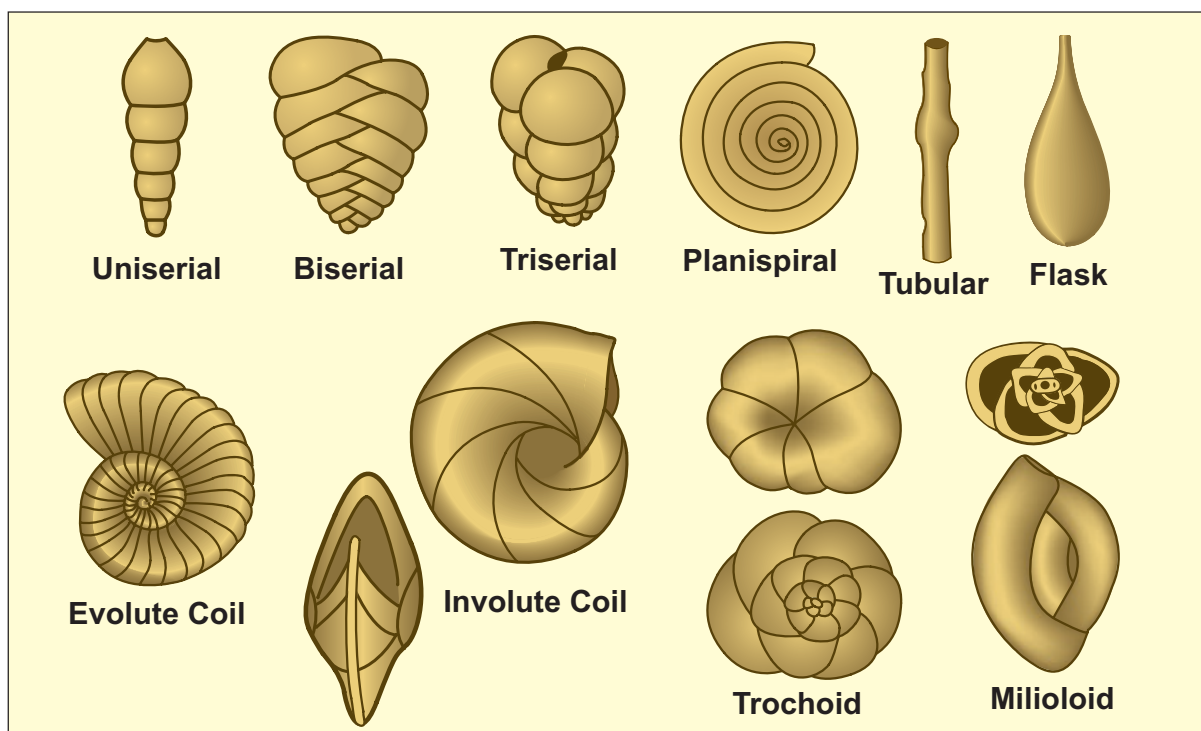


Figure 2.5. Most common shell morphologies of foraminifera. Taken from Scholle and Ulmer-Scholle (2003).

2.4.3 Ostracoda

Ostracoda are a subclass of species belonging to the group Crustacea. They range in size from 0.5 mm to more than 5 mm, and their shell consists of two valves that can be calcareous or chitinous in composition (Fig. 2.6). Ostracoda are widely distributed in almost all aquatic environments (marine, brackish and freshwater), even in wet soils (Ordoñez, 2006). They also have both benthic and planktic life forms. Currently, about 33,000 species of Ostracoda have been identified (Camacho, 1966). They can be dated back to the Ordovician and are widely distributed in rock sequences of all periods of the Phanerozoic (Saraswati and Srinivasan, 2015). The subclass Ostracoda is one of the best documented microfossil species due to their wide environmental distribution and ease of fossilization. They have many applications in biostratigraphy, paleoecology, and paleoclimate determination (Camacho, 1966; Horowitz et al., 2012).

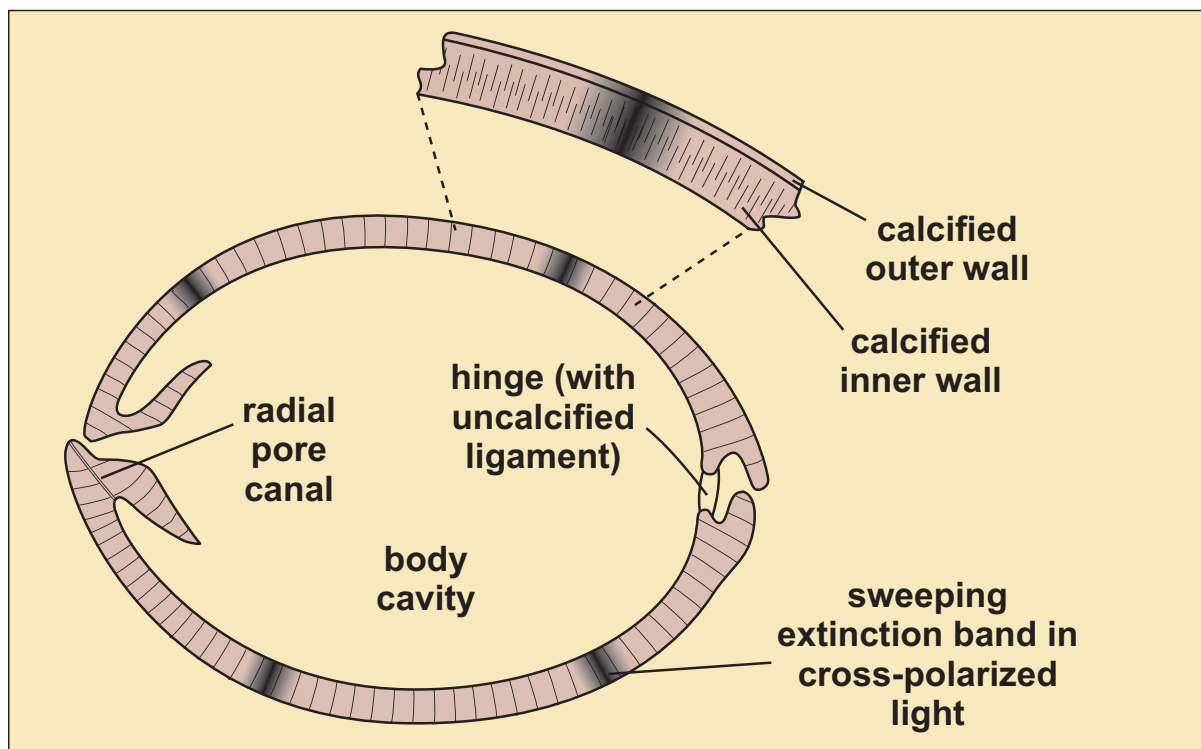


Figure 2.6. Ostracoda shell morphology and structure. Taken from Scholle and Ulmer-Scholle (2003).

2.4.4 Radiolaria

Radiolarians are unicellular marine zooplankton species composed of two layers of siliceous (opaline) skeletons in the shape of a hollow, perforated sphere or vase. There are three major

divisions within the Radiolaria group: (1) Spumellaria, (2) Nassellaria, and (3) Phaeodaria (Saraswati and Srinivasan, 2015). Phaeodaria is poorly preserved in the fossil record, as their bodies are composed of 95% organic matter and 5% silica. On the other hand, Spumellaria and Nassellaria are widely distributed in the fossil record since the Cambrian. The main difference between Spumellaria and Nassellaria is the shell morphology (Fig. 2.7). The skeletons of Spumellaria are characterized by a complex radial symmetry enclosing a central capsule connected by needles and spicules. The skeletal structure of Nassellaria is characterized by axial symmetry with tripod-like, conical, hat-shaped, and sagittal ring structures (Horowitz et al., 2012; Haq and Boersma, 1998).

Radiolarians range in size from 30 μm to 2 mm in diameter and are exclusively marine, developing mainly near the equator. Radiolarian microfossils preserve the signatures of oceanic and climatic changes, making them valuable in biostratigraphy, especially for Cretaceous deposits (Ordoñez, 2006).

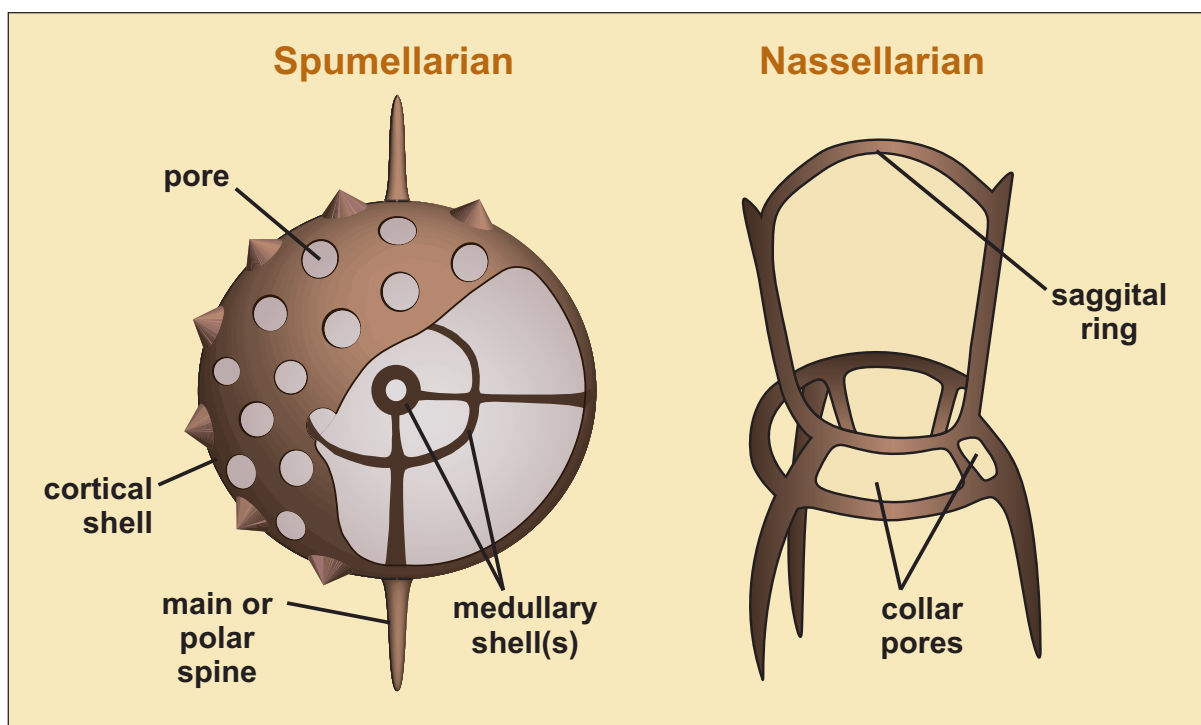


Figure 2.7. Typical radiolarian skeletal types. Taken from Scholle and Ulmer-Scholle (2003).

2.4.5 Calcareous nanoplankton

Calcareous nanoplankton are a group of calcareous algae, of which coccolithophores are the most important and abundant species. Coccolithophores are unicellular, autotrophic marine algae, generally less than 20 μm in size (Haq and Boersma, 1998; Scholle and Ulmer-Scholle, 2003). They are the major component of calcareous marine sediments, although some species have been found in coastal and freshwater environments (Saraswati and Srinivasan, 2015). Coccolithophores are composed of tiny calcareous shields called coccoliths (Fig. 2.8). Coccoliths are secreted from the cell, which then assemble into an enveloping spherical structure called a coccosphere (Ordoñez, 2006; Haq and Boersma, 1998).

Coccolithophores first appeared in the Late Triassic and are abundant from the Early Jurassic to recent times (Scholle and Ulmer-Scholle, 2003). Due to their very small size, examination under a high-power optical microscope or the SEM is required to identify these fossil species (Haq and Boersma, 1998). The study of calcareous nanoplankton has become an excellent tool for relative dating in the hydrocarbon industry because of their good recovery and short stratigraphic range. Calcareous nanofossils have also been used to determine ancient ocean currents and paleoenvironments (Saraswati and Srinivasan, 2015).

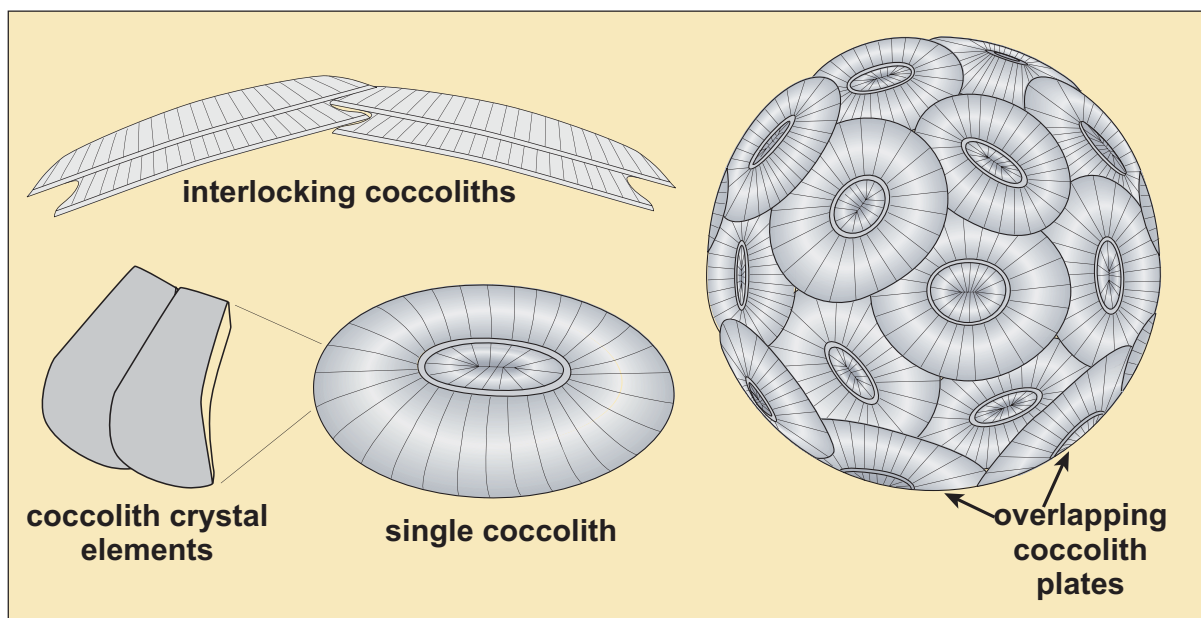


Figure 2.8. Schematic representation of the structure of coccoliths and their assembly into a coccosphere. Taken from Scholle and Ulmer-Scholle (2003).

Chapter 3

Methodology

3.1 Sampling methods and sedimentary description

The lithostratigraphic units studied correspond to the Cayo and Calentura Formations (see discussion) from the Chóngon-Colonche Cordillera. These formations are well exposed on the eastern flank of the cordillera, in the Pedro Pablo Gomez - La Rinconada transect. The Ayampe River and its tributaries flow westward, and stream erosion has created outcrops that are well suited for stratigraphic and paleontological evaluation. In June 2023, a field trip was conducted by Alejandro Vallejo and MSc. Felipe Carlosama from Yachay Tech University, Ing. Rita Andrade, Ing. Jhonatan Enríquez and Ing. Oswaldo Coronel from the Instituto de Investigación Geológico y Energético (IIGE). After accessing the study area, 6 evenly spaced and well exposed outcrops were selected for field description (Fig. 1.2).

The outcrops were arranged in chronological order, with Outcrop 1 being the earliest visited and Outcrop 6 the latest. A sedimentary graphic log was constructed at each outcrop to record the stratigraphic position of the collected samples, lithologies, sedimentary structures, and bedding styles. The stratigraphic position of all samples collected is detailed in Appendices A-F. A total of 28 samples were collected and divided into 2 groups : 16 consolidated rock samples and 12 fine-grained semiconsolidated sediment bags, referred to as bulk sediments (see Appendix G). As a general criteria, fine-grained lithologies were preferred for sampling to increase the chances of finding undisturbed microfossils, although some coarse-grained samples were also collected.

Each bulk sediment bag contained approximately 500 g of sample. The sediment bags were used to manually collect body fossils (remnants of microfossils, usually shells or spicules) for

analysis under a stereomicroscope. Bulk sediments sampling was methodical, attempting to collect representative unconsolidated sediments from each section and avoiding contamination from overlying strata to reduce errors during the microfossil identification stage.

The dimensions of the consolidated rock samples were approximately 25 x 25 cm. The polarity of each sediment sample was recorded as an aid to obtaining oriented sections of rock perpendicular to the bedding, in order to increase the probability of finding microfossils in thin sections.

3.2 Preparation of thin sections

Following the guidelines suggested by [Burnham Petrographics LLC](#), the following steps were performed to prepare the thin sections of 16 sedimentary rock samples (see Appendix G) in the laboratories of Yachay Tech University.

1. Using a SystemAbele precision rock saw (Fig. 3.1A), each sample was divided in half, keeping one half as a reference and using the other half to prepare the thin section.
2. At least 2 blocks with dimensions of 2.5 x 2.5 x 3.5 cm were cut, taking care to label (preferably with liquid paper) the sample code and polarity of each rock block. The remaining chips obtained after the cutting process were kept in the same sample bag as a reference.
3. If the rock sample is friable, it must be impregnated with a resin solution prior to polishing. The resin used to impregnate and mount the samples is Petropoxy 154, which must be mixed with a curing agent at a concentration of 10 phr (parts per hundred parts of resin, by volume).
4. To impregnate friable samples, they must first be heated on a heating plate until they reach a temperature of ~135°C to 140°C. Once the sample reached the desired temperature, the resin was applied to each side of the rock block using a wooden stick. Depending on the porosity and permeability of the sample, additional resin applications were necessary. When the resin had cured (after ~20 minutes), the process was repeated on the upside down side. The heat supply was kept constant until the resin had cured completely.

5. The polishing process required a SystemAbele universal grinding machine and a mounting tool. The mounting tool was used to secure each rock block with a side that may show representative textures/fossils facing down. The setting up of the instrument is shown in (Fig. 3.1B).
6. The polishing process was performed from the coarser grit to the finest. 4 grit sizes were used: 80, 150, 600 and 1000 grit. The polishing time for each group of 6 blocks was 1 to 2 hours per disk. The polishing time also depended on the lithology of the sample, so the polished surface was checked periodically. Once the surface was fully polished (it reflected light evenly), the rock blocks were ready to be dried.
7. The drying process was key to the development of the thin sections. If the specimen is not completely dried, water vapor can be generated between the contact surface of the specimen and the glass slide, creating bubbles that prevent a strong bond with the resin. This will result in loss of some of the sample during the final stages of preparation. Samples were dried using a heating plate at $\sim 135^{\circ}\text{C}$ to 140°C for at least 15 hours (especially for the most porous rocks). The samples were rotated regularly to distribute the heat evenly and to allow water vapor to escape easily.
8. The mounting process was performed on the heating plate at $\sim 135^{\circ}\text{C}$ to 140°C . A glass slide and a rock block were heated until they reached the desired temperature. After that, a generous layer of resin (the same from step 4) was applied to the polished surface which then was placed directly onto the glass slide squeezing out any trapped air bubble. The rock block was placed back on the heating plate with the glass slide facing down for 2 minutes. If bubbles have formed or the resin has soaked in, the glass slide was discarded and the resin from the block was cleaned with a sharp object. This process was repeated until the number of bubbles was minimal and there was an even layer of resin between the rock block and the glass slide (Fig. 3.1C). The heat supply was maintained for a few hours until the resin had cured.
9. After the mounting process, the glass slide may inevitably break due to stresses generated after the resin has cured and shrunk. To solve this problem, it was necessary to reheat the specimen and spread the resin on each crack, allowing it to flow into the voids. This created a strong bond between the cracks, so the slide was able to resist the later stages

of the process.

10. A vacuum tool was used to hold the sample and mount it in the systemAbele precision rock saw to obtain a layer of rock a few millimeters thick.
11. The slide was polished again with the smallest grit disk (1000) until the desired thickness of 30 μm was reached. The thin sections are ready when the interference colors of common minerals (usually quartz or plagioclase) can be identified in the sample. To do this, the sample must be examined periodically in a petrographic microscope during the final polishing stage.

When the thin section slides were ready, a Euromex iScope Series trinocular petrographic microscope was used to examine the thin sections for microfossil identification (Fig. 3.1D). Each slide was then thoroughly examined and an image of each identified microfossil was taken under both plane polarized light (PPL) and cross polarized light (XPL) at 100X magnification.

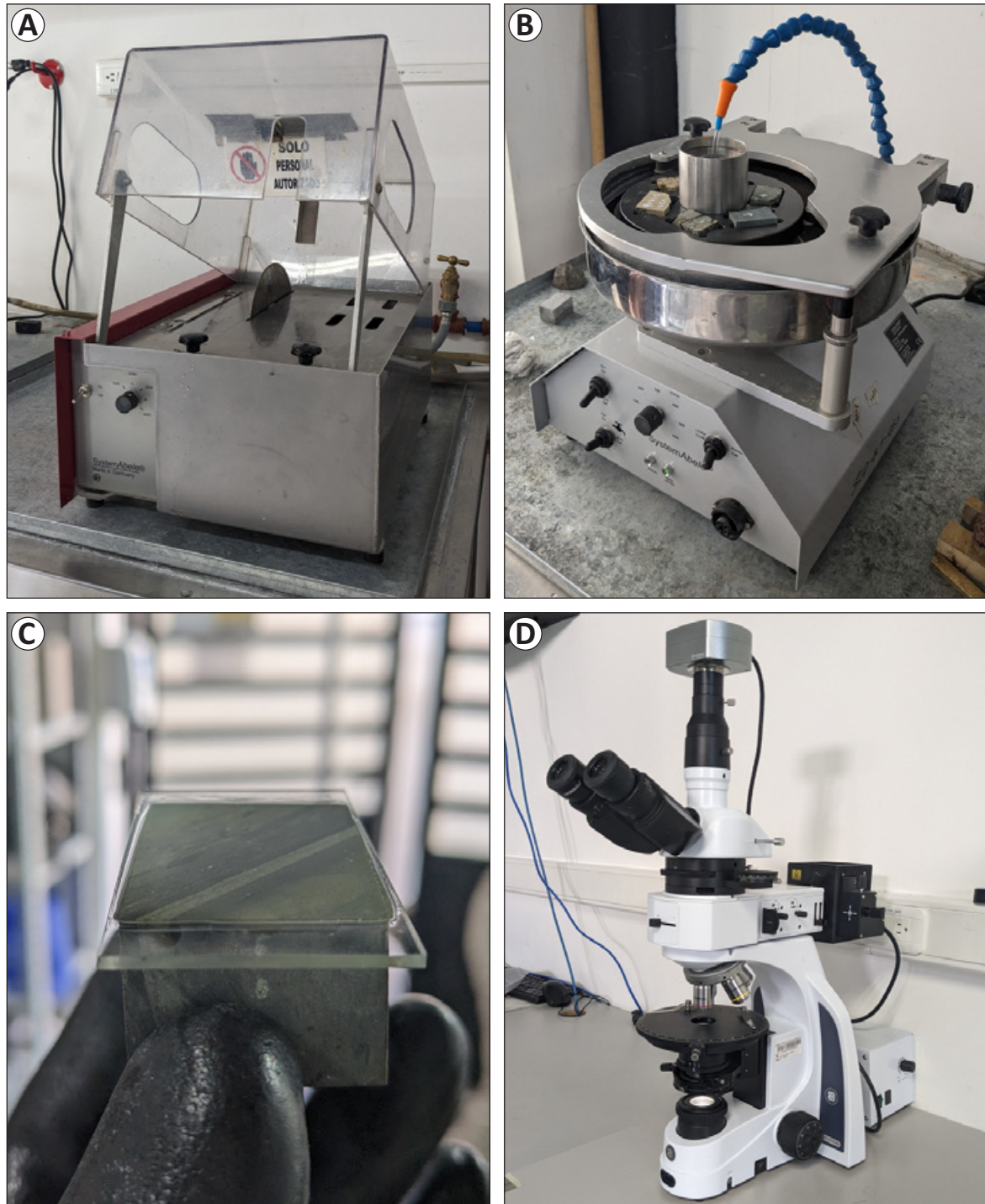


Figure 3.1. Materials used for thin section preparation and analysis available at Yachay Tech University. A) SystemAbele precision rock saw. B) Setting up the SystemAbele Universal Grinding Machine and the mounting instrument for polishing the samples. C) Ideal surface between the polished rock and the glass slide with minimal presence of bubbles. D) Euromex iScope series trinocular microscope used for thin section analysis.

3.3 Bulk sediment cleaning and fossil extraction

The cleaning procedure of the 12 semi-consolidated and unconsolidated samples (bulk sediments, see Appendix G) was carried out as follows in the laboratories of Yachay Tech University.

1. Approximately 100 g of each sample was first crushed in a jaw crusher until grains of ~0.5 cm in diameter or less were obtained.
2. Each crushed sample was placed in a 500 ml beaker. Then each beaker was filled with 100 ml of H₂O₂ at 30% concentration. After the solution was added, the samples started to react and water vapor was released from the beaker (Fig. 3.2A). This reaction is exothermic, so the beakers were left in a ventilated place until the reaction had stopped. The H₂O₂ disaggregated the samples and cleaned the silica and carbonate tests of microfossils.
3. The samples were soaked for at least 48 hours. After that, the samples were sieved manually through metal laboratory sieves. Specifically, sieves with standard mesh sizes of 18, 60, and 230 were used (Fig. 3.2B). This sieving process discarded any clay-sized sediment, and the retained sediment contained most of the microfossil content.
4. The sieved (wet) sediment was returned to a beaker and was placed in a laboratory oven at a temperature of about 56 °C for at least 5 hours. When completely dried, the samples were stored in a clearly labeled plastic bag.
5. Before repeating the process with other samples, each container, beaker, and sieve that was in contact with previous samples was covered with a pre-prepared mixture of 1 g methyl blue and 500 ml water (Fig. 3.2C). This mixture was used to clean each container during the following steps to avoid contamination between samples (contaminated microfossils will appear blue during the picking up process and were discarded).
6. Finally, each bag of sediment was examined using a stereomicroscope (Fig. 3.2D) and a Petri dish to collect all the microfossils present. A slightly moistened, fine-tipped brush was used to pick up the microfossils from the plate. The microfossils were then stored in small containers labeled with each sample code.

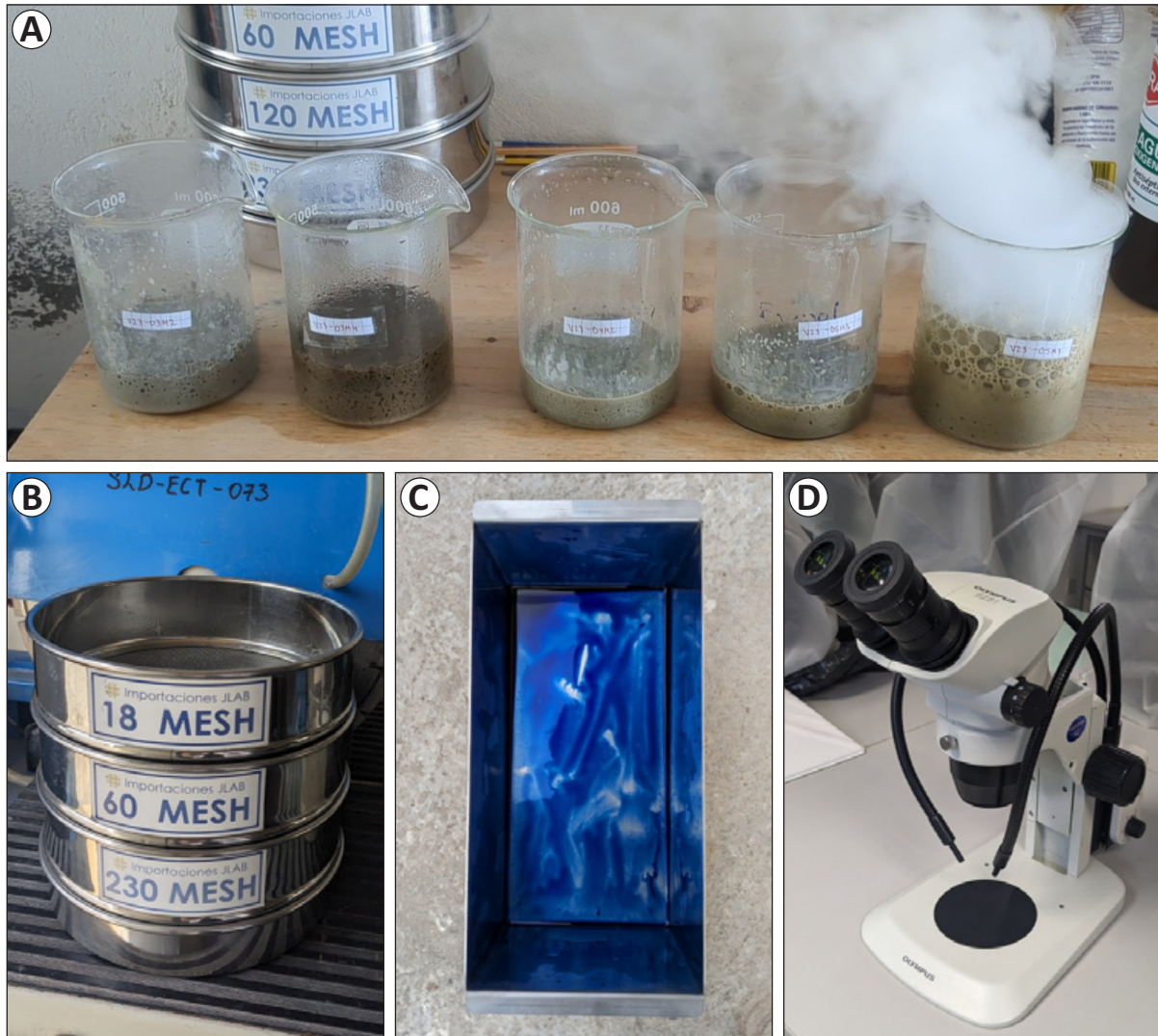


Figure 3.2. Materials available at Yachay Tech University for cleaning bulk sediments, fossil extraction, and analysis. A) Bulk sediments soaking up process with H_2O_2 at 30% concentration showing an exothermic reaction. B) Sieves and their standard mesh sizes used for sieving wet sediments. C) Container covered with a solution of methyl blue to avoid contamination between samples. D) Olympus SZ61 stereomicroscope used to pick up microfossils from bulk sediments.

Chapter 4

Results

The six outcrops studied (see location in Fig. 1.2) belong to the Cayo and Calentura Formations (see Discussion). Along with the lithological data collected in the field, a total of 28 samples were collected: 12 bulk sediment and 16 consolidated rock samples were collected from the selected outcrops (see Appendix G). A rough graphic log was constructed at each site to describe the major lithologies, sedimentary structures, and stratigraphic location of the samples. Paleontological data were obtained from both physical removal of microfossils under a stereomicroscope of the 12 samples of bulk sediments (picking-up technique), and thin section analysis of the 16 rock samples under a petrographic microscope. Consolidated rock samples were also analyzed by thin section to determine the mineral content and rock texture. Three classification schemes were used to classify volcanoclastic (Schmid, 1981), detrital (Folk et al., 1970), and carbonate (Dunham, 1962) sedimentary rocks. Finally, a lithofacies model for the studied lithologies was constructed based on the stratigraphic, petrographic, and paleontological results. The following sections describe the overall results for each outcrop in chronological order, with outcrop 1 being the first visited and outcrop 6 being the last.

4.1 Outcrop 1

Outcrop 1 is located ~6 km east of the town of Guala on the left bank of the Ayampe River (see location on Fig. 1.2). At this location, there is a steep and sparsely vegetated 10 m high and 20 m wide outcrop, E-W oriented, that belongs to the Upper Cayo member (Fig. 5.2). The outcrop has locally fractured and faulted inclined strata oriented N02E, 25NO (Fig. 4.1B). The lithology consist of light brown very fine-grained sandstones, greenish siltstones, and tuffaceous

sandstones. Thin laminations and cross-bedding structures are present throughout the outcrop (Fig. 4.1A). Two samples were collected for thin section preparation (V23-01M1 and V23-01M2, see Appendix G for the coordinates and description of the samples).

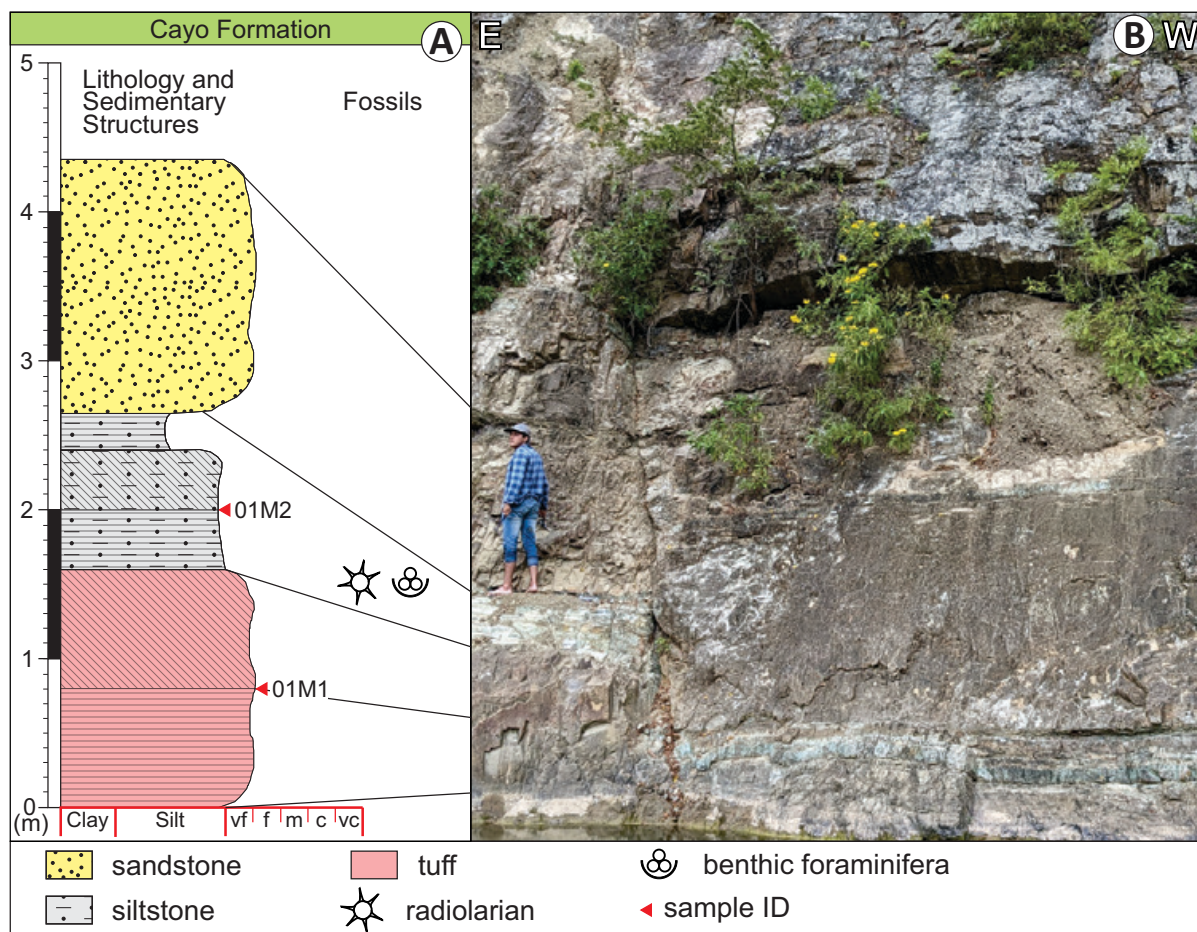


Figure 4.1. A) Graphic log of Outcrop 1 describing the lithology, grain size, sedimentary structures, and sample stratigraphic position (refer to Appendix A for a detailed description). B) Outcrop 1 studied next to the Ayampe River. See location on Fig. 1.2.

Microscopically, the sandstone 01M1 contains angular mineral grains, with the occurrence of highly weathered olivine (5%), subhedral plagioclase (10%), quartz (10%), and fossil fragments (5%) in a glassy matrix (70%). There are also post-depositional alterations such as crystallization of pyrolusite through fractures (Fig. 4.2A). Based these observations, sandstone 01M1 can be classified as a vitric tuff. Siltstone 01M2 shows 2 main textural trends. Most of the rock is matrix-supported with a clayey light-brown matrix (75%) with minor occurrences of quartz, feldspars, and fossil/lithic fragments (25%, Fig. 4.2B), which can be classified as a greywacke. Additionally, towards the top of the sequence there is a textural evolution to clast-supported,

containing a high concentration of fossil fragments and mineral grains (Fig. 4.2C), therefore it is classified as a lithic-arenite.

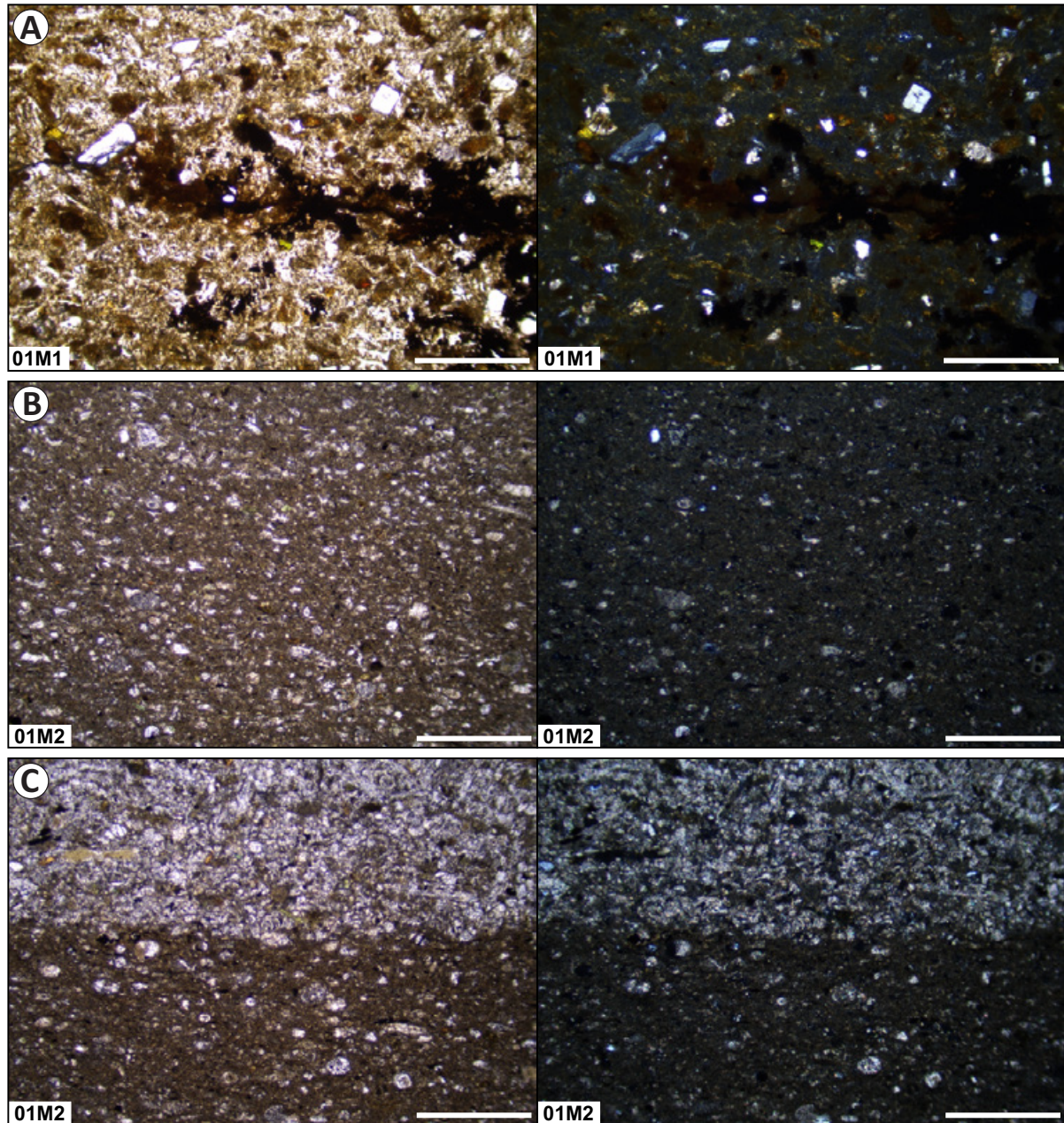


Figure 4.2. Thin sections of rock samples from Outcrop 1 (see stratigraphic location on Fig. 4.1A). The left column is in PPL and the right column is in XPL. The scale bar is 500 μm . A) Vitric tuff with a glassy matrix and pyrolusite infill fractures. B) Greywacke texture with a clayey matrix supporting fossil fragments and mineral grains. C) Textural evolution between greywacke and lithic-arenite with strong increase in calcareous fossil fragments.

4.2 Outcrop 2

Outcrop 2 is located east of the town of Guale, ~500 m east of Outcrop 1 on the right bank of the Ayampe River (see location on Fig. 1.2). In this location there is a steep 12 m high and 20 m wide outcrop, SW-NE oriented, that belongs to the Upper Cayo member (Fig. 5.2). The orientation of the strata is N30E, 25NO. The strata occurring in this outcrop are pale green, very fine grained sandstones, brown micro-conglomerates, and tuffaceous sandstones (Fig. 4.3B). There are several calcite-filled fractures and nodules at the interface and within the beds. There is a minor presence of sedimentary structures of localized thin laminations (Fig. 4.3A). Six rock samples were collected from this site (V23-02M1, V23-02M2a, V23-02M2b, V23-02M2c, V23-02M2d, and V23-02M3, see Appendix G for the coordinates/description of the samples).

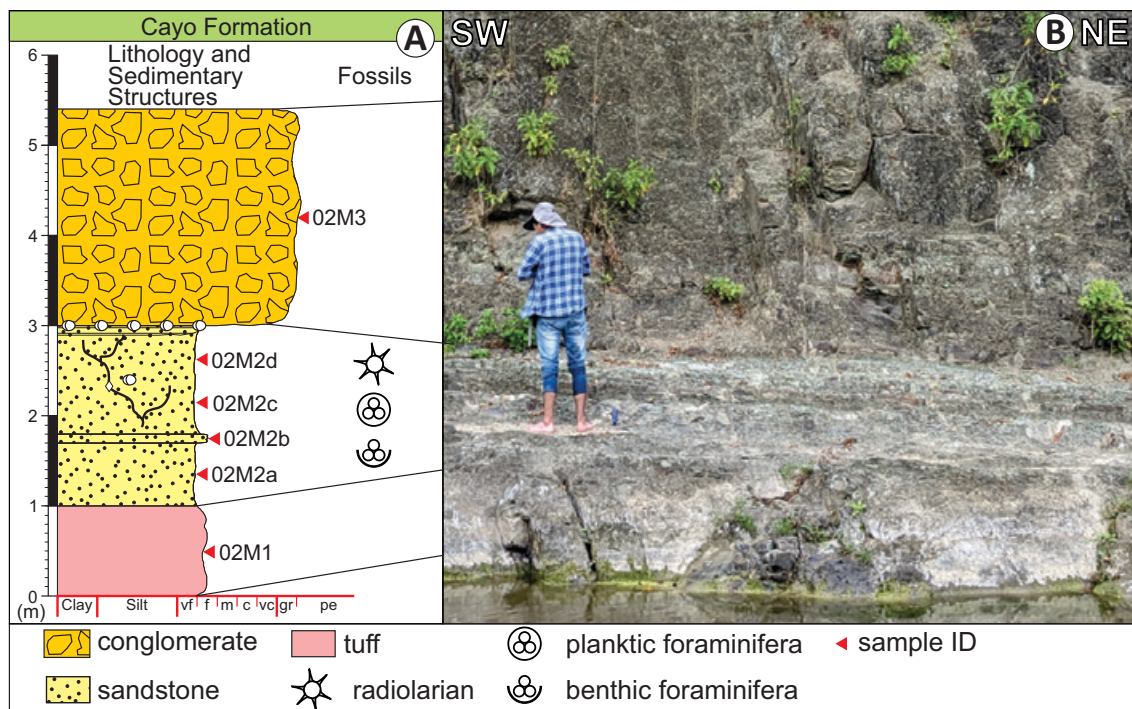


Figure 4.3. A) Graphic log of Outcrop 2 describing the lithology, grain size, sedimentary structures, and sample stratigraphic position (refer to Appendix B for a detailed description). B) Outcrop 2 studied next to the Ayampe River. See location on Fig. 1.2.

Microscopically, sandstone 02M1 has a highly altered glassy matrix (70%), more likely to smectite (yellow patches distributed along the matrix). Mineral grains present are subhedral and anhedral feldspar, olivine, and quartz. The assigned lithology for this sample is a smectite-rich vitric tuff (Fig. 4.4A). Sandstone 02M2, on the other hand, contains a brown clayey matrix (60%) and a moderate content of fossil fragments and planktic foraminifer body fossils (30%)

with a minor occurrence of microscopic mineral grains ($\sim 10\%$). Therefore, sandstone 02M2 is classified as a greywacke (Fig. 4.4B). Finally, conglomerate 02M3 has a matrix-supported texture that contains lithic fragments (10%) and subangular mineral fragments of plagioclase (40%), quartz (20%), olivine (10%), can be classified as a feldspathic microbreccia (Fig. 4.4C). In addition, some post-depositional alteration minerals can be identified such as iddingsite surrounding olivine crystals and smectite crystallization (Fig. 4.6A).

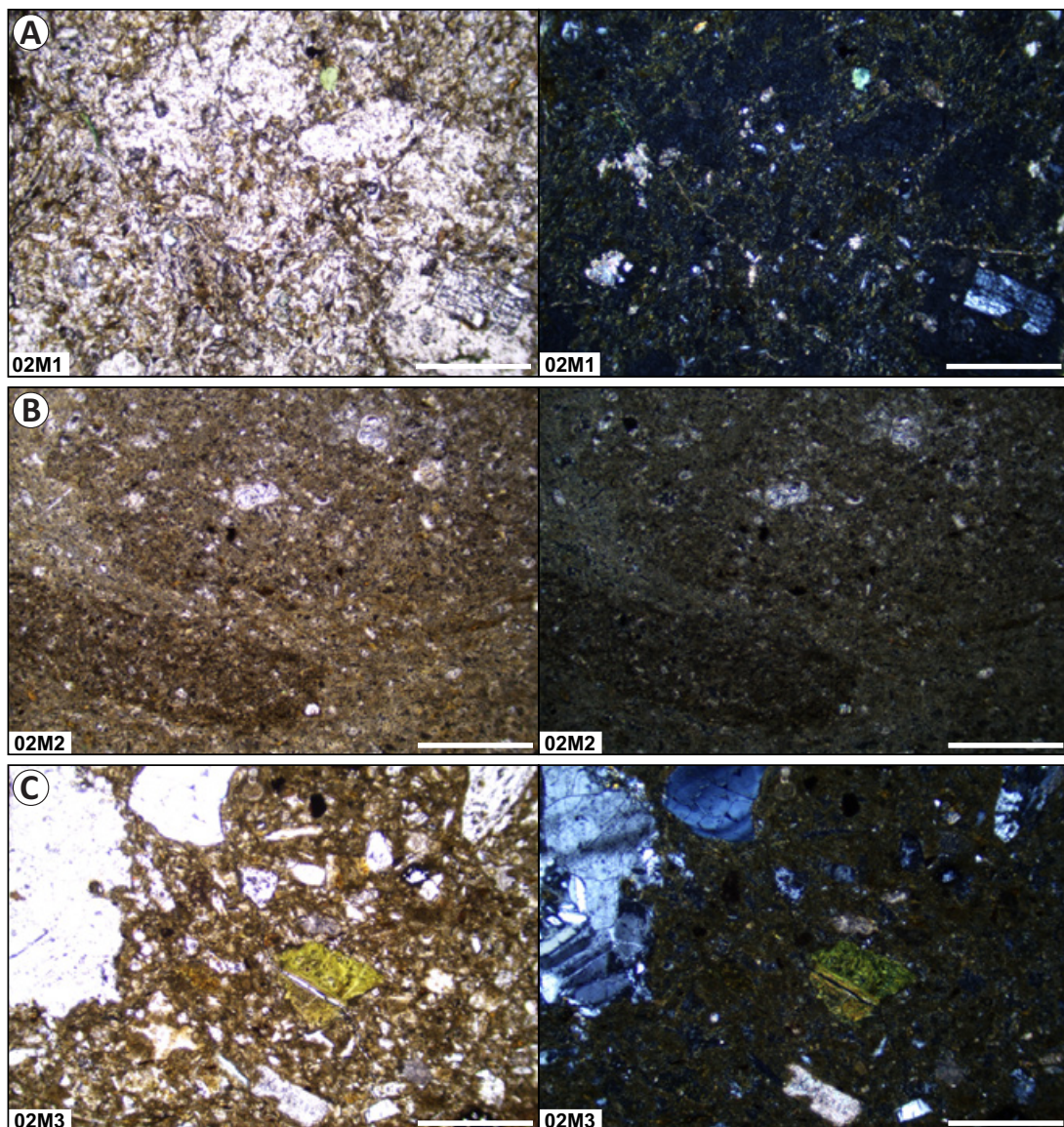


Figure 4.4. Thin sections of rock samples from Outcrop 2 (see stratigraphic location on Fig. 4.3A). The left column is in PPL and the right column is in XPL. The scale bar is $500\ \mu\text{m}$. A) Highly altered smectite-rich silicic tuff with a glassy matrix. B) Greywacke with moderate abundance of planktic foraminifera and fossil fragments. C) Matrix-supported microbreccia with high feldspar content.

4.3 Outcrop 3

Outcrop 3 is located ~300 m west of the confluence of the Ayampe and Blanco Rivers, on the right bank of the Ayampe River (see location on Fig. 1.2). At this location there is a 25 m high and 90 m wide outcrop, W-E oriented, that belongs to the Upper Cayo member (Fig. 5.2). It is composed of cyclic deposits of very fine cream to brown sandstones and siltstones oriented N19E, 49NO (Fig. 4.5B). The beds are mostly massive with some thin laminations near the top of the outcrop (Fig. 4.5A). 4 rock and bulk sediment samples were collected from this outcrop (V23-03M1, V23-03M2, V23-03M3, and V23-03M4, see Appendix G for the coordinates and description of the samples).

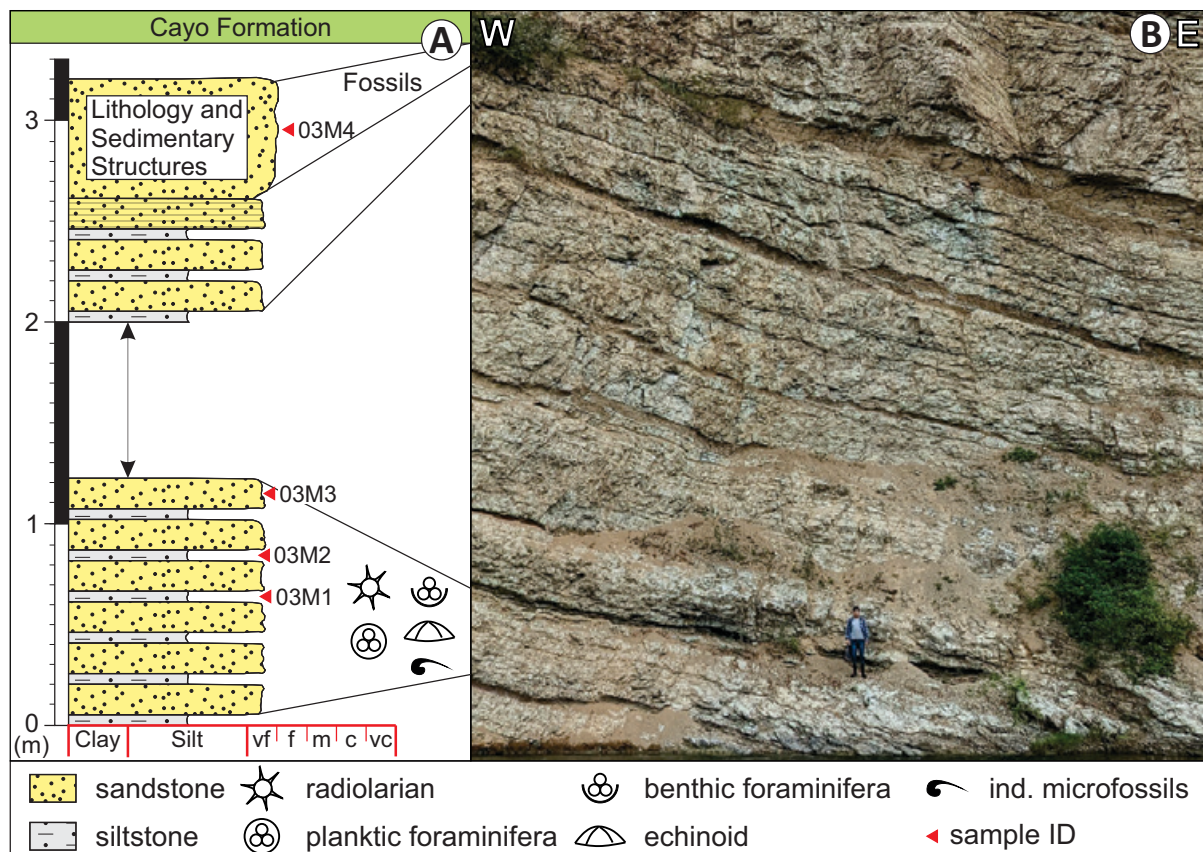


Figure 4.5. A) Graphic log of Outcrop 3 describing the lithology, grain size, sedimentary structures, and sample stratigraphic position (refer to Appendix C for a detailed description). B) Outcrop 3 studied next to the Ayampe River. See location on Fig. 1.2.

Microscopically, sandstone 03M1 has a high fossil content with abundant radiolarians, planktic foraminifera, and other fossil fragments. The texture changes from clast-supported near the

base (less than 5% of clayey tan matrix, Fig. 4.6B) to matrix-supported ($\sim 75\%$) towards the top of the sequence. Several calcite-filled fractures are also present (Fig. 4.6C). This sample is classified as a fossil-rich lithic arenite to greywacke.

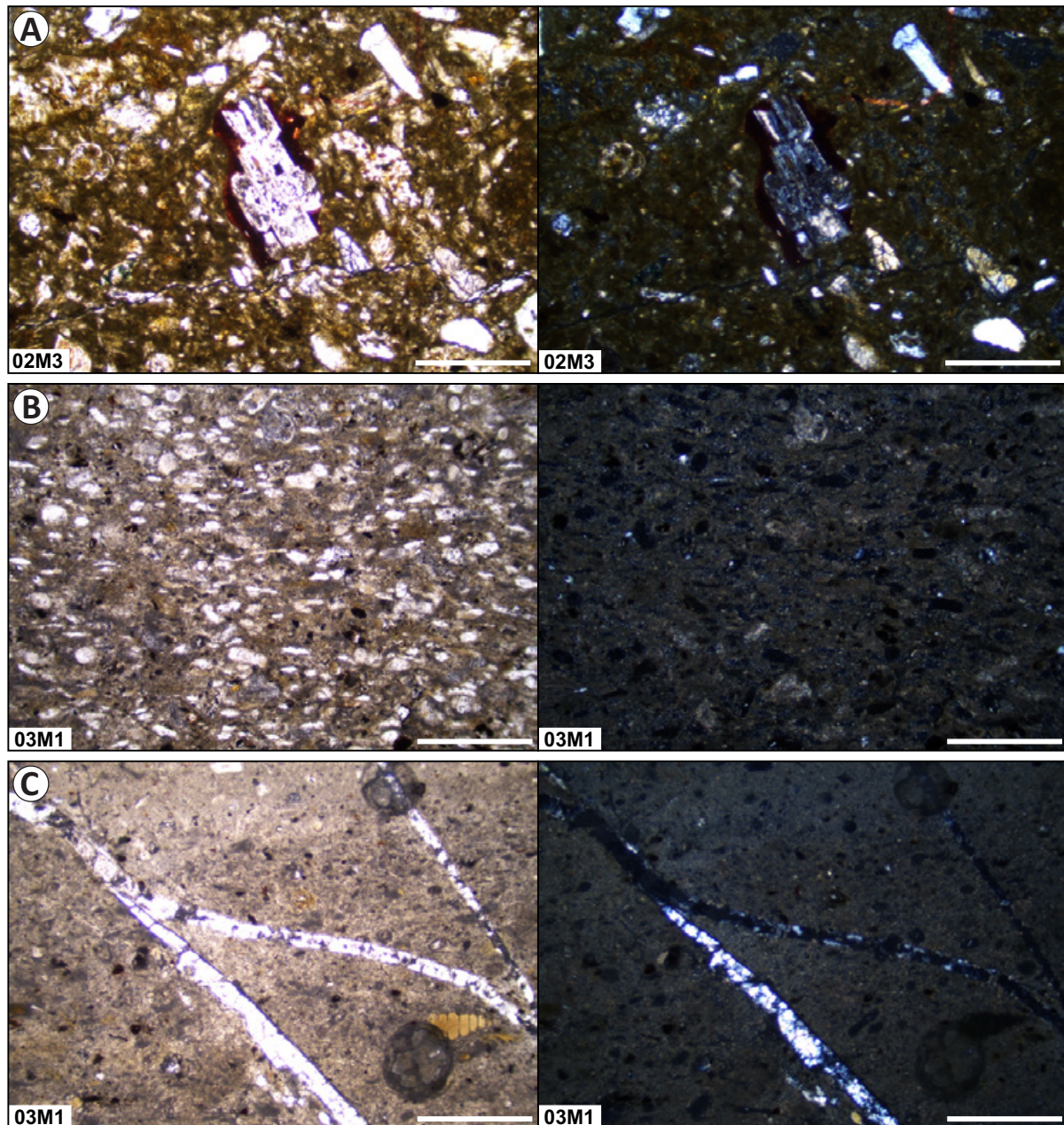


Figure 4.6. Thin sections of rock samples from outcrops 2 and 3 (see stratigraphic location on Fig. 4.3A and Fig. 4.5A). The left column is in PPL and the right column is in XPL. The scale bar is $500 \mu\text{m}$. A) Iddingsite and smectite alteration in an olivine crystal. B) Lithic arenite with abundant radiolarians and planktic foraminifera. C) Greywacke with a brown clayey matrix with the presence of calcite-filled fractures and radiolarians.

4.4 Outcrop 4

Outcrop 4 is located ~100 m west of the confluence of the Ayampe and El Plátano rivers, on the right bank of the Ayampe River (see location on Fig. 1.2). At this location, there is a 9 m high and 30 m wide outcrop, SW-NE oriented, that belongs to the Upper Cayo member (Fig. 5.2). The orientation of the strata is N80E, 35NO and it is composed of light green siltstones, very fine brown sandstones, and clast-supported breccias (Fig. 4.7B). The breccias are separated by a basal erosive surface. Thin laminations are also present (Fig. 4.7A). At this site, three samples were collected for each lithology (V23-04M1, V23-04M2, and V23-04M3, see Appendix G for the coordinates and description of the samples).

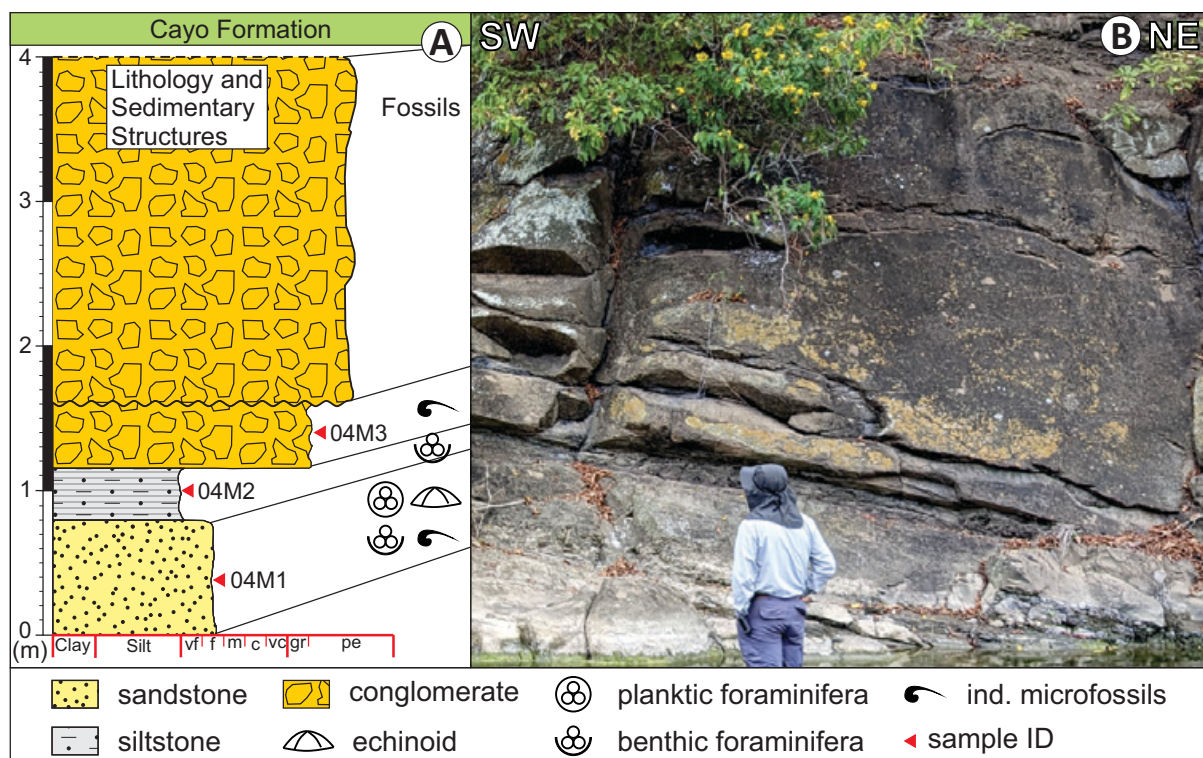


Figure 4.7. A) Graphic log of Outcrop 4 describing the lithology, grain size, sedimentary structures, and sample stratigraphic position (refer to Appendix D for a detailed description). B) Outcrop 4 studied next to the Ayampe River. See location on Fig. 1.2.

Microscopically, sandstone 04M1 contains subrounded mineral grains and lithic fragments. The minerals are mostly olivine and plagioclase (40%), while the lithic fragments are mostly volcanic glass (50%, Fig. 4.8A). This sample corresponds to a litho-feldspathic arenite. Conglomerate 04M3 contains altered glassy dacites and dark-colored lavas (Fig. 4.8B) as well as

subhedral mineral grains of olivine, plagioclase, pyroxene, and quartz (Fig. 4.8C). The surrounding matrix strongly altered to smectite. This sample is classified as a matrix-supported volcanic breccia.

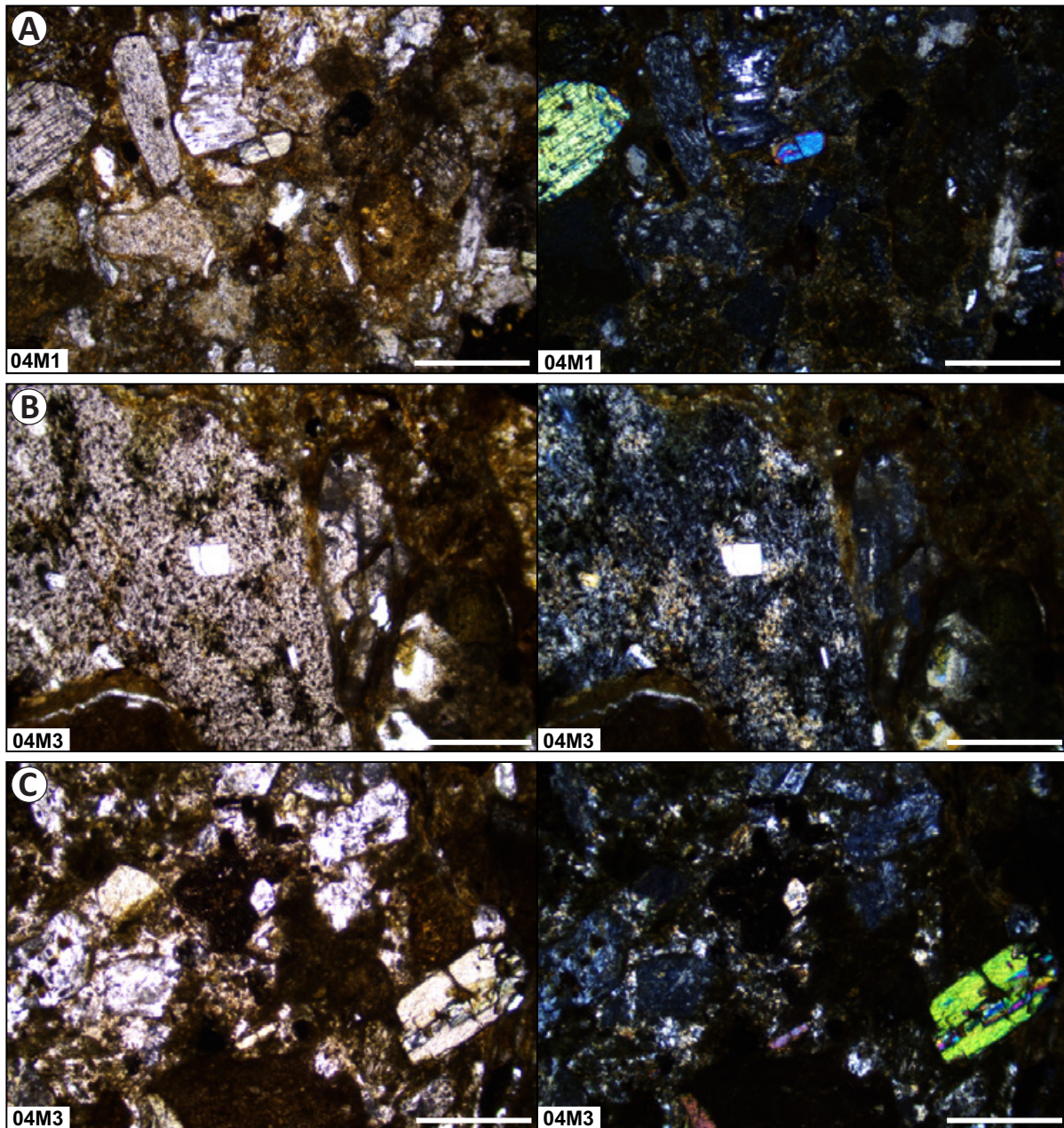


Figure 4.8. Thin sections of rock samples from Outcrop 4 (see stratigraphic location on Fig. 4.7A). The left column is in PPL and the right column is in XPL. The scale bar is 500 μm . A) Olivine, plagioclase and lithic fragments from a litho-feldspathic arenite. B) Altered dacite clasts and dark colored lavas surrounded by a smectitic matrix. C) Matrix-supported volcanic breccia with mineral grains of olivine, plagioclase, pyroxene, and quartz.

4.5 Outcrop 5

Outcrop 5 is located ~2.5 km east of Outcrop 3 and 260 m east of the confluence of the Ayampe and Chico rivers, on the right bank of the Ayampe River (see location on Fig. 1.2). At this location, there is a 8 m high and 9 m wide outcrop SW-NE oriented that belongs to the Lower Cayo member (Fig. 5.2). The orientation of the strata is N14E, 18SE and it is composed of volcanoclastic and sedimentary lithologies. Green and reddish tuffs, interbedded with light-colored siltstones, brown medium sandstones, and greenish microbreccias are the main lithologies found (Fig. 4.9B). Several sedimentary structures can be identified: parallel lamination, planar cross-bedding, wave ripples (Fig. 4.9C), convolutes (Fig. 4.9D), cross-bedding, hummocky cross-stratification and concretions (Fig. 4.9A). From this outcrop, seven rock and bulk sediment samples were collected (V23-05M1, V23-05M2, V23-05M3, V23-05M4, V23-05M6, V23-05M7, and V23-05M8, see Appendix G for the coordinates and description of the samples).

Microscopically, sandstone 05M4 contains a clast-supported texture with a smectite matrix (20%), oxides (20%), feldspars (50%), and a few grains of olivine and quartz (10%, Fig. 4.10A). This corresponds to a smectite-rich arkosic arenite. Sandstone 05M7 contains centimeter-sized crystal fragments of olivine, pyroxene, feldspar and quartz (Fig. 4.10B). The grains are clast-supported with a small amount of vitreous matrix, although some parts are pure matrix with only a few mineral grains (Fig. 4.10C). The lithology attributed to this sandstone is lithic-feldspathic arenite to greywacke.

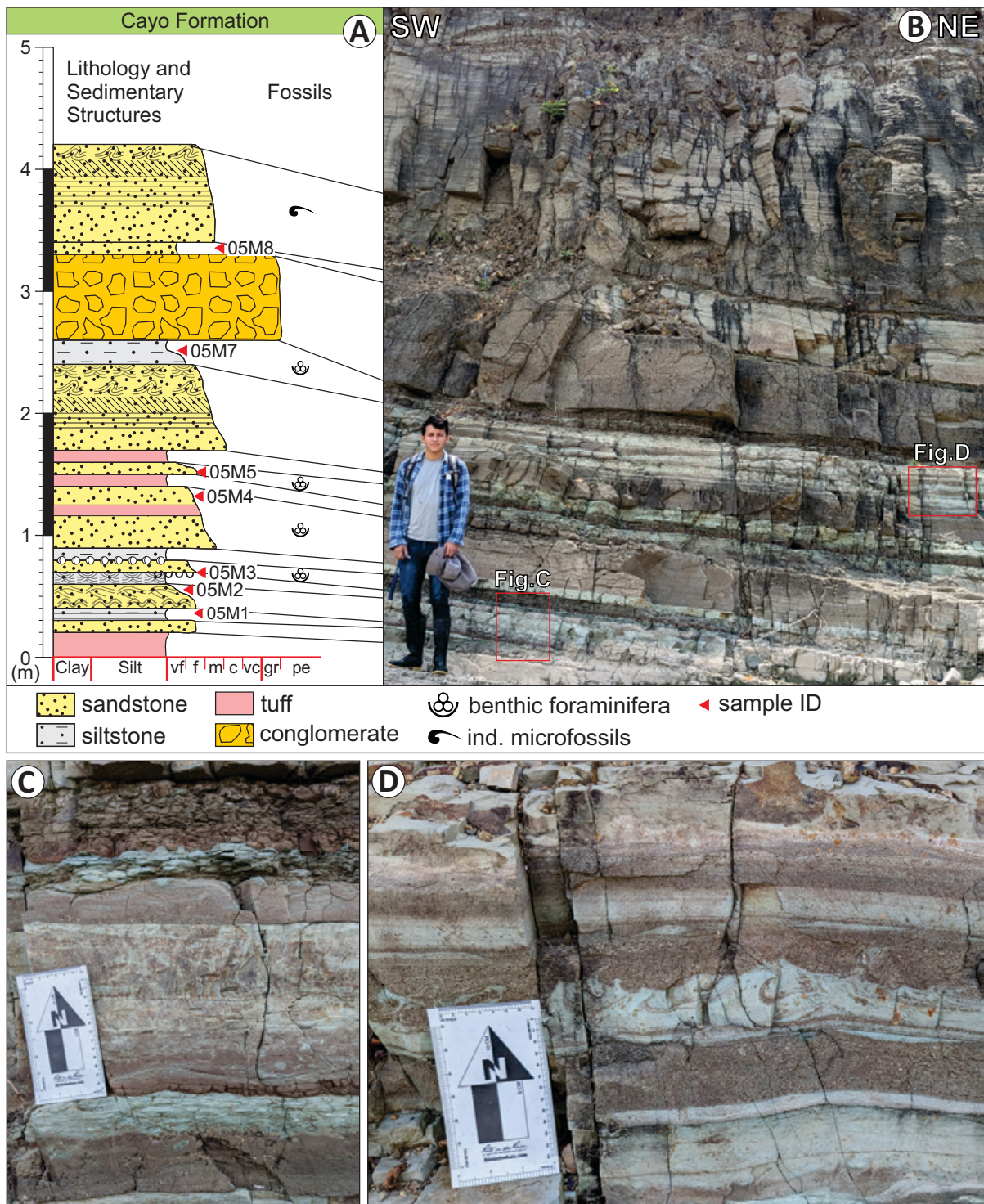


Figure 4.9. A) Graphic log of Outcrop 5 describing the lithology, grain size, sedimentary structures, and sample stratigraphic position (refer to Appendix E for a detailed description). B) Outcrop 5 studied next to the Grande River. See location on Fig. 1.2. C) Close-up showing wave ripples interbedded in cream and brown siltstones. D) Close-up showing convolutes and cross stratification within sandstone deposits.

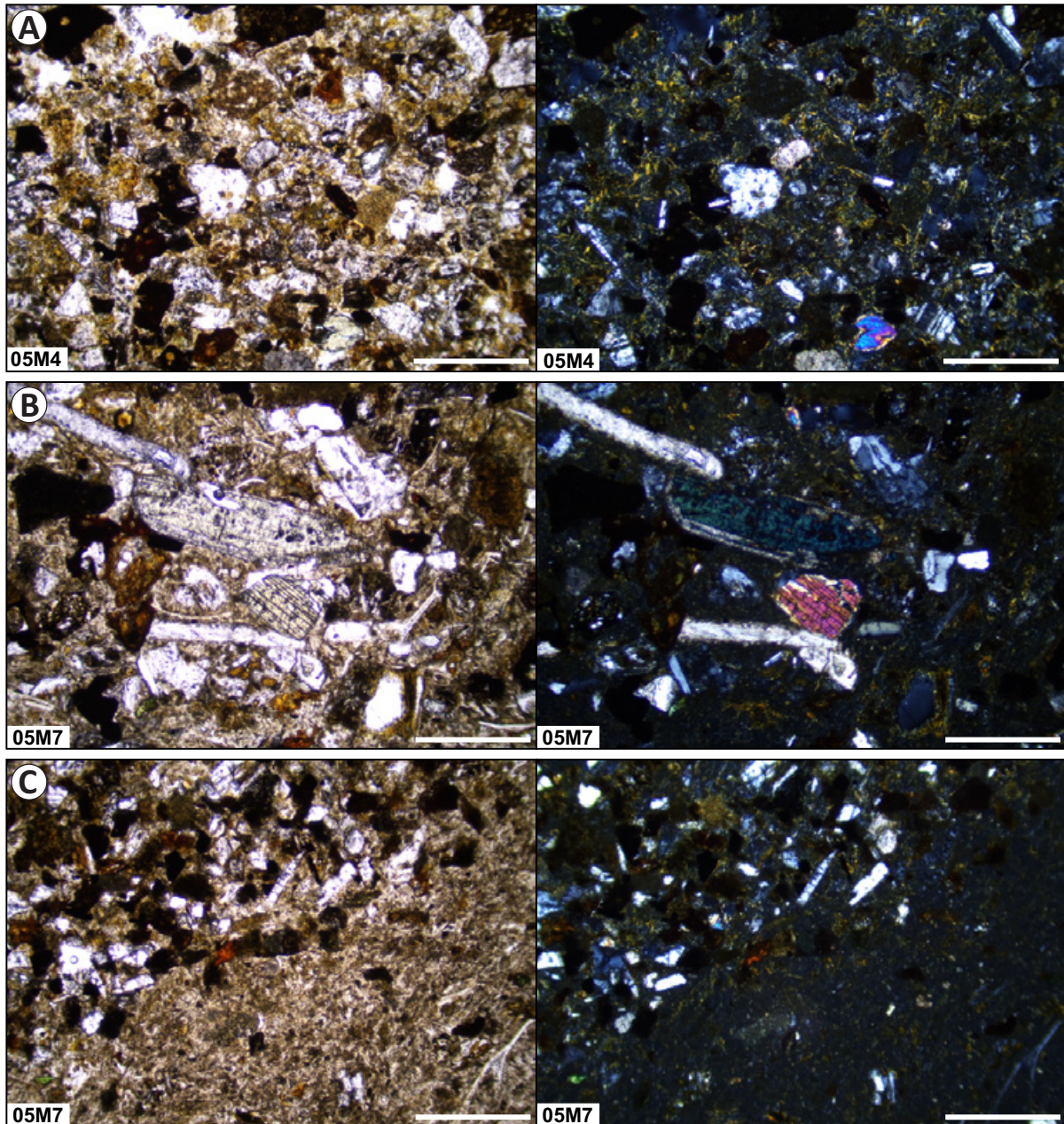


Figure 4.10. Thin sections of rock samples from Outcrop 5 (see stratigraphic location on Fig. 4.9A). The left column is in PPL and the right column is in XPL. The scale bar is 500 μm . A) Arkosic arenite with a glassy matrix strongly altered to smectite. B) Centimeter-sized reworked crystal fragments from a lithic-feldspathic arenite. C) Textural evolution from greywacke to lithic arenite in sandstone 05M7.

4.6 Outcrop 6

Outcrop 6 is located ~2.8 km east of Outcrop 5 and ~80 m north of the confluence of the Grande and Ayampe rivers, on the left bank of the Grande River (see location on Fig. 1.2). At this location, there is a 6 m high and 13 m wide outcrop, N-S oriented, that belongs to the Calentura Formation (Fig. 5.2). In this outcrop, several layers of calcareous rocks oriented N05O, 25NE can be identified (Fig. 4.11B). The rocks correspond to shales that appear black externally, although they are gray to cream in fresh surface. They are composed entirely of a micritic matrix, although some calcite lenses can be identified within the rocks (Fig. 4.11A). At this outcrop, 6 rock samples were collected for thin section preparation (V23-06M1, V23-06M2, V23-06M3, V23-06M4, V23-06M5, and V23-06M6, see Appendix G for the coordinates and description of the samples).

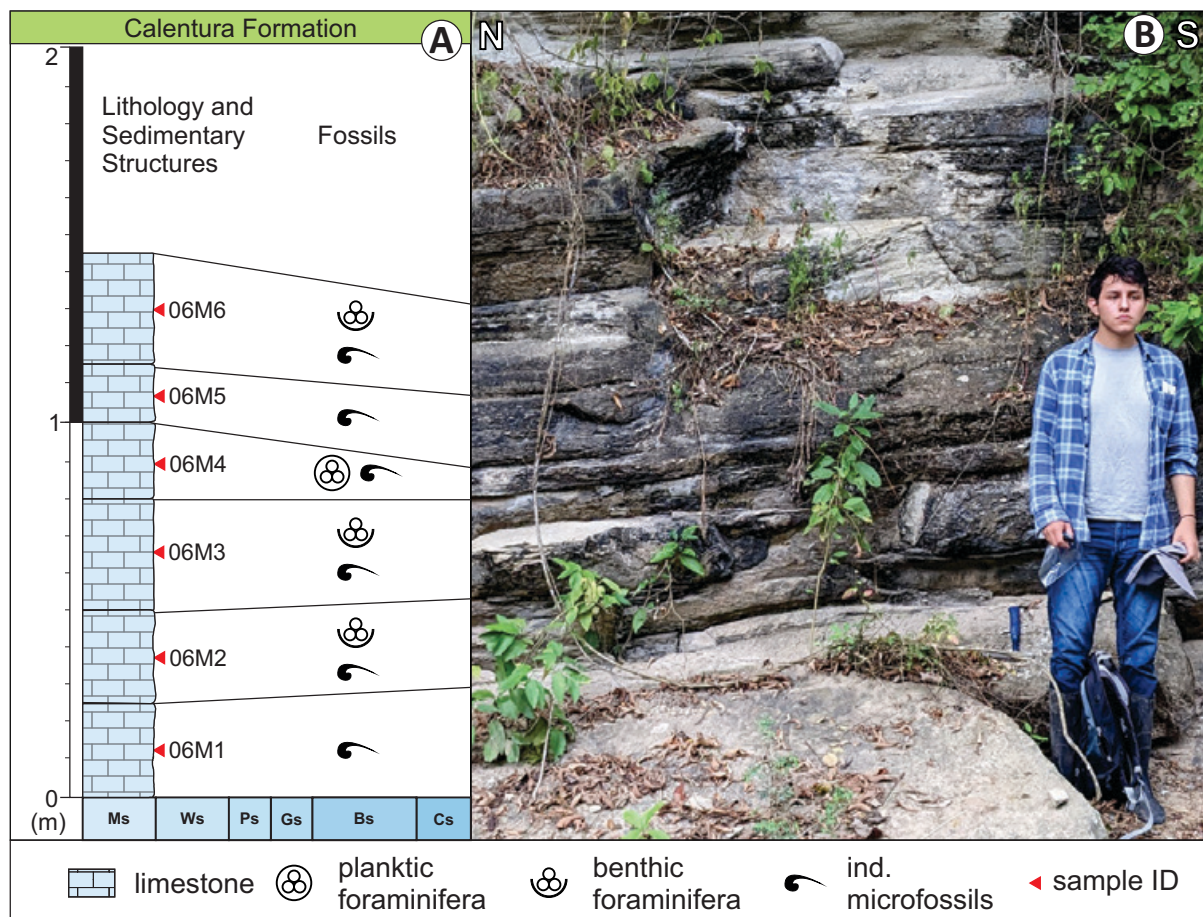


Figure 4.11. A) Graphic log of Outcrop 6 describing the lithology, grain size, sedimentary structures, and sample stratigraphic position (refer to Appendix F for a detailed description). B) Outcrop 6 studied next to the Grande River. See location on Fig. 1.2.

Microscopically, the calcareous rocks from Outcrop 6 consist of a micritic matrix (90%) that supports a few fragments and body fossils (10%, Fig. 4.10A and B). Although some parts of the rock have suffered chertification with some patches of microcrystalline quartz (Fig. 4.12C). These rock sequences are classified as carbonate mudstones.

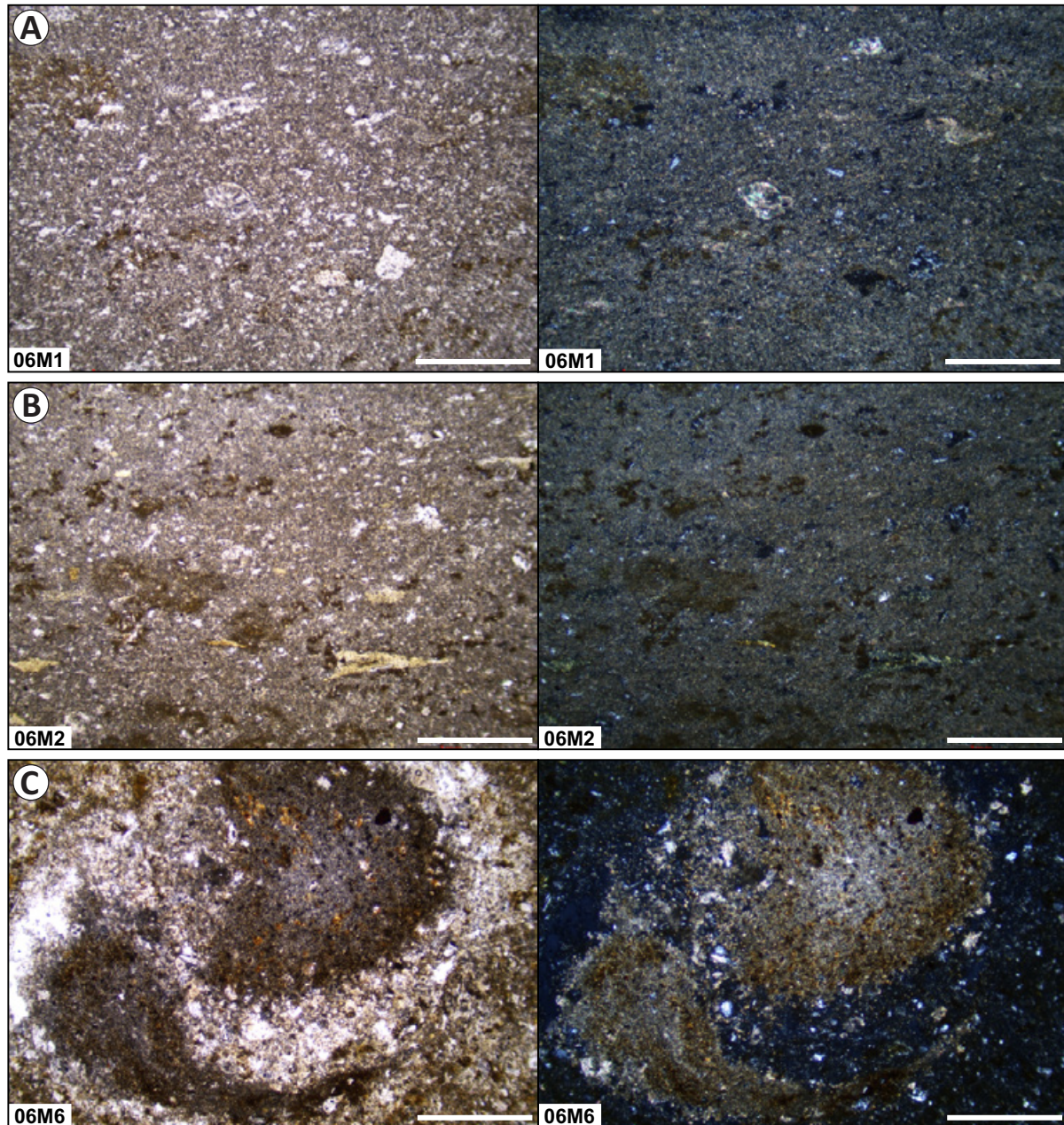


Figure 4.12. Thin sections of rock samples from Outcrop 6 (see stratigraphic location on Fig. 4.11A). The left column is in PPL and the right column is in XPL. The scale bar is 500 μm . A) and B) is the representative texture of carbonate mudstone rocks at Outcrop 6 containing fossil fragments in a micritic matrix. C) Carbonate chertification with microcrystalline quartz.

4.7 Paleontological results

A total of 171 fossil specimens/fragments were identified from bulk sediments (25) and thin sections (146). From these specimens, 13 fossil genera/species were recognized (see Table 4.1). The morphological description of each genus/species is detailed in the following sections.

Table 4.1: List of fossils identified in this study and their occurrence at each selected outcrop. See location of each outcrop in Fig. 1.2. See samples codes and coordinates in Appendix G.

Fossil Species Identified	Outcrop					
	1	2	3	4	5	6
Radiolaria						
<i>Dictyomitra multicostata</i> (Zittel)	x	x	x			
<i>Stylospongia planoconvexa</i> (Pessagno)	x		x			
Planktic foraminifera						
<i>Heterohelix</i> sp. (Ehrenberg)		x		x		x
<i>Globotruncana</i> sp. (Reiss)			x			
Benthic foraminifera						
<i>Nodosaria</i> sp. (Lamarck)	x	x	x	x	x	x
<i>Cibicides</i> sp. (Montfort)		x	x	x	x	x
<i>Cibicides subcarinatus</i> (Cushman & Deaderick)					x	
<i>Lagena</i> sp. (Walker & Jacob)			x			
<i>Gyroidinoides</i> sp. (Brotzen)					x	
<i>Hormosinella ovolum</i> (Grzybowski)			x			
<i>Praebulimina</i> sp. (Hofker)			x		x	
<i>Ellipsoglandulina</i> sp. (Silvestri)			x	x		
Echinoids				x		
Siliceous fossil fragments					x	

4.7.1 Radiolarians

Radiolarians are planktonic species that are useful to monitor past climates and environments. The identified specimens of Nasellarian and Spumellarian order (see Fig. 2.7) are described below.

Order Nassellaria
 Family Archaeodictyomitridae
 Genus *Dictyomitra*
Dictyomitra multicostata Zittel

Fig. 4.13

Description.- A single conical to subcylindrical shell (depending on the direction of the section) can be identified. The longitudinal section has an average length between 260-330 μm . The shell is divided into 9 to 10 segments that increase to a maximum diameter of 130 μm in transverse section. The length of each segment increases regularly. The outer surface of the shell is relatively smooth with the presence of depressions at each segment division.

Environment.- Marine.

Age range.- Lower Berriasian to Lower Paleocene (O'Dogherty et al., 2009).

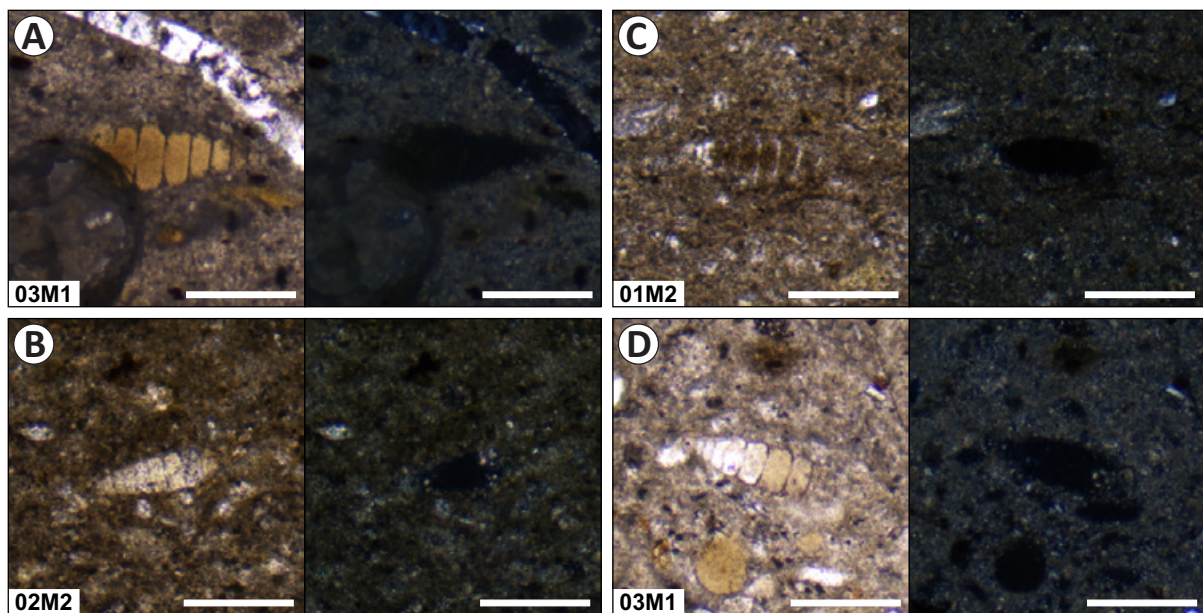


Figure 4.13. Fossil specimens of Nassellaria radiolarians. The left column is in PPL and the right column is in XPL. The scale bar is 200 μm and the magnification is 100x. A-C) *Dictyomitra multicostata*, longitudinal section. D) *Dictyomitra multicostata*, longitudinal and transverse sections.

Order Spumellaria
 Family Sponguridae
 Genus *Patellula*

Stylospongia planoconvexa Pessagno

Fig. 4.14

Description.- The basal section consists of a circular test containing a set of 8 to 10 equally spaced concentric layers and several less pronounced radiating lines from its center. The diameter of the shell is between 100-200 μm . In sections near the top of the fossil, the diameter decreases and the concentric layers become less pronounced, while a cross-shaped structure can be identified instead (as shown in Fig. 4.14B and D).

Environment.- Marine.

Age range.- Lower Cenomanian to Upper Campanian (O'Dogherty et al., 2009).

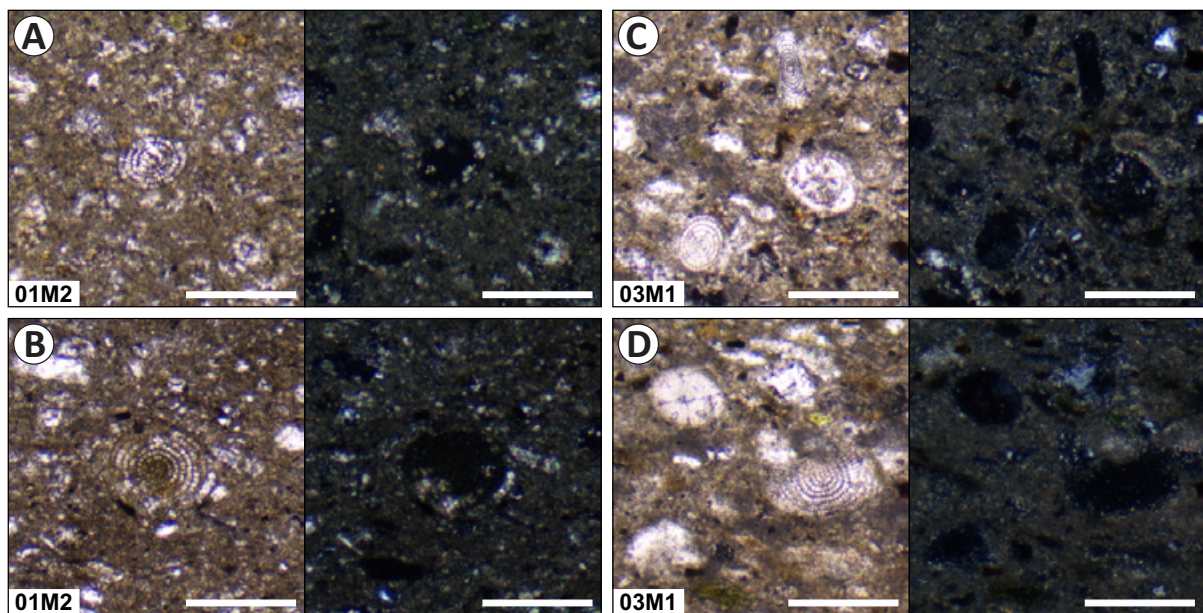


Figure 4.14. Fossil specimens of Spumellaria radiolarians. The left column is in PPL and the right column is in XPL. The scale bar is 200 μm and the magnification is 100x. A-B) *Stylospongia planoconvexa*, transverse section. C-D) Several transverse sections of *Stylospongia planoconvexa* and *Stylospongia* sp.

4.7.2 Planktic Foraminifera

Planktic species of foraminifera are the most important for biostratigraphic applications, being indispensable for relative dating. The identified specimens of the orders Rotaliida and Globotruncanida are described below.

Order Rotaliida

Family Heterohelicidae

Genus *Heterohelix*

Heterohelix sp. Ehrenberg

Fig. 4.15

Description.- Longitudinal sections (Fig. 4.15A-B) have a subtriangular outline with a height between 325-400 μm and a maximum width of 200 μm . It is composed of globular to ovoid shaped chambers arranged biserially and regularly increasing in size. Transverse sections (Fig. 4.15C-D) show a pair of circular chambers with a plane suture, each chamber having a diameter of about 100 μm . The wall composition is calcareous and/or sparitic.

Environment.- Marine.

Age range.- Upper Cretaceous (Santonian to Campanian, [Loeblich and Tappan, 1988](#)).

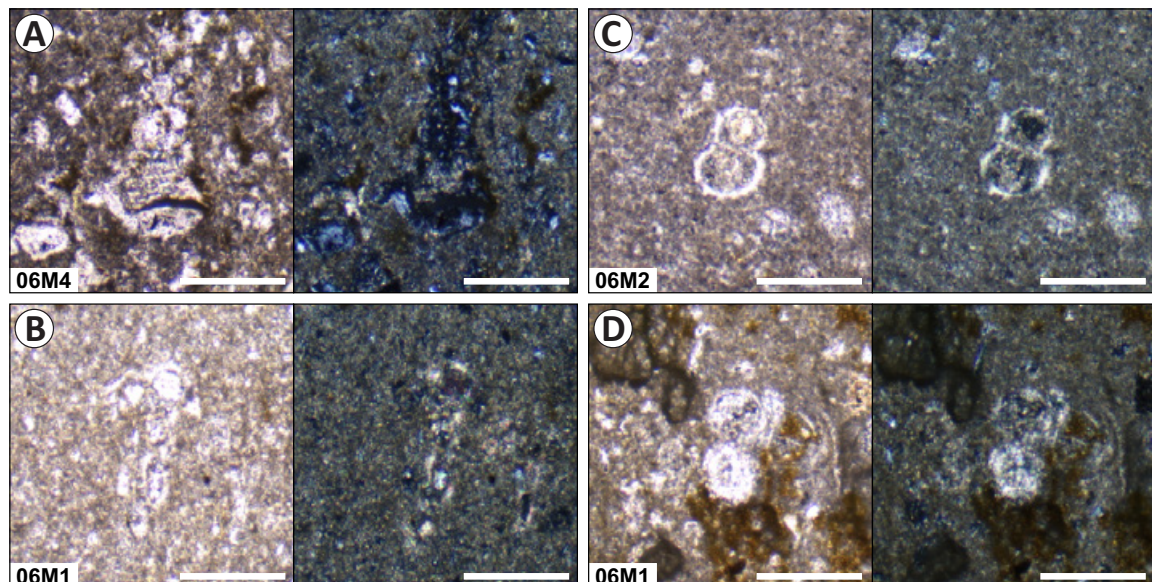


Figure 4.15. Fossil specimens of planktic foraminifera. The left column is in PPL and the right column is in XPL. The scale bar is 200 μm and the magnification is 100x. A-B) *Heterohelix* sp., longitudinal section. C-D) *Heterohelix* sp., transverse section.

Order Globotruncanida
Family Globotruncanidae
Genus *Globotruncana*
Globotruncana sp. Reiss

Fig. 4.16

Description.- Trochospiral test composed of 6 to 8 chambers that regularly increase in size. The shape of the chambers may be ovate to oblong and thick-walled. The sutures are angular and slightly curved and the umbilicus is narrowly arranged in a spiral system. The diameter ranges from 130-470 μm .

Environment.- Marine.

Age range.- Lower Jurassic to Holocene (Loeblich and Tappan, 1988).

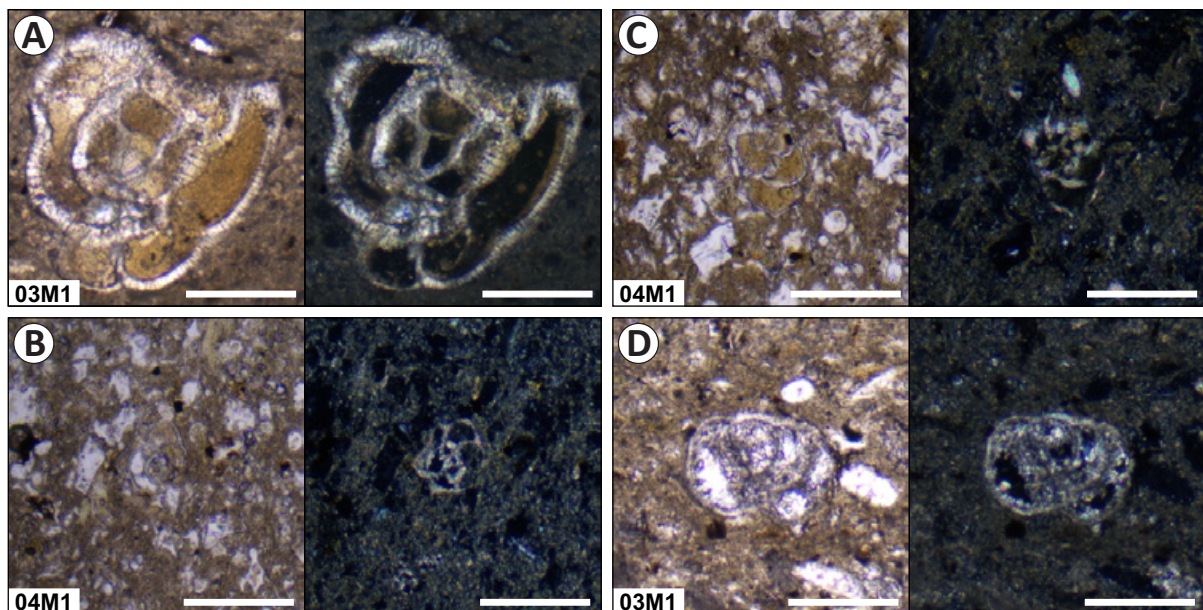


Figure 4.16. Fossil specimens of planktic foraminifera. The left column is in PPL and the right column is in XPL. The scale bar is 200 μm and the magnification is 100x. A-D) *Globotruncana* sp., transverse section.

4.7.3 Benthic Foraminifera

Benthic species of foraminifera are sensitive to changes in temperature, salinity, and nutrient availability, therefore they are important environmental indicators. The identified specimens of the orders Nodosariida, Rotaliida, Hormosinina, and Polymorphinida are described below.

Order Nodosariida

Family Nodosariidae

Genus *Nodosaria*

Nodosaria sp. Lamarck

Fig. 4.17 & Fig. 4.18

Description.- Tests are multilocular, uniserially arranged. Single-chamber arrangements are most common (Fig. 4.17C-D) and (Fig. 4.18B-D), although 2-chamber (Fig. 4.18A) or 3-chamber (Fig. 4.17A) arrangements can also be found. The overall shape of the individual chambers is ovate to globular and the dimensions are very variable with diameters ranging from 40-1000 μ . The wall composition is calcareous, hyaline, or agglutinated with a generally smooth surface without ornamentation. Fragments of broken chambers are usually attached to the specimens.

Environment.- Marine.

Age range.- Lower Jurassic to Holocene (Loeblich and Tappan, 1988).

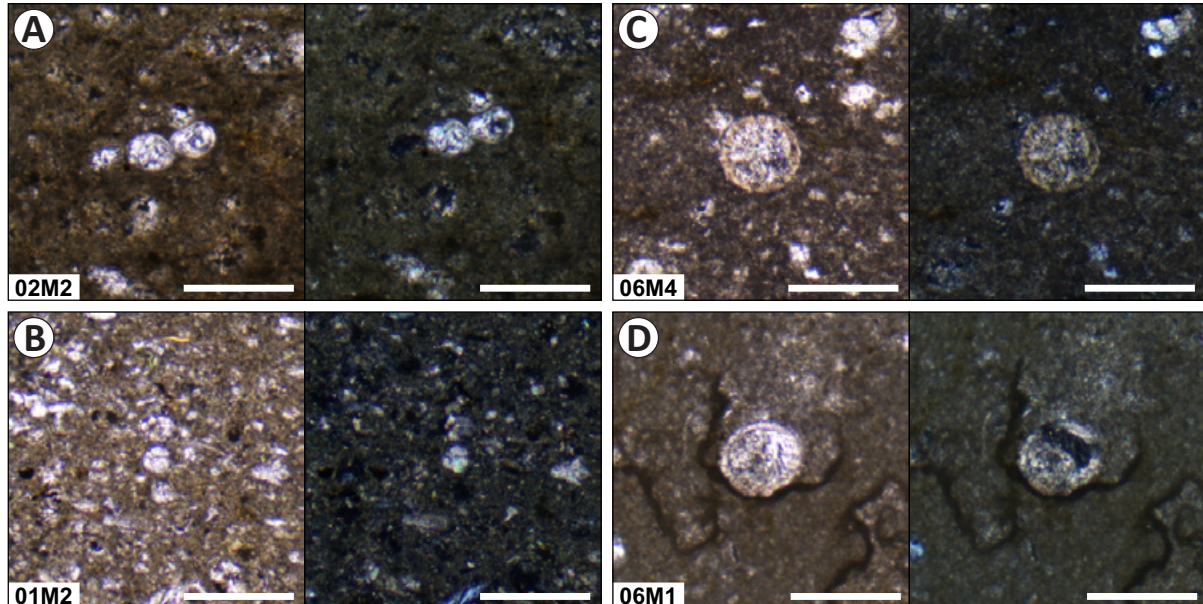


Figure 4.17. Fossil specimens of benthic foraminifera. The left column is in PPL and the right column is in XPL. The scale bar is 200 μ m and the magnification is 100x. A-B) *Nodosaria* sp., longitudinal section. C-D) *Nodosaria* sp., transverse section.

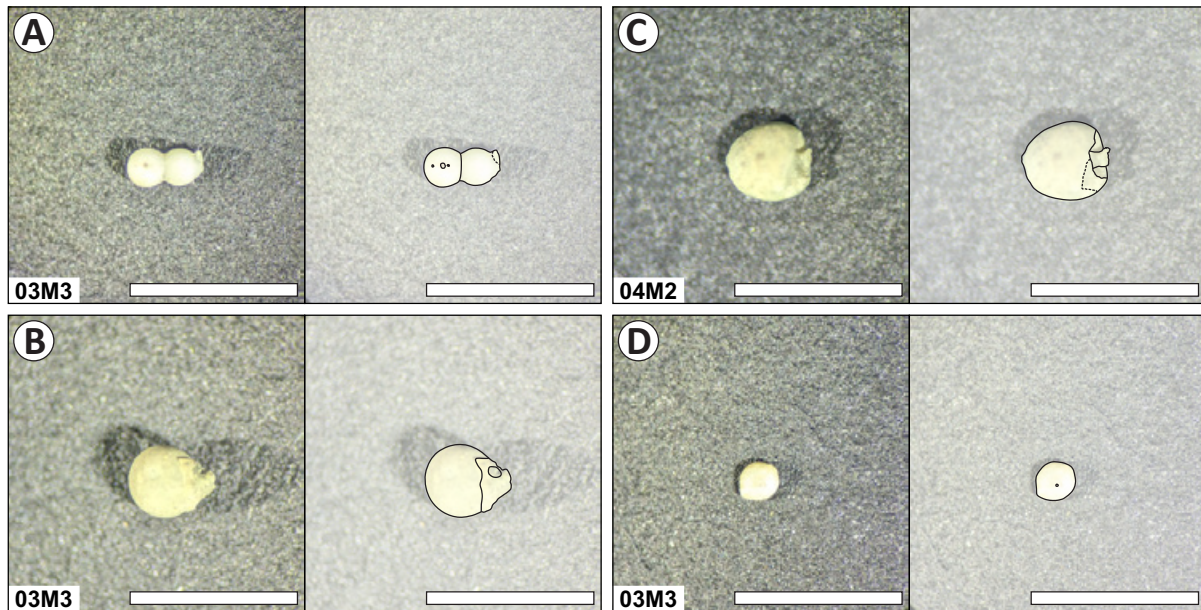


Figure 4.18. Fossil specimens of benthic foraminifera highlighting the main visible features. Images taken with an Olympus SZ61 stereomicroscope. The scale bar is 2 mm and the magnification is 45x. A) *Nodosaria* sp., 2 uniserial chambers. B-D) *Nodosaria* sp., single chambers.

Order Rotaliida

Family Cibicididae

Genus *Cibicides*

Cibicides sp. Montfort

Fig. 4.19 & Fig. 4.20A

Description.- The tests are trochospiral (chambers form a snail-like shell) with an evelute coil (Fig. 2.5). The umbilical coil is visible (involute). The wall composition is calcareous and the crystal size may be sparitic (Fig. 4.19A) or micritic (Fig. 4.19A). The wall thickness increases towards the outer chambers. The outline is ovate and smooth without ornamentation. The dimensions are about 250 μm high and 150 μm wide.

Environment.- Marine.

Age range.- Cretaceous to Holocene (Loeblich and Tappan, 1988).

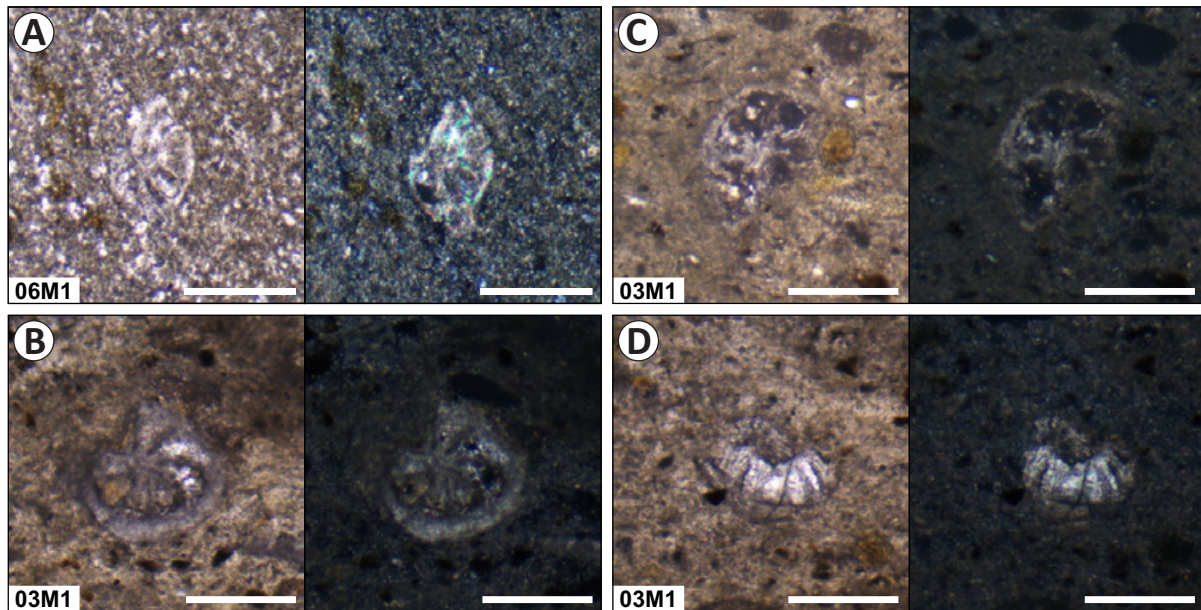


Figure 4.19. Fossil specimens of benthic foraminifera. The left column is in PPL and the right column is in XPL. The scale bar is 200 μm and the magnification is 100x. A) *Cibicides* sp., transverse section showing sparitic composition in XPL. B-C) *Cibicides* sp., transverse section and calcareous composition. D) *Cibicides* sp., dorsal view, the test is broken or dissolved.

Order Rotaliida

Family Cibicididae

Genus *Cibicides*

Cibicides subcarinatus Cushman & Deaderick

Fig. 4.20A

Description.- Calcareous perforated test trochospiral with evolute coil on spiral side. Consists of numerous chambers (8 to 9) with curved sutures. The shell is 0.65 mm high and 0.55 mm thick. The outline is ovate and smooth except for the last chamber which is prominent.

Environment.- Marine.

Age range.- Upper Albian to Maastrichtian (Ordoñez, 2006).

Order Nodosariida

Family Lagenidae

Genus *Lagena*

Lagena sp. Walker & Jacob

Fig. 4.20B

Description.- Unilocular test flask, globular to ovoid in shape with a prominent neck. The base has evenly spaced longitudinal striations. The shell is 1 mm in height and 0.8 mm in diameter.

Environment.- Marine.

Age range.- Lower Jurassic (Pliensbachian) to Holocene ([Loeblich and Tappan, 1988](#)).

Order Rotaliida

Family Cancrisidae

Genus *Gyroidinoides*

Gyroidinoides sp. Brotzen

Fig. 4.20C

Description.- Trochospiral test with evolute coil consisting of 6 to 7 seven chambers with radially curved sutures and convex involute umbilical side. The contour is rounded and smooth with a diameter of 0.7 mm.

Environment.- Marine.

Age range.- Upper Cretaceous (Cenomanian) to Holocene ([Loeblich and Tappan, 1988](#)).

Suborder Hormosinina

Family Hormosinellidae

Genus *Hormosinella*

Hormosinella ovolum Grzybowski

Fig. 4.20D

Description.- Uniserial test with ovate chambers separated by a short neck and a length of 1mm. Rounded and smooth surface.

Environment.- Marine.

Age range.- Santonian to Lower Eocene ([Bolli et al., 1994](#)).

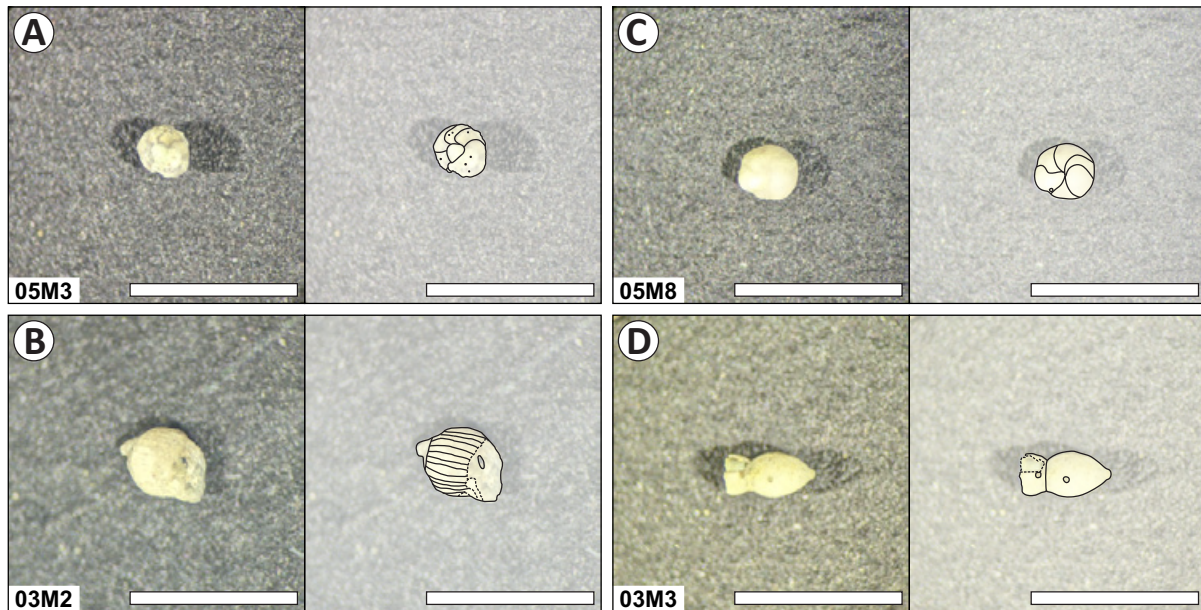


Figure 4.20. Fossil specimens of benthic foraminifera highlighting the main visible features. Images taken with an Olympus SZ61 stereomicroscope. The scale bar is 2 mm and the magnification is 45x. A) *Cibicides subcarinatus*. B) *Lagena* sp. C) *Gyroidinoides* sp. D) *Hormosinella ovolum*.

Order Rotaliida

Family Turrilinidae

Genus *Praebulimina*

Praebulimina sp. Hofker

Fig. 4.21A-C

Description.- Triserial test with poorly visible sutures. The length of the test is approximately 1 mm. Consists of ovoid inflated chambers with a smooth surface. The opening is visible at the end of the last chamber.

Environment.- Marine.

Age range.- Middle Jurassic (Bathonian) to Upper Cretaceous (Maastrichtian, [Loeblich and Tappan, 1988](#)).

Order Polymorphinida

Family Ellipsoidinidae

Genus *Ellipsoglandulina**Ellipsoglandulina* sp. Silvestri

Fig. 4.21D

Description.- Uniserial ovate test with overlapping chambers that increase greatly in size with the last chamber being two-thirds of the test length. The suture of the chambers is flat and nearly horizontal. The thickness of the test is 1.8 mm and has a smooth surface.

Environment.- Marine.

Age range.- Turonian to Holocene (Loeblich and Tappan, 1988).

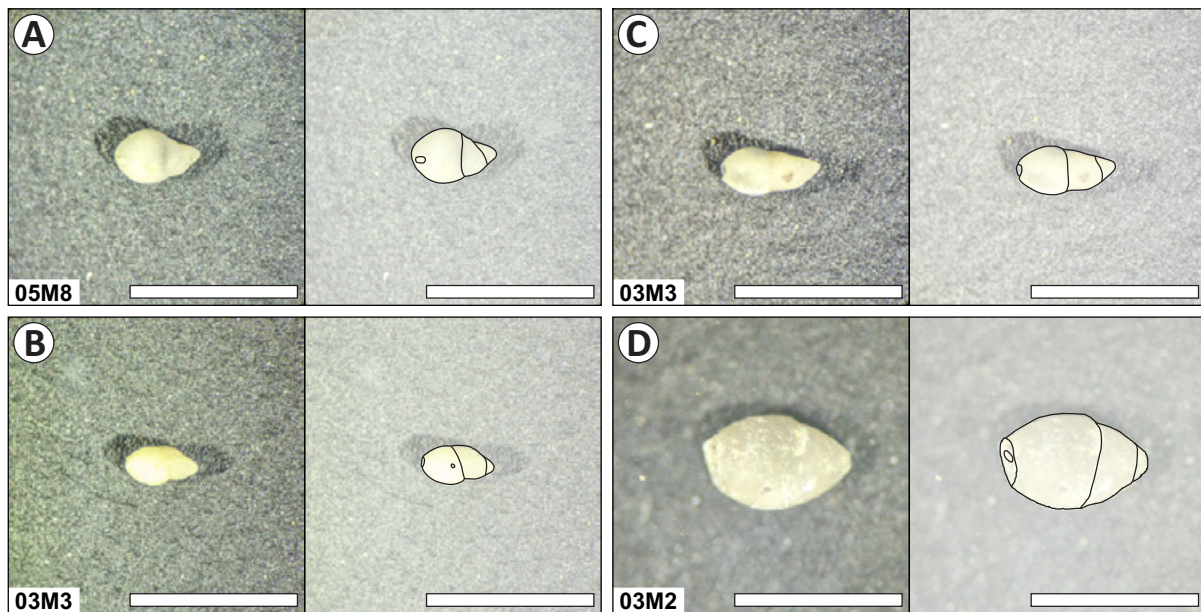


Figure 4.21. Fossil specimens of benthic foraminifera highlighting the main visible features. The scale bar is 2 mm and the magnification is 45x. A-C) *Praebulimina* sp. D) *Ellipsoglandulina* sp.

4.7.4 Other fossils

Echinoderms are widespread species that occur throughout the fossil record. In general, fragments of spicules and plates are easily recognizable. The identified fossil fragments of echinoids and other species are listed below.

Echinodermata Phylum

Echinoidea Class

Echinoids Fig. 4.22

Description.- Sparitic (Fig. 4.22A) or micritic (Fig. 4.22B) composition. Some morphologies are perforated with regularly arranged radial structures. Other structures show thick-walled segments infilled with contrasting material in small pores. The outline is ovate and can vary greatly in size. Dimensions range from 200-500 μm in diameter.

Environment.- Marine, deep-marine (Scholle and Ulmer-Scholle, 2003).

Age range.- Lower Ordovician to Holocene (Scholle and Ulmer-Scholle, 2003).

In addition, siliceous fossil fragments, more likely derived from radiolarian skeletons or echinoid/sponge spicules, are scattered throughout the rocks found at Outcrop 5 (Fig. 4.22 C-D).

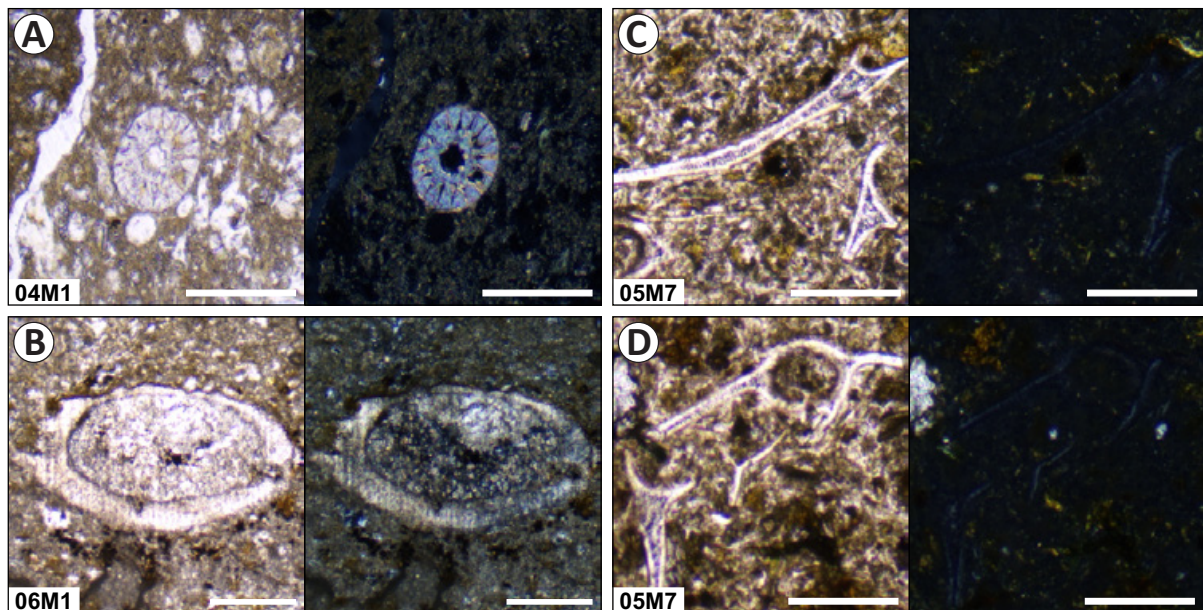


Figure 4.22. Echinoid fossils and other fragments. The left column is in PPL and the right column is in XPL. The scale bar is 200 μm and the magnification is 100x. A) Echinoid sample with sparitic composition and radial structures. B) Echinoid sample with calcareous composition and pore filled structures. C-D) Siliceous fossil fragments and spicules.

Chapter 5

Discussion

5.1 Lithofacies model

Based on petrographic and paleontological results, 10 different lithofacies of volcanoclastic and hemipelagic (i.e., terrigenous and pelagic sediments) origin have been identified (see Table 5.1). The volcanoclastic lithofacies are: (1)(Sm) poorly sorted, massive volcanoclastic sandstones, (2)(Cm) poorly sorted, subangular volcanic clasts, massive breccias, (3)(Tm, Th, Tc) massive, parallel- or cross-laminated very fine silicic tuff, and (4)(Tv) massive, vitreous-smectite matrix, fine silicic tuff. These lithofacies are characterized by a high content of mafic mineral grains and little or no fossil content. Therefore, it has been interpreted that these lithofacies were deposited in an environment of high energy, high sediment input, and rapid sediment deposition proximal to the volcanic sedimentary source. A possible cause of zeolitization in the Cayo Formation was proposed by [Machiels et al. \(2014\)](#), mainly attributed the interaction of hot volcanic glass with seawater and/or diagenesis from the cooled glass, with smectite being the major associated alteration mineral.

The hemipelagic facies are: (1)(M) slightly chertified, fossiliferous carbonate mudstones, (2)(S_{lm}, S_{lh}, S_{lc}) massive, parallel- or cross-laminated fossiliferous lithic arenites, (3)(S_{gm}, S_{gh}, S_{gc}) massive, parallel or cross-laminated fossiliferous greywackes, (4)(S_{Hm}, S_r) hummocky-cross-stratified and wave ripples fine sandstones, (5)(S_t) through-cross bedded siltstone to fine sandstone, and (6)(S_{Cv}) convolute laminated and cross-laminated fining-upward sandstones. These lithofacies may contain abundant fossiliferous or organic matter as well as reworked mafic minerals that are generally matrix-supported. It has been interpreted that these lithofacies were deposited in a relatively lower energy environment, with a smaller fraction of volcanoclastic

sediment input and a slower sedimentation rate. This resulted in the accumulation of clay-sized sediments and microfossils due to suspension settling from the water table suggesting distal deposits from the volcanic sedimentary source.

These results are in agreement with previous findings reported by different authors (e.g., [Aizprua, 2021](#); [Benitez, 1995](#); [Jaillard et al., 1995](#)) who attribute the nature of these deposits to erosion and deposition in a submarine environment of the so-called San Lorenzo arc. Therefore, the volcanoclastic facies can be interpreted as being deposited proximal to the San Lorenzo arc, while the more distal deposits correspond to the hemipelagic facies.

In addition, typical Bouma turbidite sequences (Fig. 1.1) were identified at most of the outcrops. Two distinct $T_A - T_C$ sequences were observed at Outcrop 5 (see appendix E). Several T_A and T_D single sequences were identified at Outcrop 3 (see Appendix C). Individual $T_D - T_E$ sequences are also scattered throughout Outcrops 1 and 4. These turbiditic deposits are typical of the Cayo Formation and have been previously reported by [Benitez \(1995\)](#) and [Luzieux \(2007\)](#), where they identified a wide range of turbiditic deposits from centimeter size to megaturbidites (i.e., thick, extensive deposits from an exceptionally large mass flow). The table 5.1 also describes the possible Bouma sequence classification for each lithofacies. For centimeter- to decimeter-sized turbidite deposits, clusters of 3 to 4 members can be clearly identified (i.e., Outcrops 3 and 5), but for large megaturbidites, only single members could be inferred (i.e., Outcrops 1, 2, and 4) because the scope of this study was on a smaller scale. Therefore, the main mechanism of sedimentation of these sequences was density turbiditic flows.

Table 5.1: Descriptions of the facies recognized in this study from field observations, petrography of rock samples, and microfossil content. The possible Bouma turbidite classification was also determined.

Facies Code	Fossil Occurrence	Description	Bouma-Sequence
Sm	Absent	Poorly sorted, massive volcanoclastic sandstone	T _A
Cm	Scarce	Poorly sorted, subangular volcanic clasts, massive breccia	
Tm, Th, Tc	Absent	Massive, parallel- or cross-laminated very fine vitric tuff	T _A , T _B
Tv	Scarce	Massive vitreous-smectite matrix fine vitric tuff	T _A
M	Moderate	Slightly chertified, fossiliferous carbonate mudstone	
S _{lm} , S _{lh} , S _{lc}	Abundant	Massive, parallel- or cross-laminated fossiliferous lithic arenite	T _B , T _C
S _{gm} , S _{gh} , S _{gc}	Abundant	Massive, parallel or cross-laminated fossiliferous greywacke	T _D , T _E
S _{Hm} , S _r	Scarce	Hummocky-cross-stratified and wave ripples fine sandstone	T _C
St	Scarce	Throguh-cross bedded siltstone to fine sandstone	T _C
S _{Cv}	Scarce	Convolute laminated and cross-laminated fining-upward sandstone	T _C , T _D

5.2 Relative dating

As stated by [Ordoñez \(2006\)](#), in order to develop a proper age determination based on microfossil assemblages, it is preferable to have specimens identified to the species level. Due to the low recovery of body fossils in the present study and the lack of specialized laboratory equipment such as the SEM, only the preparation of thin sections of consolidated rock samples and examination under a petrographic microscope was developed. This method complemented the fossil collection available for the study area, nevertheless, the 2D view provided by the thin sections failed to provide sufficient detail to be able to identify specimens to the species level. Therefore,

our specimens were not placed at the species level until they have been thoroughly revised, otherwise the results may be misleading. To avoid this problem, species could be classified at the genus level based on general characteristics of the fossil groups.

Relative dating based on the specimens classified at the genus level was possible, but it had some drawbacks. There are key types of fossils (known as index fossils) that have been shown to have narrow age ranges, providing a better approximation when dating sedimentary rocks. Using index fossils for relative dating is more accurate and reliable. On the other hand, generic groups of fossils are more general, have a wider distribution, and the age range assigned to them is not as precise, making them less reliable. In this study, the radiolarian *Stylospongia planoconvexa* set the upper age boundary (i.e., Campanian). Similarly, the benthic foraminifer *Hormosinella ovolum* established the lower age boundary (i.e., Santonian). The remaining fossil species/genus identified also occur in this age range. The presence of *Heterohelix* sp., which has a Campanian to Santonian age, also supports this age determination. Therefore, based on the identified fossil species/genus, the estimated age of the studied outcrops is Santonian to Campanian (Fig. 5.1).

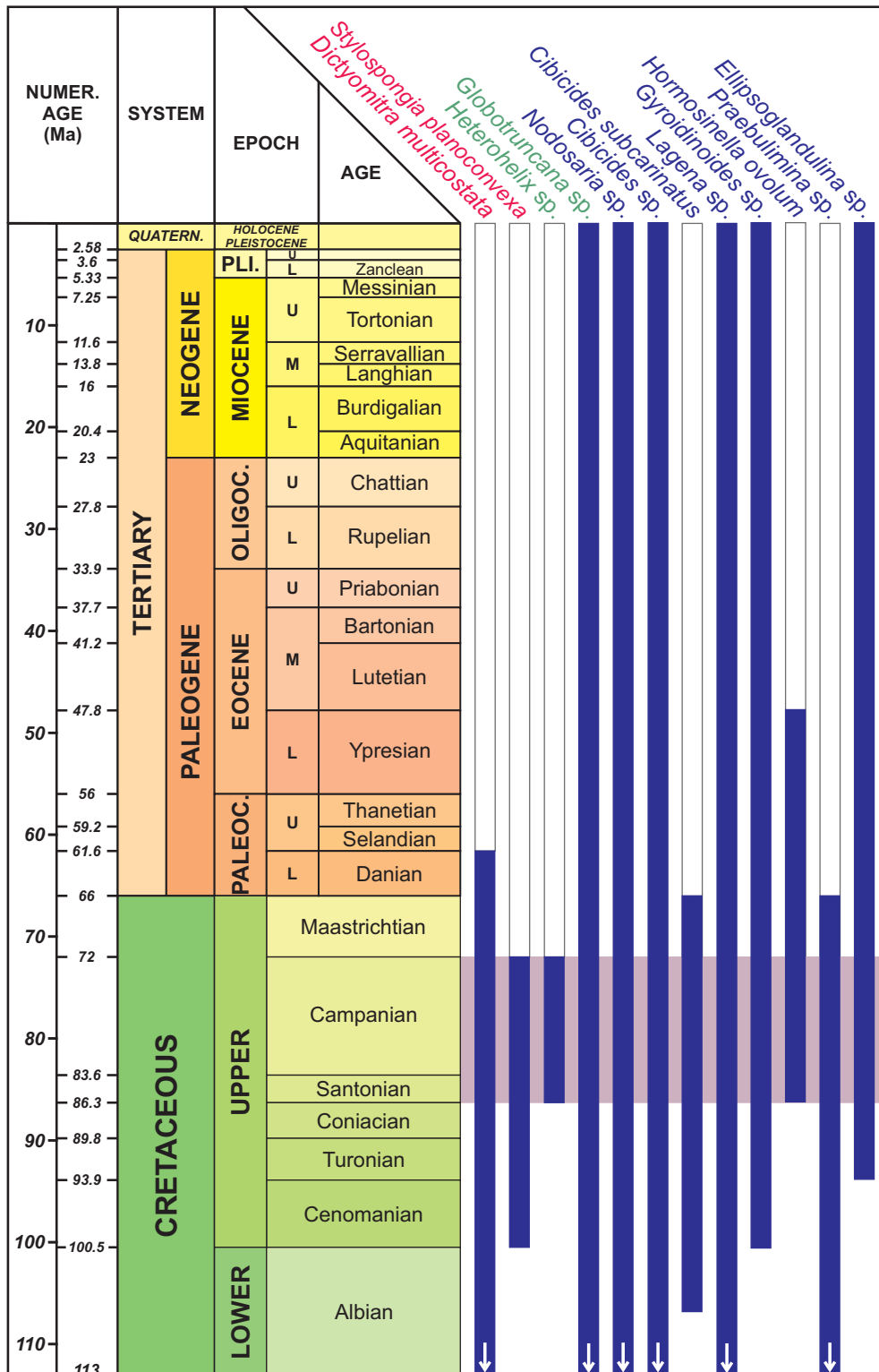


Figure 5.1. Stratigraphic distribution of identified species of radiolarians (red), planktic foraminifera (green), and benthic foraminifera (blue) in the Chongón-Colonche Cordillera. The age ranges were taken from Bolli et al. (1994); Loeblich and Tappan (1988); O’Dogherty et al. (2009); Ordoñez (2006)

5.3 Lithostratigraphic correlation

The reported calcareous black shales with dominant mudstone composition and abundant organic matrix reported in the Calentura Formation by [Luzieux \(2007\)](#) are consistent with the results obtained at the easternmost location in the study area (i.e., Outcrop 6, see location in Fig. 2.2). [Benitez \(1995\)](#) assigned these calcareous mudstone deposits as the basal member of the Cayo Formation. Later on, other authors such as [Ordoñez \(2006\)](#) differentiated the Calentura Formation in the stratigraphy of the Chongón-Colonche Cordillera. Finally, [Luzieux \(2007\)](#) also suggested a differentiation between the Cayo Formation and the Las Orquideas Formation. The currently accepted model for the basal sedimentary cover in the Chongón-Colonche Cordillera area distinguishes the Las Orquideas, Calentura, and Cayo Formations (see Fig. 5.2).

The lithology and fossil assemblages found at Outcrops 1-5 (see location in Fig. 2.2) are consistent with the volcanic debris flows and silicified turbidites that make up the Cayo Formation. In particular, Outcrop 5 is thought to correlate with the metric turbidite deposits found in the so-called Lower Member of the Cayo Formation. Finally, Outcrops 1-4 correspond to the decimetric turbiditic deposits and volcanic breccias found in the Upper Member of the Cayo Formation (Fig. 5.2). The age determination of the fossil assemblages found in the study area also supports this distribution, since the Calentura and Cayo Formations have been assigned a Santonian to Campanian age (Fig. 2.3) by various authors (e.g., [Benitez, 1995](#); [Luzieux, 2007](#); [Ordoñez, 2006](#); [Reyes and Michaud, 2012](#)).

A geological map was constructed (Fig. 2.2) based on bedding measurements taken in the field, and faults and geological formations reported by [Reyes and Michaud \(2012\)](#). The general dip direction of the deposits studied is NW, with the Outcrops 1 to 4 showing dip directions consistent with these observations. A major structural change occurs near the Casas Viejas site, marked by the presence of a fault that extends in the same orientation as the Blanco and Piñas Rivers, possibly following the fault scarp. The change in dip direction from NW to E suggests that folding of the strata due to tectonic stresses led to the formation of an anticline. Finally, the faults between Outcrops 5 and 6 are inverse faults, where older strata (Calentura Formation) have been uplifted. A similar structure can be seen near the Guayaquil area where the proven contact of the Calentura Formation has been reported ([Reyes and Michaud, 2012](#)). Further prospecting is required to delineate the extent of the Calentura Formation on this side of the Chongón-Colonche Cordillera and compliment the geological map of the coastal Ecuador.

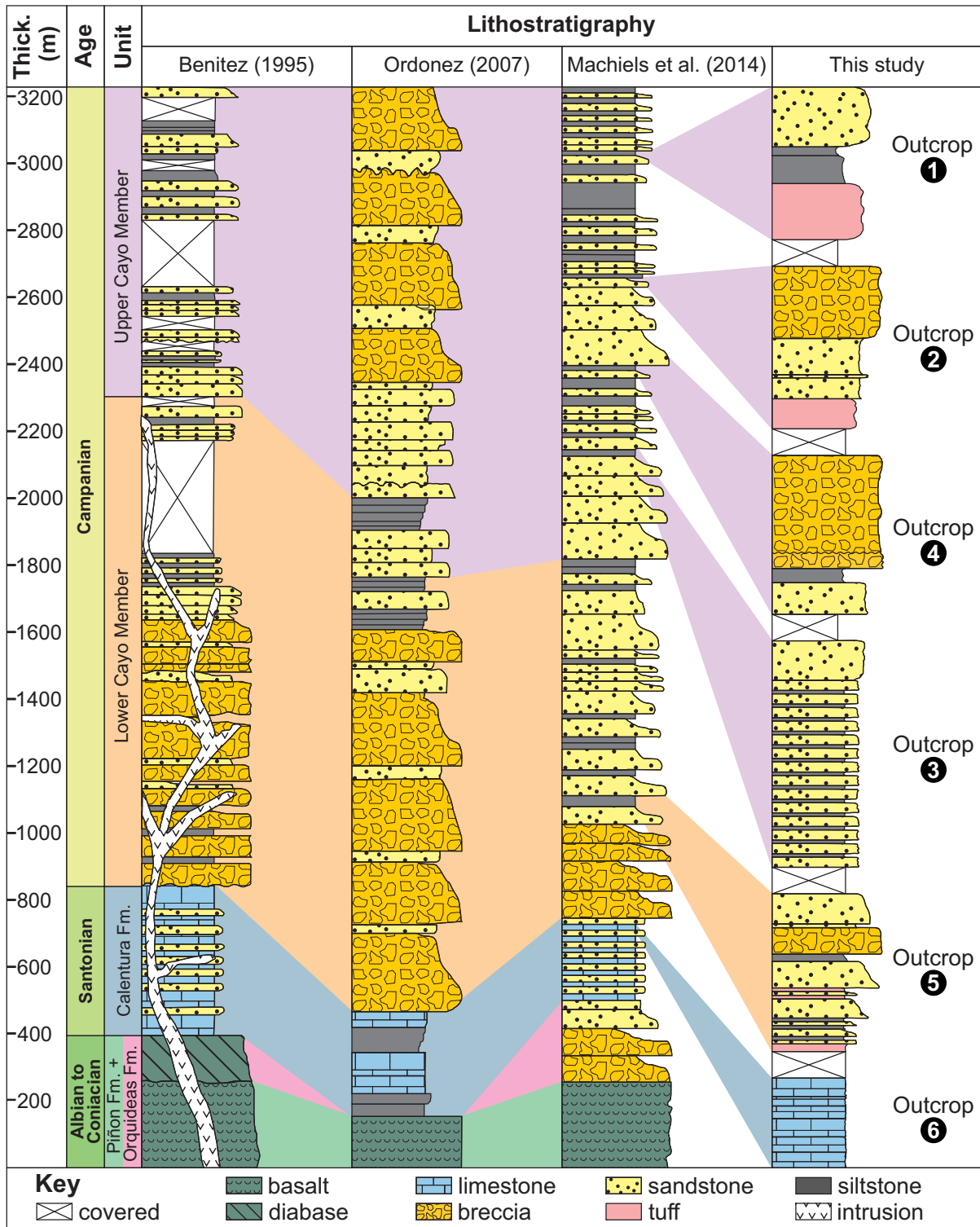


Figure 5.2. Lithostratigraphic correlation of the studied outcrops with previous studies, detailing approximate thickness and age. Modified after Benitez (1995), Ordoñez (2007) and Machiels et al. (2014).

5.4 Paleoenvironment determination

As noted by [Ordoñez \(2006\)](#), the microfossil record for this zone is rather scarce, making it impossible to apply statistical methods that require a large database of fossil occurrences to determine paleoclimates or oxygen levels. However, the reported occurrence of foraminifera, especially benthic foraminifera, can provide valuable information on depth and environmental conditions at the time of deposition.

The models proposed by [Sliter \(1972\)](#) and [Saraswati and Srinivasan \(2015\)](#) to explain depth distribution patterns based on the occurrence of benthic foraminifera were used to infer the paleoenvironment at the time of deposition (Fig. 5.3). In general, a high concentration of benthic foraminifera indicates a shallow environment, whereas an increase in the concentration of planktic foraminifera and radiolarians indicates a transition to a deeper environment. Due to the lack of planktic foraminifera in this study (see Table 4.1), it can be assumed that the paleoenvironments that deposited the studied outcrops are mostly from relatively shallow environments (upper to mid slope).

Since most of the strata deposited in the Cayo Formation are turbiditic in origin, it was expected that they would contain benthic foraminifera from a wide range of marine environments. Therefore, it is assumed that some shallow environment species such as *Cibicides* sp. or *Nodosaria* sp. found in assemblages with deeper environment species may have been reworked. As a discriminating factor, it was assumed for all deposits that the depositional environment was the deepest possible based on their fossil content. The following sections discuss the paleoenvironments determined for the Calentura and Cayo Formations based on the fossil assemblages at each outcrop (see Table 4.1).

5.4.1 Calentura formation

- **Outer Shelf (Outcrop 6)**

The fossil assemblage at Outcrop 6 includes the foraminifera *Heterohelix* sp., *Nodosaria* sp. and *Cibicides* sp. (see Table 4.1), suggesting an inner shelf to upper slope environment (~ 30 to 300 m, Fig. 5.3). In addition, the identified carbonate mudstones, which contain an organic-rich matrix, suggest an anoxic environment in which most of the fossil content was reduced by anaerobic bacteria, resulting in a clay-sized calcareous matrix. This also explains the scarcity and high alteration of the fossil specimens found. This is supported

by [Ordoñez \(2006\)](#) who attributes this to two possible causes, (1) a marine transgression or (2) upwelling events. Either event could have caused a corresponding increase in nutrient input to these environments, greatly increasing organic activity and depleting oxygen levels. Due to the nature of the calcareous deposits at Outcrop 6, the environment of deposition can be restricted to the outer shelf.

5.4.2 Cayo Formation

- **Inner to Outer shelf (Outcrops 1,2 and 4)**

Outcrops 2 and 4 are characterized by inner to outer shelf species such as the planktonic foraminifera *Heterohelix* sp. and the benthic species *Cibicides* sp. and *Nodosaria* sp. The occurrence of other fossils such as the radiolarian *Dictyomitra multicostata* and echinoids is also reported. Similarly, Outcrop 1 also contains radiolarians, specifically *Dictyomitra multicostata* and *Stylospongia planoconvexa*. Some single chambers of *Nodosaria* sp. are also present (see Table 4.1). The high content of radiolarians suggests a deep to mid slope environment, although the lack of benthic foraminifera makes defining a specific paleoenvironment difficult (Fig. 5.3).

- **Upper slope (Outcrop 5)**

The fossil assemblage at Outcrop 5 is mainly composed of benthic foraminifera ranging from shelf environments (*Cibicides* sp. and *Nodosaria* sp.), upper slope (*Gyroidinoides* sp.) to middle slope (*Praebulimina* sp., see Table 4.1). Assuming that the shallower species were reworked, a narrower approximation for depositional depth might be upper slope (Fig. 5.3). Due to the lack of planktic foraminifera, deeper environments are also discarded.

- **Middle slope (Outcrop 3)**

The fossil content of Outcrop 3 is the most diverse in this study. It contains the radiolarians *Dictyomitra multicostata*, the *Stylospongia planoconvexa*, and the planktic foraminifera *Globotruncana* sp. suggesting a continental slope environment. The benthic foraminifera assemblage consisting of *Nodosaria* sp., *Hormosinella ovolum* and *Praebulimina* sp. supports the upper to lower slope environment (see Table 4.1 and Fig. 5.3). Due to the nature of the fine-grained turbiditic sediments, these deposits are more likely to be part of a mid slope environment.

Based on these results, it is more likely that the paleoenvironment in the studied area for the Cayo Formation is upper to middle slope, which was also stated by [Ordoñez \(2006\)](#), who assigned a bathyal paleoenvironment (700-1000 m deep). As mentioned above, although benthic foraminifera from shallower environments are reported, it is more likely that these fossils were reworked and transported prior to deposition. Therefore, the paleoenvironment attributed to the Calentura Formation is outer shelf, and for the Cayo Formation it ranges from outer shelf to mid slope.

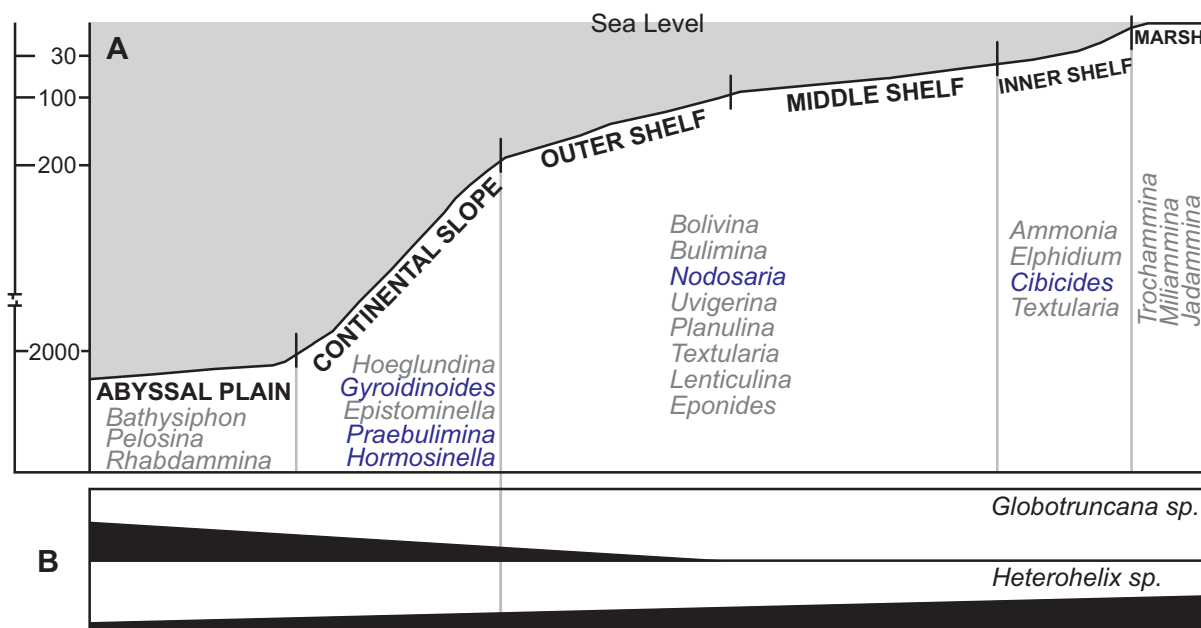


Figure 5.3. Depth assemblages of Upper Cretaceous foraminifera in marine environments. Modified after [Saraswati and Srinivasan \(2015\)](#) and [Sliter \(1972\)](#). A) Major fossil assemblages of benthic foraminifera distribution marginal marine, continental shelf, and continental slope environments highlighting the species used for this study. B) Generalized depth distribution of the planktic foraminiferal genera used in this study.

Chapter 6

Conclusions

The Calentura Formation has not been reported on the western side of the Chongón-Colonche Cordillera, between the Pedro Pablo Gomez - La Rinconada transect. Petrographic, sedimentologic and paleontologic analyses were developed on rock samples collected in the six selected outcrops. It was determined that the sequences correspond to volcanoclastic and hemipelagic deposits. By comparing microfossil assemblages, it was concluded that the studied deposits are of Santonian to Campanian age, which is in agreement with the literature. The stratigraphic columns of previous authors were compared with those developed in this study and it was determined that two formations occur: Cayo and Calentura, both of Upper Cretaceous age. Future mapping campaigns must be developed to delineate the occurrence of the Calentura Formation in this area.

Several decimetric turbidite to megaturbidite sequences have been identified based on field observations of lithologies and sedimentary structures. The sequences include complete T_C - T_D and T_D - T_E Bouma sequences as well as incomplete sequences of possibly single T_A and T_D members. The Cayo Formation shows several lithofacies that may have been derived from a nearby volcanic source and deposited on a continental slope. This feature is typical of the Cayo Formation as reported by previous authors.

Petrographic studies determined the mineral content and sedimentary textures of the rock samples. Based on these results and field measurements, 10 lithofacies of mainly lithic arenites, graywackes, tuffs, calcareous mudstones and volcanic breccias were identified in the zone. Alteration of glassy material was evident, supporting previous findings of zeolite minerals in the zone.

The lithostratigraphic correlation showed that the described rock sequences correlate with

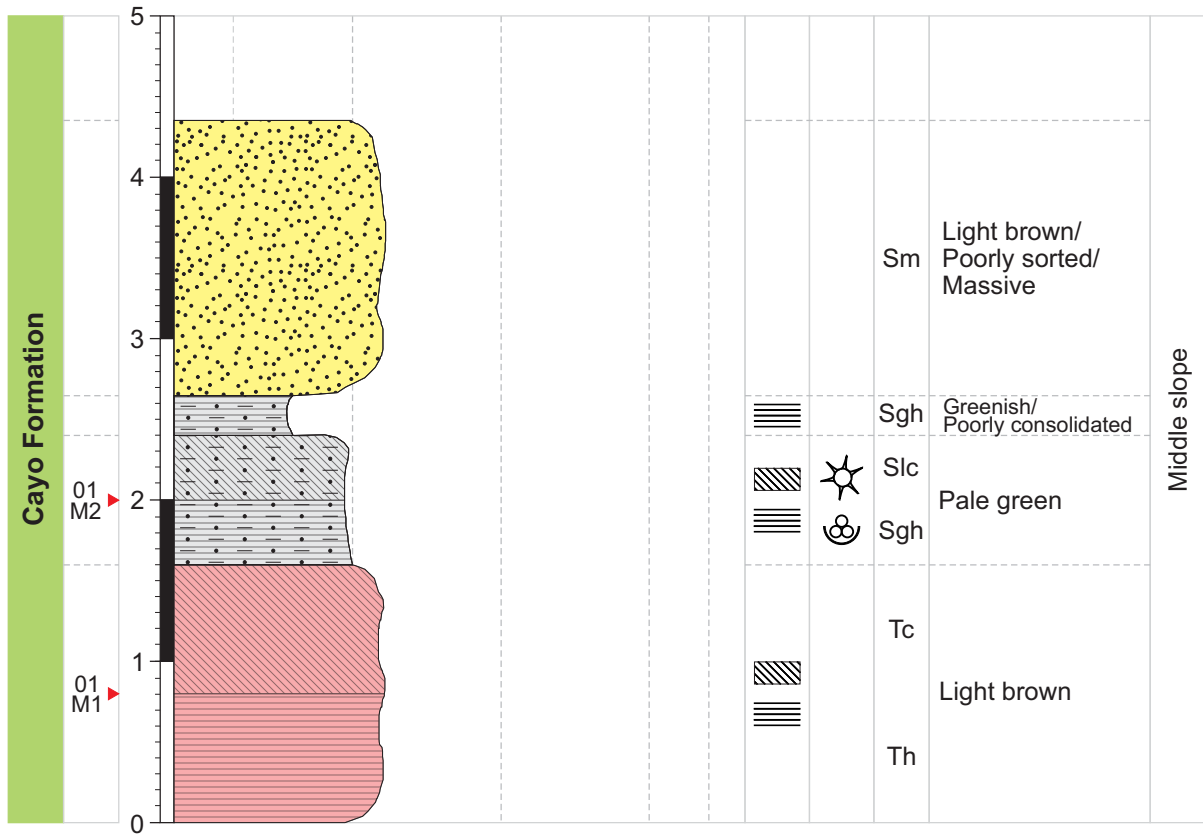
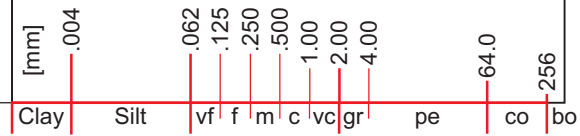
the Upper Calentura (Outcrop 6), Lower Cayo (Outcrop 5) and Upper Cayo (Outcrops 1-4) formations. The variations in the dip angle measurements of the strata and the presence of local faulting suggest a high level of tectonic disturbance, which should be further investigated in a specialized study.

Among the identified microfauna, 11 species/genus were identified, mainly from radiolarians, benthic and planktonic foraminifera. The microfossil species used for dating the studied rocks were *Stylospongia planoconvexa*, *Hormosinella ovolum*, and *Heterohelix* sp. Foraminifera fossil species revealed the depositional environments. Although *Cibicides* sp. and *Heterohelix* sp. species suggest a shallow environment origin, their interdigitation with deeper environment species (i.e., *Praebulimina* sp., *Hormosinella ovolum*, and *Gyroidinoides* sp.) suggests that these fossils were reworked, confirming a turbiditic environment. The fossil assemblages of benthic foraminifera allowed the determination of outer shelf environments for the Calentura Formation and outer shelf to mid slope environments for the Cayo Formation.

Appendix A

Graphic Log Outcrop 1

Stratigraphic Unit	Sample Code	Thickness [m]	Tuff				Lapilli	Agg.	Sedimentary Structures	Fossils	Lithofacies	Notes	Environment
			f		c								
			Ms	Ws	Ps	Gs	Bs	Cs					
			Mudstone		Sandstone		Conglomerate						



Locality
 ID: V23-01 (Outcrop 1)
 Units: meters
 Scale: 1:40

Location
 Latitude: -1.675843
 Longitude: -80.70258
 Elevation: 129 m
 Country: Ecuador

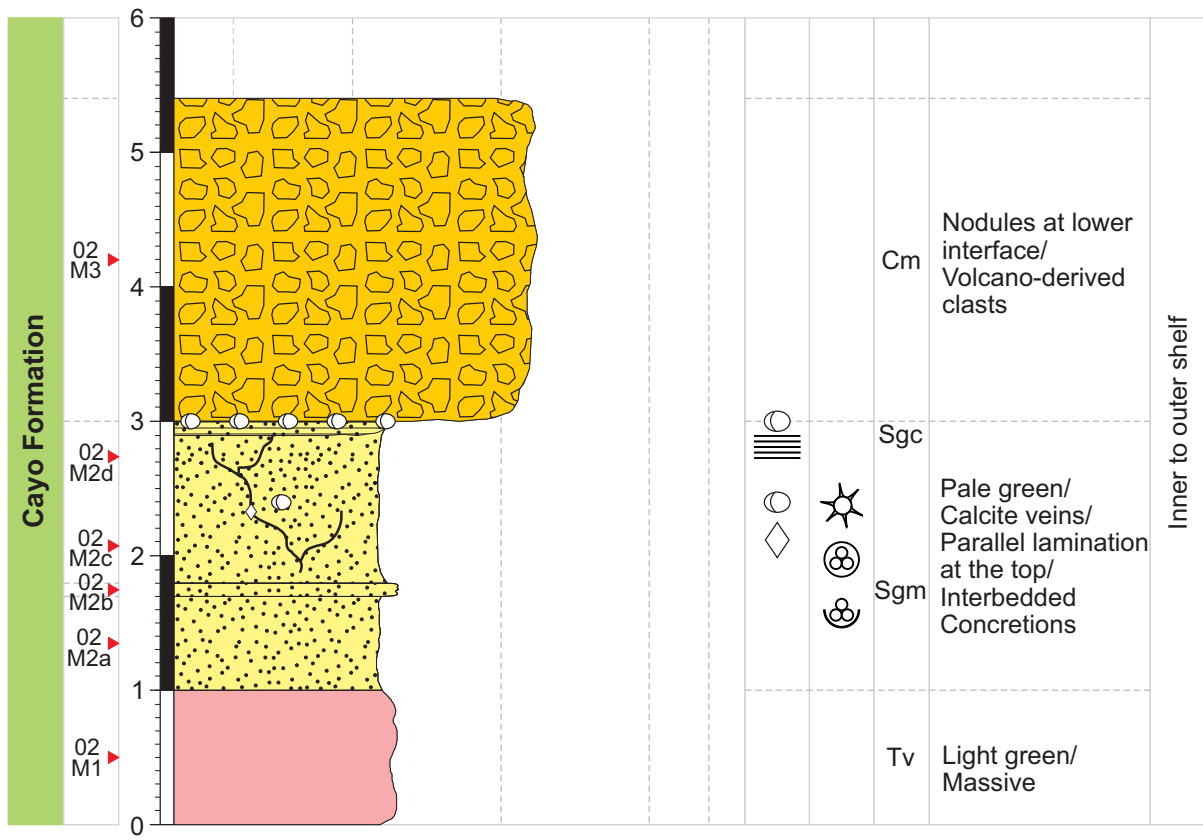
Author
 Alejandro Vallejo

LEGEND	
sandstone	radiolarian
siltstone	benthic foraminifera
tuff	
parallel lamination	planar cross bedding

Appendix B

Graphic Log Outcrop 2

Stratigraphic Unit	Sample Code	Thickness [m]	Tuff				Lapilli	Agg.	Sedimentary Structures	Fossils	Lithofacies	Notes	Environment										
			f		c																		
			Ms	Ws	Ps	Gs	Bs	Cs															
			Mudstone		Sandstone		Conglomerate																
		[mm]	.004	.062	.125	.250	.500	1.00	2.00	4.00	64.0	256											
			Clay	Silt	vf	f	m	c	vc	gr	pe	co	bo										



Locality
ID: V23-02 (Outcrop 2)
Units: meters
Scale: 1:55
Location
Latitude: -1.673092
Longitude: -80.69874
Elevation: 105 m
Country: Ecuador
Author
Alejandro Vallejo

Lithology		LEGEND	
conglomerate	parallel lamination	concretion/nodule	calcite
sandstone	radiolarian	planktic foraminifera	benthic foraminifera
tuff			

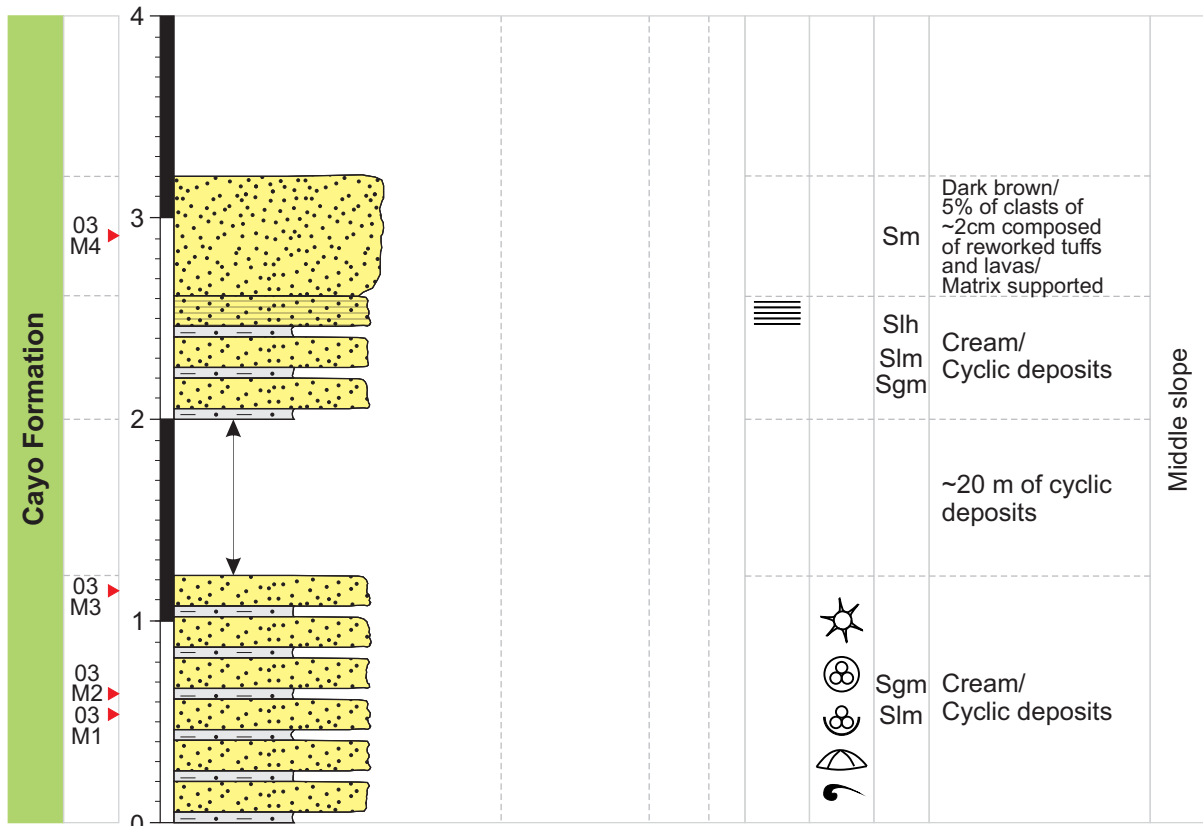
Appendix C

Graphic Log Outcrop 3

Stratigraphic Unit	Sample Code	Thickness [m]	Tuff				Lapilli	Agg.	Sedimentary Structures	Fossils	Lithofacies	Notes	Environment
			f	c									
			Ms	Ws	Ps	Gs	Bs	Cs					
			Mudstone		Sandstone		Conglomerate						

[mm] .004 .062 .125 .250 .500 1.00 2.00 4.00 64.0 256

Clay Silt vf f m c vc gr pe co bo



Locality
ID: V23-03 (Outcrop 3)
Units: meters
Scale: 1:35
Location
Latitude: -1.677158
Longitude: -80.66843
Elevation: 144 m
Country: Ecuador
Author
Alejandro Vallejo

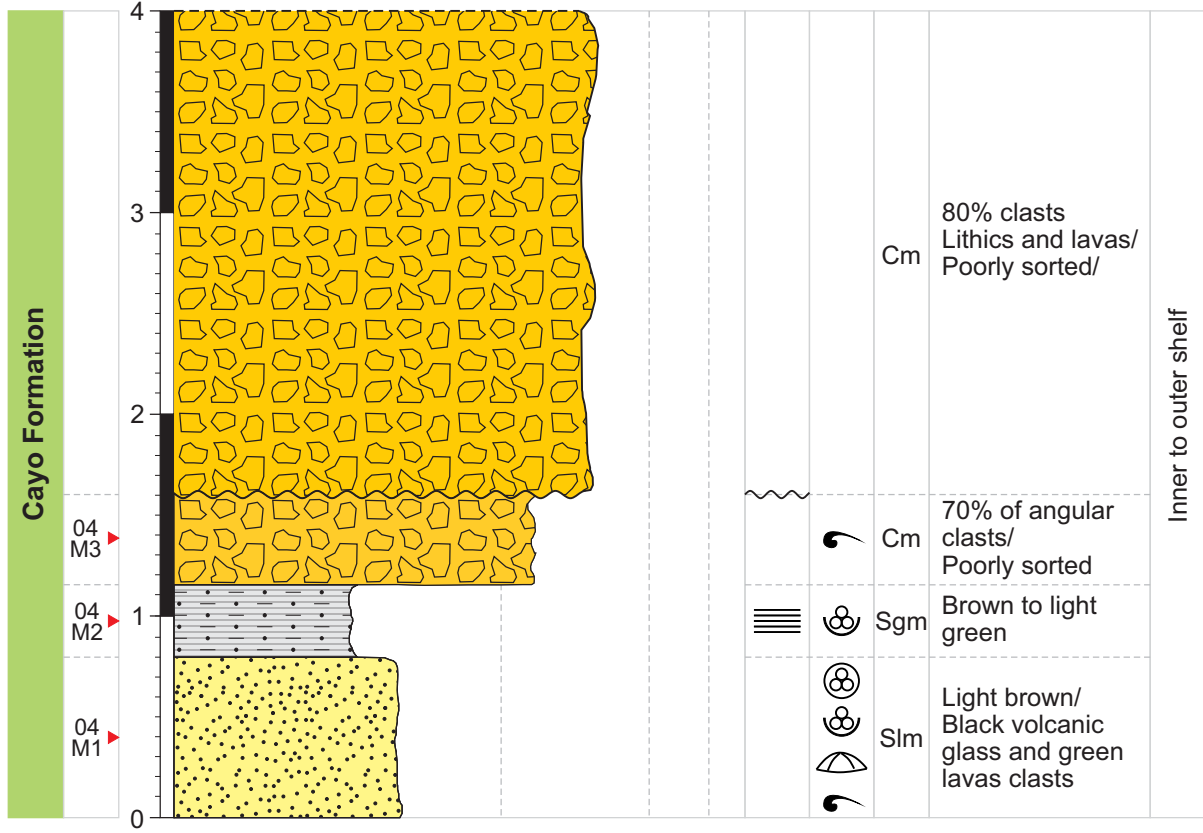
LEGEND	
	sandstone
	siltstone
	parallel lamination
	radiolarian
	planktic foraminifera
	benthic foraminifera
	echinoid
	ind. microfossils

Appendix D

Graphic Log Outcrop 4

Stratigraphic Unit	Sample Code	Thickness [m]	Tuff				Lapilli	Agg.	Sedimentary Structures	Fossils	Lithofacies	Notes	Environment
			f	c									
			Ms	Ws	Ps	Gs	Bs	Cs					
			Mudstone		Sandstone		Conglomerate						

[mm] .004 .062 .125 .250 .500 1.00 2.00 4.00 64.0 256
 Clay Silt vf f m c vc gr pe co bo



Locality
 ID: V23-04 (Outcrop 4)
 Units: meters
 Scale: 1:35

Location
 Latitude: -1.67224
 Longitude: -80.68964
 Elevation: 125 m
 Country: Ecuador

Author
 Alejandro Vallejo

LEGEND

Lithology

- sandstone
- siltstone
- conglomerate

Sedimentary Structures

- parallel lamination

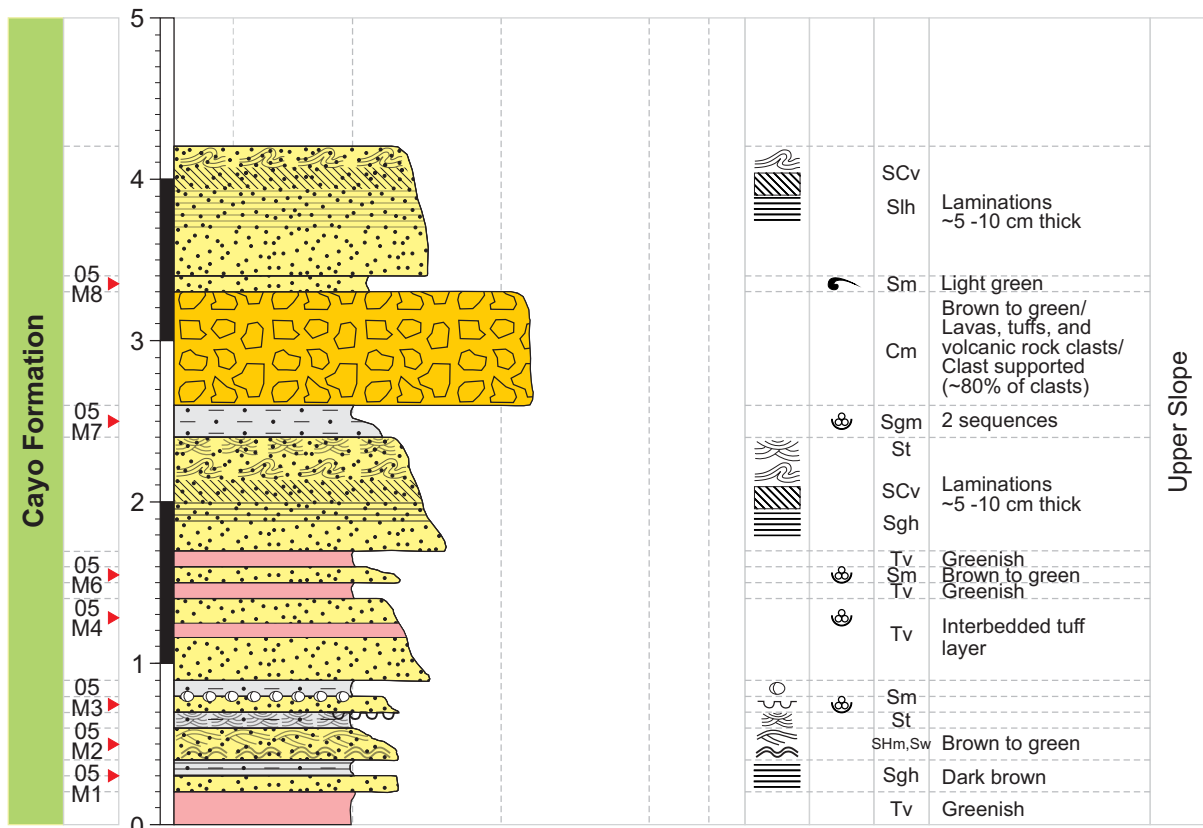
Fossils

- planktic foraminifera
- benthic foraminifera
- echinoid
- ind. microfossils
- erosive surface

Appendix E

Graphic Log Outcrop 5

Stratigraphic Unit	Sample Code	Thickness [m]	Tuff				Lapilli	Agg.	Sedimentary Structures	Fossils	Lithofacies	Notes	Environment											
			f		c																			
			Ms	Ws	Ps	Gs	Bs	Cs																
			Mudstone		Sandstone		Conglomerate																	
		[mm]	.004	.062	.125	.250	.500	1.00	2.00	4.00	64.0	256												
			Clay	Silt	vf	f	m	c	vc	gr	pe	co	bo											



Locality
 ID: V23-05 (Outcrop 5)
 Units: meters
 Scale: 1:40

Location
 Latitude: -1.667773
 Longitude: -80.64843
 Elevation: 153 m
 Country: Ecuador

Author
 Alejandro Vallejo

Lithology

- sandstone
- siltstone
- tuff
- conglomerate

Sedimentary Structures

- parallel lamination
- wave ripple/load cast
- concretion/nodule
- trough cross-bedding
- hummocky cross-stratif.
- planar cross-bedding
- convolute

Fossils

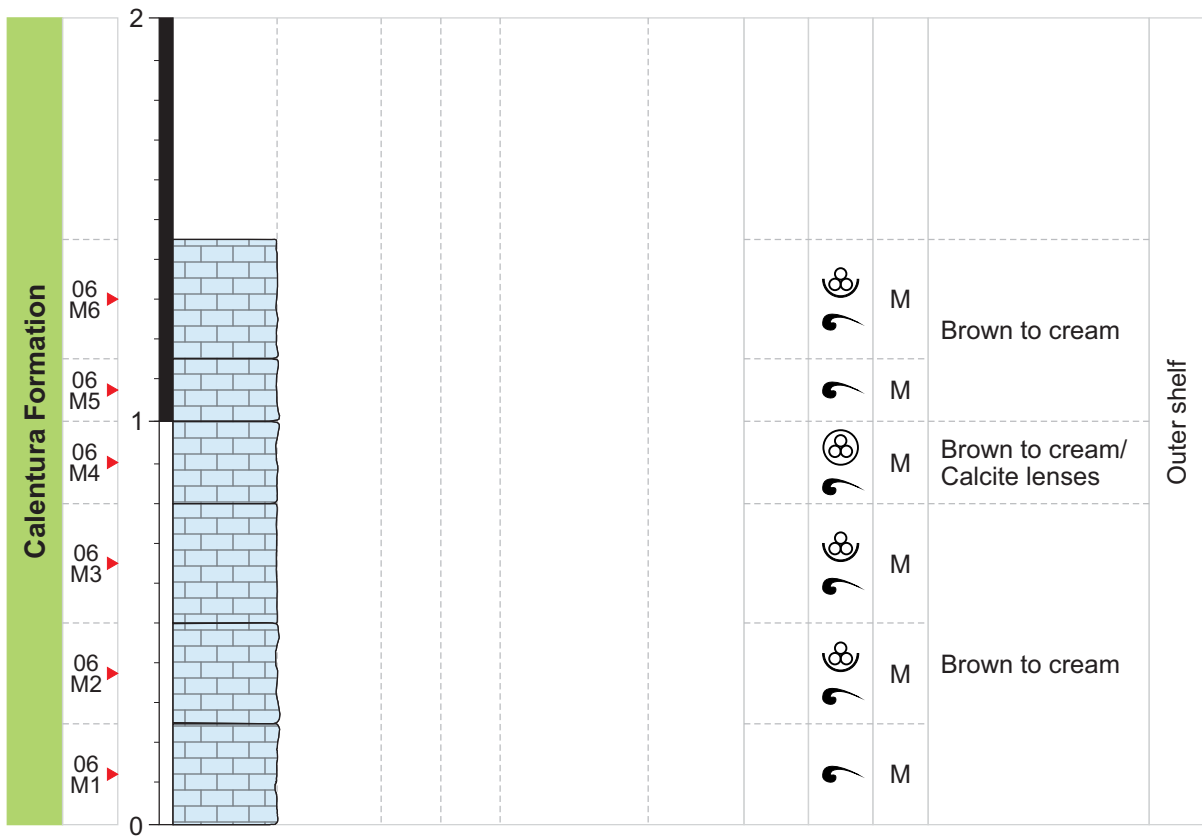
- benthic foraminifera
- ind. microfossils

Appendix F

Graphic Log Outcrop 6

Stratigraphic Unit	Sample Code	Thickness [m]	Tuff				Lapilli	Agg.					
			f	c									
			Ms	Ws	Ps	Gs	Bs	Cs					
			Mudstone		Sandstone		Conglomerate						
		[mm]	.004	.062	.125	.250	.500	1.00	2.00	4.00	64.0	256	
			Clay	Silt	vf	f	m	c	vc	gr	pe	co	bo

Sedimentary Structures	Fossils	Lithofacies	Notes	Environment
------------------------	---------	-------------	-------	-------------



Locality	
ID:	V23-06 (Outcrop 6)
Units:	meters
Scale:	1:20
Location	
Latitude:	-1.654795
Longitude:	-80.62703
Elevation:	183 m
Country:	Ecuador
Author	
Alejandro Vallejo	

LEGEND	
Lithology	
	limestone
Fossils	
	planktic foraminifera
	benthic foraminifera
	ind. microfossils

Appendix G

List of Collected Samples and Location

Table G.1: List of collected of rock samples (16) used for thin section analysis and bulk sediments (12) used for cleaning and physical removal of microfossils.

Sample Code*	Outcrop	Type	Coordinates (UTM 17S)	
			Easting	Northing
01-M1	1	Rock sample	533081	9814766
01-M2	1	Rock sample	533081	9814766
02-M1	2	Rock sample	533509	9815070
02-M2a	2	Bulk sediment	533509	9815070
02-M2b	2	Rock sample	533509	9815070
02-M2c	2	Bulk sediment	533509	9815070
02-M2d	2	Bulk sediment	533509	9815070
02-M3	2	Rock sample	533509	9815070
03-M1	3	Rock sample	536880	9814620
03-M2	3	Bulk sediment	536880	9814620
03-M3	3	Bulk sediment	536880	9814620
03-M4	3	Bulk sediment	536880	9814620
04-M1	4	Rock sample	534521	9815164
04-M2	4	Bulk sediment	534521	9815164
04-M3	4	Rock sample	534521	9815164
05-M1	5	Bulk sediment	539105	9815657
05-M2	5	Bulk sediment	539105	9815657
05-M3	5	Bulk sediment	539105	9815657
05-M4	5	Rock sample	539105	9815657
05-M6	5	Bulk sediment	539105	9815657
05-M7	5	Rock sample	539105	9815657
05-M8	5	Bulk sediment	539105	9815657
06-M1	6	Rock sample	541485	9817091
06-M2	6	Rock sample	541485	9817091
06-M3	6	Rock sample	541485	9817091
06-M4	6	Rock sample	541485	9817091
06-M5	6	Rock sample	541485	9817091
06-M6	6	Rock sample	541485	9817091

* The sample ID is defined as follows: V23-01-M1a (V23 refers to sampling age - outcrop number - M1 refers to the sample number in a single bed ("a" stands for numerous samples taken in the same bed).

Bibliography

- Aizprua, C. (2021). *Forearc crustal structure and controlling factors on basin formation across the southernmost Northern Andes*. PhD thesis, Université de Lille; Norwegian University of Science and Technology
- Bellier, J.-P., Mathieu, R., and Granier, B. (2010). Short treatise on foraminiferology (essential on modern and fossil foraminifera) [court traité de foraminiférologie (l'essentiel sur les foraminifères actuels et fossiles)]. *Carnets de Géologie*, CG2010.
- Benitez, S. (1995). *Evolution géodynamique de la province côtière sud-équatorienne au Crétacé supérieur-Tertiaire*. PhD thesis, Université Joseph-Fourier-Grenoble I.
- Benítez, S., Jaillard, E., Ordoñez, M., C, N., and Berrones, G. (1993). Late cretaceous to eocene tectonic-sedimentary evolution of southern coastal ecuador : geodynamic implications.
- Bolli, H., Saunders, J., and Perch-Nielsen, K. (1989). *Plankton Stratigraphy: Volume 1, Planktic Foraminifera, Calcareous Nannofossils and Calpionellids*. Cambridge Earth Science Series. Cambridge University Press.
- Bolli, H. M., Beckmann, J.-P., and Saunders, J. B. (1994). *Benthic foraminiferal biostratigraphy of the south Caribbean region*. Cambridge University Press.
- Bristow, C. and Hoffstetter, R. (1977). Ecuador: Lexique international de stratigraphie. *Paris, 5a2*.
- Burnham Petrographics LLC (n.d). User's manual instructions for using petropoxy 154. Online. Accessed on 2023-12-29.
- Camacho, H. (1966). *Invertebrados fósiles*. Manuales de EUDEBA.: Ciencias naturales. EU-DEBA.

- Cohen, K., Finney, S., Gibbard, P., and Fan, J. (2013). Cohen, k.m., finney, s.c., gibbard, p.l., fan, j.x. 2013. the ics international chronostratigraphic chart. episodes 36, 199-204. *Episodes*, 36.
- Collinson, J., Collinson, J., Mountney, N., and Mountney, N. (2019). *Sedimentary Structures*. Dunedin Academic Press.
- Deniaud, Y. (1998). Evolucion tectono-sedimentaria de las cuencas costeras neógenas del ecuador. *Convenio Petroproduccion/ORSTOM. Quito, Ecuador, 74p*.
- Dunham, R. J. (1962). Classification of carbonate rocks according to depositional textures.
- Feininger, T. and Bristow, C. R. (1980). Cretaceous and paleogene geologic history of coastal ecuador. *Geologische Rundschau*, 69(3):849–874.
- Folk, R. L., Andrews, P. B., and Lewis, D. (1970). Detrital sedimentary rock classification and nomenclature for use in new zealand. *New Zealand journal of geology and geophysics*, 13(4):937–968.
- Goossens, P. J. and Rose Jr, W. I. (1973). Chemical composition and age determination of tholeiitic rocks in the basic igneous complex, ecuador. *Geological Society of America Bulletin*, 84(3):1043–1052.
- Haq, B. U. and Boersma, A. (1998). *Introduction to marine micropaleontology*. Elsevier.
- Horowitz, A., Ringer, G., and Potter, P. (2012). *Introductory Petrography of Fossils*. Springer Berlin Heidelberg.
- Jackson, L. J., Horton, B. K., and Vallejo, C. (2019). Detrital zircon u-pb geochronology of modern andean rivers in ecuador: Fingerprinting tectonic provinces and assessing downstream propagation of provenance signals. *Geosphere*, 15(6):1943–1957.
- Jaillard, E., Benitez, S., and Mascle, G. H. (1997). Les déformations paléogènes de la zone d'avant-arc sud-équatorienne en relation avec l'évolution géodynamique. *Bulletin de la Société géologique de France*, 168(4):403–412.
- Jaillard, E., Lapierre, H., Ordoñez, M., Alava, J. T., Amortegui, A., and Vanmelle, J. (2009). Accreted oceanic terranes in ecuador: southern edge of the caribbean plate? *Geological Society, London, Special Publications*, 328(1):469–485.

- Jaillard, E., Ordoñez, M., Benitez, S., Berrones, G., Jiménez, N., Montenegro, G., and Zambrano, I. (1995). Basin Development in an Accretionary, Oceanic-Floored Fore-Arc Setting; Southern Coastal Ecuador During Late Cretaceous-Late Eocene Time. In *Petroleum Basins of South America*. American Association of Petroleum Geologists.
- Lebrat, M., Megard, F., Juteau, T., and Calle, J. (1985). Pre-orogenic volcanic assemblages and structure in the western cordillera of Ecuador between 140's and 220's. *Geologische Rundschau*, 74:343–351.
- Loeblich, A. R. and Tappan, H. (1988). *Foraminiferal Genera and Their Classification*. Springer, New York, NY.
- Luzieux, L. (2007). *Origin and Late Cretaceous-Tertiary evolution of the Ecuadorian forearc*. PhD thesis, ETH Zurich.
- Machiels, L., Garces, D., Snellings, R., Vilema, W., Morante, F., Paredes, C., and Elsen, J. (2014). Zeolite occurrence and genesis in the late-cretaceous Cayo arc of coastal Ecuador: Evidence for zeolite formation in cooling marine pyroclastic flow deposits. *Applied Clay Science*, 87:108–119.
- Mégard, F., Noblet, C., Mourier, T., Laj, C., Lebrat, M., and Roperch, P. (1987). L'occident équatorien: un terrain océanique pacifique accolé au continent sud-américain. *Bulletin de l'Institut Français d'Études Andines*, 16(1):39–54.
- O'Dogherty, L., Carter, E. S., Dumitrica, P., Goriccan, S., De Wever, P., Bandini, A. N., Baumgartner, P. O., and Matsuoka, A. (2009). Catalogue of mesozoic radiolarian genera. part 2: Jurassic-cretaceous. *Geodiversitas*, 31(2):271–356.
- Ordoñez, M. (2006). *Micropaleontología ecuatoriana: Datos bioestratigráficos y paleoecológicos de las cuencas: Graben de Jambelí, Progreso, Manabí, Esmeraldas y Oriente; del levantamiento de la península de Santa Elena, y de las cordilleras Chongón Colonche, costera y Occidental*. Petroproducción y Centro de Investigaciones Geológicas de Guayaquil.
- Ordoñez, M. (2007). Asociaciones de radiolarios de la cordillera Chongón-Colonche, Ecuador (coniaco-eoceno). In *4th European Meeting on the paleontology and stratigraphy of Latin America, Extend. Abstract.-Cuadernos Museo Geominero*, volume 8, pages 291–299.

- Prothero, D. and Schwab, F. (2004). *Sedimentary Geology*. W. H. Freeman.
- Reyes, P. and Michaud, F. (2012). Mapa geológica de la margen costera ecuatoriana (1: 500000).
- Reynaud, C., Jaillard, É., Lapierre, H., Mamberti, M., and Mascle, G. H. (1999). Oceanic plateau and island arcs of southwestern Ecuador: their place in the geodynamic evolution of northwestern South America. *Tectonophysics*, 307(3-4):235–254.
- Saraswati, P. K. and Srinivasan, M. (2015). *Micropaleontology: Principles and applications*. Springer.
- Schmid, R. (1981). Descriptive nomenclature and classification of pyroclastic deposits and fragments: Recommendations of the IUGS subcommission on the systematics of igneous rocks. *Geologische Rundschau*, 70:794–799.
- Scholle, P. A. and Ulmer-Scholle, D. S. (2003). *A Color Guide to the Petrography of Carbonate Rocks: Grains, textures, porosity, diagenesis*. American Association of Petroleum Geologists.
- Sliter, W. (1972). Cretaceous foraminifers—depth habitats and their origin. *Nature*, 239(5374):514–515.
- Spikings, R., Cochrane, R., Villagomez, D., Van der Lelij, R., Vallejo, C., Winkler, W., and Beate, B. (2015). The geological history of northwestern South America: from Pangaea to the early collision of the Caribbean large igneous province (290–75 Ma). *Gondwana Research*, 27(1):95–139.
- Tamay Granda, J. V. (2018). Estructura de cuencas intramontañosas del sur de Ecuador en relación con la tectónica de la cordillera de los Andes a partir de datos geofísicos y geológicos.
- Vallejo, C., Spikings, R. A., Horton, B. K., Luzieux, L., Romero, C., Winkler, W., and Thomsen, T. B. (2019). Late Cretaceous to Miocene stratigraphy and provenance of the coastal forearc and western cordillera of Ecuador: Evidence for accretion of a single oceanic plateau fragment. In *Andean tectonics*, pages 209–236. Elsevier.
- Vallejo, C., Winkler, W., Spikings, R. A., Luzieux, L., Heller, F., and Bussy, F. (2009). Mode and timing of terrane accretion in the forearc of the Andes in Ecuador. In *Backbone of the Americas: Shallow Subduction, Plateau Uplift, and Ridge and Terrane Collision*. Geological Society of America.

Van Melle, J., Vilema, W., Faure-Brac, B., Ordoñez, M., Lapierre, H., Jimenez, N., Jaillard, E., and Garcia, M. (2008). Pre-collision evolution of the piñón oceanic terrane of sw ecuador: stratigraphy and geochemistry of the “calentura formation”. *Bulletin de la Société géologique de France*, 179(5):433–443.